

United States
Environmental Protection
Agency

Atmospheric Research and Exposure
Assessment Laboratory
Research Triangle Park, NC 27711

EPA/600/8-89/041
March, 1989

Research and Development



User's Guide to the
Complex Terrain
Dispersion Model Plus
Algorithms for
Unstable Situations
(CTDMPLUS):

Volume 1. Model
Description and User
Instructions



Research and Development



User's Guide to the Complex Terrain Dispersion Model Plus Algorithms for Unstable Situations (CTDMPLUS):

Volume 1. Model Description and User Instructions



EPA/600/8-89/041
March 1989

**USER'S GUIDE TO THE COMPLEX TERRAIN DISPERSION MODEL
PLUS ALGORITHMS FOR UNSTABLE SITUATIONS (CTDMPLUS)
VOLUME 1: MODEL DESCRIPTION AND USER INSTRUCTIONS**

by

Steven G. Perry*

Atmospheric Sciences Modeling Division
Atmospheric Research and Exposure Assessment Laboratory
Research Triangle Park, NC 27711

Donna J. Burns and Lucy H. Adams

Computer Sciences Corporation
Research Triangle Park, NC 27709

Robert J. Paine, Michael G. Dennis,** Michael T. Mills****

Environmental Research and Technology, Inc.
Concord, MA 01742

David G. Strimaitis, Robert J. Yamartino,** Elizabeth M. Insley****

Sigma Research Corporation
Westford, MA 01886

*On assignment from the National Oceanic and Atmospheric Administration,
U.S. Department of Commerce

**Authors of the original CTDM user's manual (EPA/600/8-87/058a), much of
which remains in this manual for CTDMPLUS.

**ATMOSPHERIC RESEARCH AND EXPOSURE ASSESSMENT LABORATORY
OFFICE OF RESEARCH AND DEVELOPMENT
U.S. ENVIRONMENTAL PROTECTION AGENCY
RESEARCH TRIANGLE PARK, NC 27711**

NOTICE

All the information in this document has been funded wholly or in part by the U.S. Environmental Protection Agency; the portions on the original CTDM were funded under Contract No. 68-02-3421 to Environmental Research and Technology, Inc. This document has been subjected to the Agency's peer and administrative review, and it has been approved for publication as an EPA document. Mention of trade names or commercial products does not constitute endorsement or recommendation for use.

ABSTRACT

The Complex Terrain Dispersion Model Plus Algorithms for Unstable Situations (CTDMPLUS) is a refined air quality model for use in all stability conditions for complex terrain applications. It contains, in its entirety, the technology of CTDM for stable and neutral conditions. However, CTDMPLUS can also model daytime, unstable conditions, and has a number of additional capabilities for improved user friendliness. Its use of meteorological data and terrain information is different than current EPA models; considerable detail for both types of input data is required and is supplied by preprocessors specifically designed for CTDMPLUS. CTDMPLUS requires the parameterization of individual hill shapes using the terrain preprocessor and the association of each model receptor with a particular hill (except for receptors in flat terrain, which CTDMPLUS can also model).

In modeling stable to neutral conditions, a central feature of CTDMPLUS is its use of a critical dividing-streamline height (H_c) to separate the flow in the vicinity of a hill into two separate layers. Flow in the upper layer has sufficient kinetic energy to pass over the top of the hill, while streamlines in the lower layer are constrained to flow in a horizontal plane around the hill. Two separate components of CTDMPLUS compute ground-level concentrations resulting from plume material in each of these flows: LIFT handles the flow above H_c , and WRAP handles the flow below H_c .

In modeling unstable (convective) conditions, the model relies on a probability density function (PDF) description of the vertical velocities to estimate the vertical distribution of pollutant concentration. Terrain distortions of plume parcel trajectories are accounted for, as are deflections of the daytime mixed layer height.

Hourly profiles of wind and temperature measurements are used by CTDMPLUS to compute plume rise, plume penetration, convective scaling parameters, the value of H_c , and the Froude number above H_c . In stable/neutral conditions the profiles of turbulence data (σ_θ or σ_v , and σ_w values) are used to compute plume σ_y and σ_z values at plume height.

The model calculates on an hourly (or appropriate steady averaging period) basis how the plume trajectory (and, in stable/neutral conditions, the shape) is deformed by each hill. The computed concentration at each receptor is then derived from the receptor position on the hill and the resultant plume position and shape.

This user guide is divided into two volumes: Volume 1 describes the model and how to use it, while Volume 2 contains code listings. Auxiliary user manuals describe the terrain and meteorological preprocessors. The CTDMPLUS technical descriptions of algorithms for stable/neutral conditions remain virtually unchanged from those of the original CTDM manual (Paine et al., 1987). However, due to improvements in user friendliness, sections of this CTDMPLUS manual pertaining to user instructions and model structure have changed significantly from those for CTDM.

TABLE OF CONTENTS

Abstract	iii
Figures.....	vii
Tables	ix
Symbols and Abbreviations	x
Acknowledgements	xvi
1 INTRODUCTION	1-1
1.1 BACKGROUND	1-1
1.2 MODEL APPLICABILITY AND TECHNICAL LIMITATIONS	1-2
1.3 OVERVIEW OF CTDMPPLUS SOFTWARE COMPONENTS	1-3
1.3.1 Terrain Preprocessor	1-3
1.3.2 Meteorological Preprocessor, METPRO	1-5
1.3.3 Receptor Generator, RECGEN	1-6
1.3.4 Complex Terrain Dispersion Model PPlus Algorithms for Unstable Situations, CTDMPLUS	1-6
1.3.5 Interactive Set-up Program, SETUP	1-6
1.3.6 Concentration Postprocessors	1-7
1.3.7 Menu Driver Program	1-7
1.4 CTDMPPLUS COMPUTER CONSIDERATIONS	1-7
1.4.1 Software Considerations	1-7
1.4.2 Hardware Limitations	1-8
2 TECHNICAL DESCRIPTION	2-1
2.1 OVERVIEW OF THE CTDMP PLUS ALGORITHMS FOR UNSTABLE CONDITIONS (CTDMPLUS)	2-1
2.1.1 Pollutant Releases into Stable/Neutral Layers	2-1
2.1.2 Pollutant Releases into Unstable Layers	2-6
2.2 CALCULATION OF METEOROLOGICAL VARIABLES	2-11
2.2.1 Mixed-Layer Height	2-12
2.2.2 Wind Speed	2-13
2.2.3 Wind Direction	2-14
2.2.4 Potential Temperature Gradient	2-15
2.2.5 Turbulence Intensities	2-16
2.3 PLUME RISE CALCULATIONS	2-17
2.3.1 Momentum Rise	2-17
2.3.2 Neutral/Unstable Buoyant Final Rise	2-17
2.3.3 Neutral/Stable Buoyant Final Rise	2-18
2.4 DISPERSION PARAMETERS FOR STABLE/NEUTRAL CONDITIONS	2-19
2.4.1 Plume Spread Due to Turbulence	2-19

TABLE OF CONTENTS (continued)

2.4.2	Allowance for Source-Induced Effects	2-22
2.5	THE LIFT COMPONENT	2-23
2.5.1	Overview of LIFT	2-23
2.6	THE WRAP COMPONENT	2-31
2.6.1	Overview of WRAP	2-31
2.6.2	WRAP Structure	2-31
2.7	RECEPTORS NOT TREATED BY LIFT OR WRAP	2-37
2.7.1	Receptors Not Influenced by Hills	2-38
2.7.2	Receptors Upwind of the Impingement Point	2-38
2.8	PLUME PENETRATION INTO ELEVATED STABLE LAYERS	2-40
2.9	THE VERTICAL DISTRIBUTION FUNCTION	2-41
2.9.1	The Probability Density Function (PDF)	2-41
2.9.2	Terrain Influences On the PDF	2-47
2.10	TERRAIN INFLUENCE ON MIXING HEIGHT	2-53
2.10.1	Estimate of the Elevated Temperature Gradient	2-55
2.11	THE HORIZONTAL DISTRIBUTION FUNCTION	2-56
3	USER INSTRUCTIONS FOR RUNNING CTDMPPLUS	3-1
3.1	OVERVIEW	3-1
3.2	INPUT DATA REQUIREMENTS	3-6
3.2.1	General Program Specifications	3-7
3.2.2	Terrain Data	3-11
3.2.3	Receptor Data	3-11
3.2.4	Meteorological Profile Data	3-11
3.2.5	Meteorological Surface Data	3-15
3.2.6	Meteorological Rawinsonde Data	3-15
3.2.7	Hourly Emissions Data	3-15
3.3	CTDMPLUS OUTPUT FILES	3-15
3.3.1	CTDMPLUS Output Listing	3-15
3.3.2	Concentration File	3-19
3.4	ADDITIONAL COMPUTER NOTES	3-20
3.5	CTDMPLUS SUBROUTINE STRUCTURE	3-22
4	USER INSTRUCTIONS FOR AUXILIARY PROGRAMS	4-1
4.1	RECEPTOR GENERATOR	4-1
4.2	INTERACTIVE SETUP PROGRAM	4-2
4.3	GRAPHICAL CONCENTRATION DISPLAYS	4-2
4.3.1	CHIRET	4-11

TABLE OF CONTENTS (continued)

4.3.2	CHIDIS	4-11
4.3.3	CONTOUR	4-15
5	INSTRUCTIONS FOR USING THE MENU DRIVER	5-1
5.1	INTRODUCTION	5-1
5.2	USER INSTRUCTIONS	5-1
5.2.1	File Naming	5-1
5.2.2	Directory Setup	5-1
5.2.3	Initiating the Program	5-5
5.2.4	Terrain Preprocessor Programs	5-5
5.2.5	Receptor Generator	5-9
5.2.6	Meteorological Preprocessors	5-9
5.2.7	Running CTDMPLUS	5-12
5.2.8	Concentration Postprocessors	5-15
	References	Ref-1
	Appendix A Details of LIFT and WRAP Algorithms	A-1
	Appendix B Test Case for CTDMPLUS	B-1

FIGURES

2-1	Idealized picture of how the dividing-streamline plane and the plane of stagnation streamlines "cut" into a plume	2-4
2-2	Depiction of plume behavior as it passes over a hill as seen from the side	2-5
2-3	Depiction of plume behavior as it is deflected around a hill as seen from above	2-7
2-4	Depiction of plume behavior as it passes over a hill as seen from above	2-8
2-5	Idealized stratified flow about hills indicating domain of individual CTDMPLUS component algorithms	2-25
2-6	Illustration of the relationship between the crosswind-average concentration profiles at s_0 and s , and the plume from one of the many point-source elements representing the flux of material across the plane at s_0	2-27
2-7	Illustration of terrain effect on the vertical distribution of plume material above H_c as modeled in LIFT	2-29
2-8	Typical streamline patterns in two-dimensional flow around an elliptical cylinder	2-32
2-9	Top view of a plume in two-dimensional flow around a hill	2-34
2-10	Sketch of the flow around an ideal cylinder of elliptical cross-section	2-36
2-11	Treatment of receptors upwind of the impingement point	2-39
2-12	Illustration of the use of image sources to model possible paths	2-43
2-13	Illustration of the bi-Gaussian distribution of P_v	2-45
2-14	Comparison of normalized crosswind integrated concentration contours	2-46
2-15	Illustration of the intercept method used for finding a second estimate of the vertical velocity that carries a parcel in a deformed flow over a hill	2-49
2-16	Illustration of the weighted-average approach	2-50
2-17	Illustration of the linear interpolation method used iteratively	2-51
2-18	Fluid modeling results from Perry and Snyder (1989) showing deflections in the z_i streamline	2-54
2-19	Typical profile of mean potential temperature	2-57
3-1	Interaction among components of the CTDMPLUS system	3-2
3-2	Outline of the main program CTDMPLUS	3-23
3-3	Outline of the subroutine SEQMOD	3-28
3-4	Outline of the subroutine DAYCALC.....	3-30
4-1	Portion of a sample interactive session from the RECGEN program	4-3

FIGURES (continued)

4-2	Receptor display from the interactive RECGEN program	4-4
4-3	Example of a receptor file generated by the interactive RECGEN program	4-5
4-4	Display from a sample session of SETUP: "OPTIONS" input file for METPRO	4-7
4-5	Display from a sample session of SETUP: "PROFILE" input file for METPRO	4-8
4-6	Display from a sample interactive session of SETUP: "SURF1" input file for METPRO	4-9
4-7	Display from a sample interactive session of SETUP: listing of files required by CTDMPLUS	4-10
4-8	Sample interactive session for program CHIRET, a portion of the concentration display postprocessor	4-12
4-9	Sample screen display from the CHIDIS program showing user options for concentration displays	4-13
4-10	Sample screen display from the CHIDIS program showing previously displayed receptors plus the current one and the concentration value	4-14
5-1	Directory setup	5-4
5-2	Screen display from the menu driver system, showing the main selection menu	5-6
5-3	Screen display from the menu driver system, showing the terrain preprocessor menu	5-7
5-4	Sample display from the menu driver system, showing the FITCON options screen	5-8
5-5	Sample screen display from the menu driver system, showing the HCRIT options screen ...	5-10
5-6	Screen display from the menu driver system, showing the meteorological preprocessor menu	5-11
5-7	Sample screen display from the menu driver system, showing the selection of a file for use with METPRO	5-13
5-8	Sample screen display from the menu driver system, showing the list of files selected for use with CTDMPLUS	5-14
5-9	Sample screen display from the menu driver system, showing the concentration postpro- cessor menu	5-16
5-10	Sample screen display from the CONTOUR program, showing the concentration isopleths and hill contours	5-17

TABLES

3-1	Format of the "FOPTIONS" FITCON options file	3-3
3-2	Format of the "HOPTIONS" HCRIT options file	3-4
3-3	Contents of the "CTDM.IN" file	3-8
3-4	Surface roughness length (meters) for land-use types and seasons	3-10
3-5	Format of the "TERRAIN" input data file	3-12
3-6	Format of the "RECEPTOR" input data file	3-13
3-7	Format of user-created "PROFILE" file	3-14
3-8	Format of the "SURFACE" file	3-16
3-9	Format of the "RAWIN" file	3-17
3-10	Variable emissions input format	3-18
3-11	Format of text concentration output file	3-21
5-1	Components in the CTDMPLUS menu driver	5-2
5-2	Standard CTDMPLUS file extensions	5-3

LIST OF ABBREVIATIONS AND SYMBOLS

ABBREVIATIONS

CTDM	Complex Terrain Dispersion Model
CTDMPLUS	Complex Terrain Dispersion Model PPlus Algorithms for Unstable Situations
CWIC	Crosswind Integrated Concentration
ERF	Error Function
EPA	Environmental Protection Agency
GLC	Ground-Level Concentration
HDF	Horizontal Distribution Function
PC	Personal Computer
PDF	Probability Density Function
RTDM	Rough Terrain Diffusion Model
VPTG	Vertical Potential Temperature Gradient

SYMBOLS

α	Major axis length of an ellipse, m (also denoted as L_a)
A_z	Term used in F_z formulation
b	Minor axis length of an ellipse, m (also denoted as L_b)
b_1, b_2, b_3	Factors involved in B_1, B_2 terms in WRAP calculation
B	Function of h/L used in computation of wind direction adjustment with height
B_0	Parameter used in analytical expression for convolution integral I
B_1, B_2	Factors involved in vertical term in WRAP concentration calculation
C	CTDMPLUS modeled concentration ($\mu\text{g}/\text{m}^3$)
d	Stack-top inner diameter, m; also crosswind distance from plume centerline (m)
dQ	Source strength of a point source element (g/s)
$d\theta/dz$	Vertical potential temperature gradient (K/m)
f	Coriolis parameter = $1.458 \times 10^{-4} \cdot \sin(\text{latitude}), \text{sec}^{-1}$
F_b	Buoyancy flux parameter
Fr	Hill Froude number
F, F_b	Buoyancy flux (m^4/s^3)
f_z	Vertical distribution function in Gaussian plume equation
g	Acceleration due to gravity = $9.8 \text{ m}/\text{s}^2$

LIST OF ABBREVIATIONS AND SYMBOLS (continued)

G	Soil heat flux, W/m^2 ; also, a constant used in determining vector wind speed from scalar wind speed and σ_θ ; also denotes Green's function
G_m	Maximum probability of P_w
h	Stable mixed layer height, m; also final plume height, m; also hill height function (m)
h_R	Height of receptor above reference base height (m)
h_R'	Modified height of receptor (relative to plume height) due to terrain effects (m)
h_s	Height of the stack top above the common stack base (m)
H	Height at the top of the hill above common stack base, m; also the sensible heat flux (W/m^2)
H_c	Critical dividing streamline height (m)
i_y	Horizontal component of the turbulence intensity
i_z	Vertical component of the turbulence intensity
I	Convolution integral of Green's function with the hill height function
k	von Karman constant (0.4)
K_y	Eddy diffusivity, horizontal component (m^2/s)
K_z	Eddy diffusivity, vertical component (m^2/s)
l	Mixing length, m; also crosswind distance from plume centerline to receptor (m)
l_n	Mixing length in neutral conditions (m)
l_s	Mixing length in stable conditions (m)
L	Monin-Obukhov length (m)
L_a	Major axis length of an ellipse (m--also denoted as a)
L_b	Minor axis length of an ellipse (m--also denoted as b)
L_n, L_z	Parameters used in analytical expression for convolution integral I
L_x	Length scale of hill in along-wind direction (m)
L_y	Length scale of hill in cross-wind direction (m)
m	Modified inverse length scale = $n(1 + L_x^2/L_y^2)^{1/2}$; also trajectory slope in PDF
n	Ratio of N/u (m^{-1})
N	Brunt-Vaisala frequency (s^{-1})
N_0	Value of N at S_0 (flat terrain value)
P	Plume penetration factor

LIST OF ABBREVIATIONS AND SYMBOLS (continued)

P_w	Probability density function of vertical lift
p	Perturbation pressure (Boussinesq flow)
Q	Emission rate (g/s)
r	Ratio of ellipse major axis length to minor axis length, $r = a/b$
R	Displacement from a reference point, m; ($R^2 = x^2 + y^2 + z^2$)
R_i	Richardson number
R_L	Parameter used in analytical expression for convolution integral I
s, S	Square of the Brunt-Vaisala frequency; stability parameter (s^{-2})
s_0	Downwind distance at which the plume impinges upon or is deflected by terrain (m)
S_T	Speed of the incident flow at the tower location (u_T, v_T), (m/s)
S_w	Speed of the incident flow approaching a hill (m/s)
t	Travel time (s)
T_a	Ambient air temperature (K)
T_h	Factor for streamline distortion in the vertical (height correction factor)
T_L	Distortion factor due to terrain effects in the horizontal direction
T_L	Lagrangian time scale (s)
T_{L0}	Value of T_L at s_0 (flat terrain value), (s)
T_s	Stack gas temperature (K)
T_u	Factor for wind speed distortion due to terrain influences
T_y	Terrain-effect factor equal to ratio of σ_y^*/σ_y^*
T_z	Terrain-effect factor equal to ratio of σ_z^*/σ_z^*
T_{σ_v}	Terrain-effect factor equal to ratio of σ_v/σ_{v0}
T_{σ_w}	Terrain-effect factor equal to ratio of σ_w/σ_{w0}
U	Total scalar wind speed (m/s)
u	Scalar wind speed, along-flow component (m/s)
u_*	Friction velocity (m/s)
u_g	Geostrophic wind speed (m/s)
u_s	Stack-top wind speed (m/s)
u_v	Vector wind speed (m/s)

LIST OF ABBREVIATIONS AND SYMBOLS (continued)

u', v', w'	Perturbation wind velocities (Boussinesq flow) in downwind, crosswind, and vertical directions, respectively (m/s)
u	Cross-flow wind speed component (m/s)
w	Vertical component of the wind speed (m/s)
\hat{w}	Mode of vertical wind component (m/s)
w_*	Convective velocity scale (m/s)
w_d	Mean downdraft velocity in unstable conditions (m/s)
w_s	Stack gas exit velocity (m/s)
X	Non-dimensional alongwind distance
x	Alongwind coordinate (m)
x_0	Alongwind coordinate at S_0 , the impingement point of the approach flow on the hill (m)
x_m	Length parameter used in analytical expression for convolution integral I
x_r, y_r, z_r	Position in space of the receptor
x_s, y_s, z_s	Position in space of the plume release
y	Distance in cross-wind direction (m)
y_R	Crosswind distance of receptor from plume centerline (m)
Y_R'	Modified crosswind distance of receptor from plume centerline due to terrain effects (m)
z	Measurement height, m ; also receptor height (m)
z_0	Surface roughness length (m)
z_b	z_i - stack height (m)
z_i	Convective (daytime) mixed layer height (m)
z_m	Height of a streamline above the base of the hill far upwind (m)
z'	Height above terrain surface (m)
α	Wind speed shear (vertical component) (s^{-1})
α_1, α_2	Parameters used in analytical expression for convolution integral I
α_w	Direction of the incident flow approaching a hill (deg)
β	Strain function from theory of Hunt and Mulhearn (1973) used in computation of T_y, T_z , also, rotation angle between wind flow and stagnation streamline; also the asymmetry factor in the PDF model
δ_z	Vertical deflection experienced by a streamline due to terrain influences (m)
$\Delta\alpha$	Wind direction change within the mixed layer (degrees)

LIST OF ABBREVIATIONS AND SYMBOLS (continued)

Δh	Plume rise (m)
ϵ	Variable used to relate between scalar and vector wind speeds, a function of σ_θ
$\Delta \theta$	Jump in potential temperature at the top of the mixed layer (K)
η	Height of a streamline above the surface of the hill; also denotes deflection of streamlines in the vertical (Appendix A)
γ	Constant of proportionality between the mixing length in a stable atmosphere and σ_w/N ; $\gamma = 0.52$
Γ	Constant of proportionality between the mixing length in a neutral atmosphere and z ; $\Gamma = 0.36$
μ, ν	Elliptical coordinates
μ_0	Value of μ along the boundary of an ellipse
μ_s, ν_s	Elliptical coordinates of the source
μ_T, ν_T	Elliptical coordinates of the point where wind speed and direction are measured (tower)
ϕ_T	Wind direction measured at the tower location (μ_T, ν_T), (m/s)
Ψ_m	Stability correction for wind profile formulation in the surface layer
Ψ_s	Stream function through the source
ρ_0	Initial unperturbed fluid density in Boussinesq flow
σ	Generic representation of either σ_y or σ_z due to ambient turbulence (m)
σ_{tb}	σ_y, σ_z due to buoyancy-enhanced dispersion (m)
σ_{ts}	σ_y, σ_z due to source-induced turbulence (m)
σ_θ	Standard deviation of wind direction (deg)
σ_v	Standard deviation of the crosswind component of the wind speed (m/s)
σ_{v0}	Value of σ_v at s_0 (flat terrain value)
σ_w	Standard deviation of vertical wind speed (m/s)
σ_{w0}	Value of σ_w at s_0 (flat terrain value)
σ_y	Crosswind distance from plume centerline in a Gaussian plume at which the concentration falls to $e^{-1/2}$ of the value at the plume centerline, m
σ_{y0}	Value of σ_y at s_0 (m)
σ_y^*	Growth in σ_y between s_0 and the receptor position of interest for flat terrain (m)
σ_y^*	Growth in σ_y between s_0 and the receptor position of interest with terrain influences considered (m)

LIST OF ABBREVIATIONS AND SYMBOLS (continued)

σ_{ya}	σ_y due to ambient turbulence, accounting for terrain-influenced changes in turbulence parameters (m)
σ_{ye}	Effective σ_y , accounting for effect of strain in the flow over terrain on horizontal diffusion
σ_z	Vertical distance from plume centerline in a Gaussian plume at which the concentration falls to $e^{-1/2}$ of the value at the plume centerline (m)
σ_{zo}	Value of σ_z at s_o (m)
σ_z^*	Growth in σ_z between s_o and the receptor position of interest for flat terrain
σ_z^{**}	Growth in σ_z between s_o and the receptor position of interest with terrain influences considered (m)
σ_{za}	σ_z due to ambient turbulence, accounting for terrain-influenced changes in turbulence parameters (m)
σ_{ze}	Effective σ_z , accounting for effect of strain in the flow over terrain on vertical diffusion
Θ	Potential temperature (K)
θ_o	Surface potential temperature (at $z = 0$) (K)
θ_m	Mean potential temperature of the mixed layer (K)

ACKNOWLEDGEMENTS

The authors wish to thank the following contributors to the development of CTDMPLUS: Katherine A. Brehme, Gary A. Briggs, William H. Snyder, Nicholas Z. Karasek, Ronald E. Stogner, and Kenneth J. Galluppi. For their contributions to this expanded and improved user's manual, we also thank David J. Sullivan, Jeanne R. Eichinger, Christine D. Rafferty, Kathleen Rea, Francis Pooler, and Thomas Pierce.

Special thanks are extended to Francis A. Schiermeier, Peter L. Finkelstein, and all the members of the EPA CTDM Technology Transfer Work Group for their steady support of the efforts to extend and improve CTDM.

The authors of the original CTDM User's Guide wish to identify two important contributors to the development of the CTDM code. During the formative stage of the effort, Akula Venkatram identified and developed the two-layer approach that remains a central feature of CTDMPLUS. His guidance and insight in the development of the theoretical basis of the model greatly contributed to its technical integrity. Donald DiCristofaro produced much of the code for the earlier versions of CTDM, and his participation in the many revisions to that code helped to maintain its clarity and efficiency.

SECTION 1

INTRODUCTION

1.1 BACKGROUND

The Complex Terrain Model Development (CTMD) project was initiated by the U.S. Environmental Protection Agency (U.S. EPA) to develop a practical, refined plume model for elevated point sources near complex terrain. Accomplishments of this model development project are summarized by Strimaitis et al. (1987). The major result of this effort was the Complex Terrain Dispersion Model (CTDM), which was completed and released to the user community in early 1988.

Nighttime, stably-stratified conditions are generally associated with maximum short-term impacts from elevated sources in complex terrain, as concluded by participants of an EPA workshop (Hovind et al., 1979). CTDM was developed primarily to model these conditions.

However, since many air quality standards are written for averaging periods that generally include daytime/unstable conditions, additional algorithms for estimating impacts from elevated sources in complex terrain during unstable/convective conditions have been developed and integrated with CTDM to form CTDMPLUS (CTDM PLUS Algorithms for Unstable Situations). CTDMPLUS also includes several features designed to improve user friendliness.

CTDMPLUS differs from currently available complex terrain models in the following areas:

- In stable/neutral conditions, the structure of the two-layer flow (above/below the dividing-streamline height, H_c) is explicit in the formulation, and plume material that straddles the interface remains in the respective layers (the plume is not treated as if it were all in one layer or the other). Above H_c , the material is deflected and distorted, and the rate of dispersion is altered. Below H_c , the stagnation streamline divides the flow, and only material that diffuses onto the stagnation streamline is able to reach the surface of the hill. The stagnation streamline and the concentration pattern wrap around the terrain. Plumes that lie to one side of the stagnation streamline pass around the terrain.
- The rate of plume growth depends on the turbulence and, in the case of σ_z , it also depends on the degree of stratification. Sector averaging in the lateral direction is not used.
- For plumes released into daytime convective layers, a probability density function (PDF) approach is used to describe the vertical distribution of pollutants, and convective scaling concepts are utilized to parameterize the lateral dispersion coefficient. CTDMPLUS considers the effect of terrain on pollutant trajectories and on mixed-layer height deflections.

- Partial plume penetration into elevated stable layers is considered.
- The three-dimensional nature of the terrain is used in the flow distortion calculations.
- Vertical variations of windspeed, wind direction, and turbulence intensities are determined through either interpolation of input measurements or surface layer scaling.

1.2 MODEL APPLICABILITY AND TECHNICAL LIMITATIONS

CTDMPLUS is a point-source Gaussian¹ plume dispersion model designed to estimate hourly-averaged concentrations of plume material at receptors on or near isolated terrain features. Although multiple sources and multiple terrain features are modeled by CTDMPLUS, the plumes impinging on a downwind "hill" are assumed to be influenced by upwind features only in the effects found in the on-site meteorological measurements.

The following restrictions and assumptions about CTDMPLUS should be understood:

- CTDMPLUS contains no wake algorithms for simulating the mixing and recirculation found in cavity zones in the lee of a hill. Therefore, sources within the lee of terrain features will not be modeled with consideration given to wake effects. Estimates of concentrations at receptors in the lee will not be reliable when such zones are present.
- The path taken by a plume through an array of hills cannot be simulated. The model relies on measurements of the flow obtained in the neighborhood of the source to define the incident flow field for each of the terrain segments independently. If there is a strong channelling of the flow due to large-scale terrain features (e.g., a valley setting), then this influence is reflected in the modeling only insofar as it is to be contained in the meteorological measurements. Any changes to the plume size caused by one hill are not carried forward to subsequent simulations downwind. For situations when an individual hill is difficult to isolate from a complex terrain structure, CTDMPLUS results may not be reliable.
- Real terrain features are approximated by ideal shapes (determined by the terrain preprocessor). CTDMPLUS considers elliptically-shaped horizontal contours and overall Gaussian shaped (vertical profile) hills.
- CTDMPLUS does not simulate calm meteorological periods. Therefore, under these conditions, either no concentrations are estimated or (at the user's option) the following assumptions about plume height variables are made in order to provide modeled concentrations:

¹ A skewed bi-Gaussian PDF approach is used in unstable conditions in describing the vertical pollutant distribution.

1. Minimum scalar wind speed = 1.0 m/s
2. Minimum σ_z = 0.2 m/s
3. Minimum σ_w = 0.01 m/s

These minimum values are discussed further in Section 2.2.

- CTDMPPLUS assumes that the meteorological data are representative of the entire averaging period, and apply to the entire spatial domain. Spatial variability resolved by an array of meteorological towers cannot be used directly in the model.
- Hill slopes are assumed not to exceed 15°, so that the linearized equations of motion for Boussinesq flow (described in Appendix A) are applicable.

These restrictions are consistent with the primary purpose of the model, namely, that of estimating pollutant concentrations on nearby downwind terrain.

1.3 OVERVIEW OF CTDMPPLUS SOFTWARE COMPONENTS

The package contains:

- CTDMPPLUS (transport and diffusion model)
- a terrain preprocessor (Mills et al., 1987)
- a meteorological preprocessor (Paine, 1987)
- a receptor coordinate generator
- graphical concentration display programs

Section 3 describes the interaction of these programs in detail. In addition, the system includes:

- a PC-based menu driver that enables the user to select pre-existing files for use with the programs in CTDMPPLUS, run the programs, and view output files
- an interactive program that allows the user to modify model input files easily and run CTDMPPLUS in a case-study mode.

All of the programs, except the three graphics programs (PLOTCON, RECGEN, and CHIDIS), are written in FORTRAN 77. The graphics programs and menu driver are written in Pascal.

1.3.1 Terrain Preprocessor

The CTDMPPLUS user must first define terrain elements to be modeled as discrete hills [see discussion in Appendix A of the terrain preprocessor user's guide (Mills et al., 1987)]. An (x, y) origin point

must also be established prior to contour digitization so that the locations specified for the stacks, meteorological tower, hills, and receptors are consistent. A file containing (x , y) points along hill contours must then be generated for each hill (see Table 1 of the terrain preprocessor guide for the format of this file). The spacing between the points should be small enough so that the orientation and shape of each contour is accurately represented. The contour digitization method is left to the user's discretion; a graphics pad can be used or the map can be sent to a vendor that specializes in digitization work.

The CTDMPLUS terrain preprocessor consists of two programs that process digitized contour data to provide hill shape parameters in a format suitable for direct input to CTDMPLUS, and a third program that displays the results (see the terrain preprocessor manual for complete description and user instructions). The first program, FITCON, evaluates and edits each contour and processes the data by numerical integration to determine the following parameters for an equivalent ellipse: semi-major and semi-minor axis lengths, contour centroid coordinates, and the orientation of the ellipse.

These parameters are input to the second terrain preprocessor program, HCRIT, which determines, for the portion of the hill above several given elevations, the best-fit inverse-polynomial (vertical) profiles along the hill major and minor axes. The center coordinates of the fitted hill are calculated as the mean of the ellipse center coordinates for those contours above a given critical elevation. The orientation of the fitted hill is calculated as a vector average of the ellipse orientations weighted by the ellipse eccentricity. HCRIT provides an input file for CTDMPLUS that contains the following information for each critical elevation:

- Ellipse parameters corresponding to the contour at a critical elevation
- Coordinates of the center of the fitted hill
- Orientation of the major axis of the fitted hill with respect to north
- The length scale and exponents for the inverse polynomial fits along the hill major and minor axes.

CTDMPLUS uses the contour representations to provide hill shape information above the critical dividing streamline height for each hour and each hill using interpolation between values specified at "critical" elevations.

The third program, PLOTCON, generates the following screen displays to aid in the evaluation of the hill fitting process:

- Map of the digitized input contours
- Map of digitized contours that have been qualified and edited

- Map of the digitized contours and their associated fitted ellipses
- For each critical elevation, a map showing the digitized contours and the contours of the fitted hill at elevations corresponding to the elevations of these digitized contours that are above the critical elevation.

1.3.2 Meteorological Preprocessor, METPRO

The CTDMPLUS meteorological preprocessor, METPRO, uses on-site measurements of wind, temperature, turbulence, and surface characteristics to provide predicted values of the nocturnal surface layer height, h , or the daytime mixed-layer height, z_i and computed values of the surface friction velocity, u_* , the Monin-Obukhov length, L , and surface roughness length, z_0 . These values allow CTDMPLUS to estimate profiles of wind, temperature, and turbulence above and below the range of measurements.

METPRO has four modes of operation:

- Mode 0: Run for one or a few nighttime (stable) hours (surface characteristics such as surface roughness, albedo, and Bowen ratio are assumed to be constant for all model hours); no off-site or upper air data files are required.
- Mode 1: Run for any number of stable hours that need not be contiguous, such as only nighttime hours for several days; no off-site or upper air data are required, but site characteristics are allowed to vary each hour.
- Mode 2: Same as Mode 1, but off-site surface data are read to obtain cloud cover data.
- Mode 3: Run for a series of contiguous hours that must come in blocks of complete calendar days, although the days need not be contiguous; off-site and upper air files are required.

Input requirements are the least for Mode 0 and the most extensive for Mode 3. Mode 3 features the determination of convective mixing heights, a computation that requires input for an entire day at a time. The other modes do not compute this figure, but do provide all other variables.

The METPRO preprocessor output is an ASCII file that is read in by CTDMPLUS. The distinct, modular nature of this method of processing input data for CTDMPLUS makes it possible for a user to substitute an alternative meteorological preprocessor as long as the output format of "SURFACE" is the same as if it were produced by METPRO. METPRO is described in detail in a separate user's guide (Paine, 1987).

1.3.3 Receptor Generator, RECGEN

The receptor generator program, RECGEN, is an interactive program written in Pascal that computes receptor coordinates along selected contours. The program creates a file containing the receptor information directly input to CTDMPPLUS (file "RECEPTOR"). RECGEN also displays the contour lines and receptor locations on the monitor screen. The user can easily add receptors, in addition to those produced by RECGEN, using a text editor.

RECGEN reads the output plot file from the terrain preprocessor FITCON. For each contour, the user has the choice of (1) supplying a fixed receptor spacing along the contour, (2) supplying a fixed number of receptors to be generated along the contour, or (3) having no receptors on the contour. RECGEN is described in greater detail in Section 4.1.

1.3.4 Complex Terrain Dispersion Model Plus Algorithms For Unstable Situations, CTDMPPLUS

The main CTDMPPLUS program performs the plume transport and dispersion calculations for the entire period of simulation. It takes the files prepared by the meteorological and terrain preprocessors, together with the source, receptor, and (if necessary) rawinsonde and emission files, and executes under the control of the options specified in an input file named "CTDM.IN". Modeled concentrations can be stored in a binary or an ASCII output file, "CONC", if desired. The model lists all of the control data describing the simulation, and pertinent source, receptor, and terrain data, to the file "CTDM.OUT". In case-study mode, extensive tables of selected variables are also listed for computations performed for each source, hill, and receptor. Technical aspects of CTDMPPLUS are described in detail in Section 2 and Appendix A; user instructions are described in Section 3.

1.3.5 Interactive Setup Program, SETUP

The interactive setup program allows the user to create or modify existing input files for METPRO and CTDMPPLUS. The program uses the explicit input file names required by METPRO and CTDMPPLUS in its search for existing files. Files that can be modified are "OPTIONS", "SURF1", and "SURF2" for input to METPRO; "CTDM.IN", "SURFACE", and "TERRAIN" for input to CTDMPPLUS; and "PROFILE", which is input to both programs. Of course, all METPRO and CTDMPPLUS input files can also be created and edited by the user with any text editor that creates ASCII files.

The interactive setup program creates a batch stream to execute system commands such as renaming and deleting files and executing the programs. Therefore, this program may not be directly portable between operating systems. The interactive setup program is described in detail in Section 4.2.

1.3.6 Concentration Postprocessors

There are three concentration postprocessor programs: CHIRET, CHIDIS, and CONTOUR. CHIRET processes the receptor and concentration information and creates a file used by CHIDIS and CONTOUR. CHIDIS and CONTOUR can be used to display predicted concentrations from CTDMPPLUS on a map of hill contours. Concentrations for a series of hours can be displayed sequentially, but each hill must be done individually.

CHIDIS is a Pascal program that will draw the hill contours and provide a spatial display of concentrations for each hour. For a given hour, the receptor with the highest concentration is displayed as a blinking, filled circle. The user can continue to display receptor locations in descending order of predicted concentration. The current receptor blinks and all the previous receptors are displayed as non-blinking filled circles. Information about the current receptor can be presented at the top of the plot if desired.

CONTOUR is a Pascal program that grids the concentration and receptor data and draws concentration isopleths on a background of hill contours. CONTOUR is a part of the menu driver and is not a stand-alone program.

CHIRET and CHIDIS are described in Section 4.3; CONTOUR is described in Section 5.2.8.

1.3.7 Menu Driver Program, DRIVEIT

DRIVEIT is a menu driver program, written in Pascal, that displays lists of available files, prompts the user to choose the necessary files to run the various programs in CTDMPPLUS, and executes the desired program. The user is led through the file selection process and responses are evaluated to detect potential errors which can be viewed in the diagnostic output file. The menu driver requires that file names have certain extensions and be located in specific directories. The menu driver is described in detail in Section 4.4.

1.4 CTDMPPLUS COMPUTER CONSIDERATIONS

1.4.1 Software Considerations

The complete CTDMPPLUS package is designed to be run on an IBM[®]-compatible personal computer (PC) system. However, all the essential portions can be satisfactorily run on other computer systems. Most of the programs are written in ANSI standard FORTRAN 77 and should therefore be compiler independent. The PC-based executables were created using the Ryan-McFarland RM/FORTRAN[™] compiler. Three programs, PLOTCON, RECGEN, and CHIDIS, are written in Pascal and were compiled with Borland International Turbo Pascal[®]. Finally, a text editor capable of creating ASCII input files is needed.

1.4.2 Hardware Limitations

With the exception of a math co-processor chip, the programs that are included in the modeling system require no special hardware in order to run. Attempts to run the modeling system without a math co-processor will cause a runtime error number of 4001. The graphics programs use a procedure that automatically detects the graphic system being used and scales the screen output accordingly. The largest program, CTDMPPLUS, requires a core space of about 360K bytes. When this program is run with the menu driver, a core space of 640K bytes is required.

The terrain preprocessor requires input of digitized terrain information that can be obtained either from an outside vendor or by using a graphics board.

The interactive setup program (SETUP), which is a FORTRAN 77 program, is designed for a PC MS-DOS[®] operating system, in that file manipulation commands are based on MS-DOS[®]. With some minor modifications, SETUP could be made to run on other computer systems.

SECTION 2

TECHNICAL DESCRIPTION

This section contains a description of the basic theoretical components of CTDMPLUS, and provides the user with an overview of the subroutine structure in the code. An overview of the model is first presented in subsection 2.1. Subsection 2.2 discusses the calculation of meteorological variables at plume height. Subsection 2.3 describes the methods of computing plume rise. Subsections 2.4 through 2.7 refer to the modeling approach for stable/neutral conditions: 2.4 contains information on dispersion coefficients; 2.5 describes LIFT, the part of CTDMPLUS that computes concentrations at receptors in that part of flow that is neutral or weakly stratified; 2.6 describes WRAP, the portion of CTDMPLUS that computes concentrations at receptors in the strongly stratified part of the flow; and a brief note about receptors which are not located on hills is contained in Subsection 2.7. Subsections 2.8 through 2.11 refer to model components for computations in unstable conditions. Subsection 2.8 discusses plume penetration into elevated stable layers; 2.9 describes the probability density function (PDF) model of the vertical pollutant distribution and adjustments for terrain; 2.10 describes the terrain adjustments to the daytime mixed layer height and their relationship to the PDF model; and 2.11 describes the horizontal distribution function and lateral dispersion coefficient.

2.1 OVERVIEW OF THE COMPLEX TERRAIN DISPERSION MODEL PLUS ALGORITHMS FOR UNSTABLE SITUATIONS (CTDMPLUS)

CTDMPLUS is a point-source steady-state plume dispersion model designed to estimate hourly-averaged concentrations of plume material at receptors near an isolated hill or near a well-defined segment of an array of hills. Emphasis is given to simulating situations in which the flow is toward the terrain, and in which maximum concentrations are expected on either the windward side of the impacted terrain or near the terrain crest. The original model (developed under contract with Environmental Research and Technology (ERT) Inc. and named CTDM) was designed primarily to model the important situation of stable plume impaction on the windward side of terrain. The model has since been expanded with compatible algorithms to model all stability conditions, thus permitting the computation of concentration impacts over continuous diurnal periods. The new model components were developed and incorporated without alterations to the original CTDM methods. Therefore, CTDMPLUS will produce concentrations identical to those from CTDM for releases into stable or neutral layers.

2.1.1 Pollutant Releases into Stable/Neutral Layers (An Overview)

In stable/neutral conditions, CTDMPLUS retains the Gaussian formulations of CTDM. The Gaussian plume model for simulating the dispersion of pollutants from a continuous point-source describes a

plume by its average properties as a function of distance along the flow downwind of the point of release. The concentration of material in the plume is prescribed by a Gaussian distribution in a plane perpendicular to the flow. The vertical distribution in this plane has a length scale denoted as σ_z , and the lateral distribution has a scale denoted as σ_y . Complete reflection of the plume at the ground assures that no plume material disappears from the atmosphere. The concentration of plume material at any point downwind of the source is determined by the size of the plume (σ_y and σ_z), the wind speed, the strength of the source, and the distance of the sampling point from the axis of the plume. For example, if the plume is narrow in the vertical (σ_z is substantially less than the height of the axis of the plume), the peak concentration is found right at the center of the plume. Sampling points away from the center detect lower concentrations. Over level ground, peak ground-level concentrations are found when σ_z is of the same order as the height of the plume.

When a hill is present, the path of the plume changes as it flows over or around the hill causing a shift in the relative position of a receptor and the center of the plume. But there are also mechanisms for changing the rate at which the material diffuses toward the surface, and for allowing the center of the plume to impinge on the surface of the hill. These mechanisms are generally responsible for increasing peak concentrations expected over terrain beyond those concentrations that would have been expected for the same meteorological conditions over flat terrain.

In the absence of stratification, all streamlines in the flow pass over a hill. The centerline of a plume in this flow follows the streamline that passes through the source of that plume. As the plume grows in the vertical and horizontal directions (in the plane perpendicular to the flow), plume material diffuses across adjacent streamlines, eventually reaching the set of streamlines that marks the surface of the terrain. Distortions in the flow which are induced by the hill change the position and relative spacing of the streamlines from their initial distribution, and therefore change the shape of the plume as it passes over the hill. As a result, ground-level concentrations (GLCs) of plume material change in two ways: The first and most obvious change in the GLCs is the shift in the distribution on the surface of the hill, arising from the change in the shape of the plume. Typically, the plume stretches in the horizontal as it passes over the crest of a simple three-dimensional hill and this stretching produces a wider "footprint" over the hill. The second change in the GLCs is the change in magnitude, arising from the effect of the distortion on the rate of diffusion of plume material across streamlines. Typically, spacing between streamlines is reduced in the vertical and expanded in the horizontal, while the speed of the flow increases over the crest. These changes tend to increase the diffusion in the vertical and reduce it somewhat in the horizontal, thereby altering the magnitude of the GLCs over the hill. If the diffusion were not altered by the distortion in the flow, the peak concentration would not change from the flat terrain value.

The nature of the flow changes dramatically when the flow is very stably stratified. A two-layer structure develops in which the flow in the lower layer primarily deflects around the hill, while the flow in the upper layer travels over the top of the hill. A critical height H_c defines the boundary of these two layers in CTDMPLUS. This concept was suggested by theoretical arguments of Drazin (1961) and Sheppard (1956) and was demonstrated through laboratory experiments by Riley et al. (1976), Brighton (1978), Hunt and Snyder (1980), Snyder et al. (1980), and Snyder and Hunt (1984). In the layer above H_c , the approach flow has sufficient kinetic energy to transport a fluid parcel up and over the hill against the density gradient of the ambient stratification. In the layer below H_c , the approach flow has insufficient kinetic energy to push the parcel over the hill, so the flow below H_c is restricted to lie in a nearly horizontal plane, allowing little motion in the vertical. Consequently, plume material below H_c travels along and around the terrain rather than over it.

Above H_c , the flow is similar to that just described above although the degree of distortion depends on the stratification. Below H_c , the flow is approximated as an ideal, steady, two-dimensional flow. Within this flow, only one streamline at each elevation touches and follows the surface of a hill, and is referred to as the stagnation streamline. Plume material reaches the surface of the hill only if it reaches the stagnation streamline. If the plume centerline lies along the stagnation streamline and if it also lies below H_c , the center of the plume impinges on the hill. But if it lies to one side of the stagnation streamline, the centerline will pass to one side of the hill.

The position of H_c and the stagnation streamline relative to the centerline of the plume dominates the degree to which a hill in stratified flow is able to alter the peak ground-level concentration obtained in the absence of the hill. Figure 2-1 illustrates this. In the model, the H_c surface slices the plume into two pieces as the hill is encountered. Plume material now residing below H_c is sliced once again by the stagnation streamline. Concentrations on the surface of the hill above H_c are determined by the cut made by the H_c surface because this now coincides with the bottom of the plume, which is in contact with the surface. Concentrations on the surface of the hill below H_c are determined by the cut made by the plane of the stagnation streamline because this cut coincides with the sides of the plume segments that are in contact with the surface of the hill. As illustrated, receptors on the hill "see" concentrations that are much nearer the center of the plume than do receptors in the absence of the hill. Figures 2-2 and 2-3 provide further insight into how the plume is modeled by CTDMPLUS in stable to neutral layers.

Figure 2-2 addresses plume material above H_c . The upper portion illustrates what the plume may actually look like in vertical cross-section as it travels along the surface. Material below H_c is removed at s_0 , and the remaining material is distorted in the flow and reflected from the surface of the hill. The size of the plume in the vertical at s depends on the amount of distortion in the shape of the plume as well as the

PLUME CROSS-SECTION

LOOKING DOWNWIND

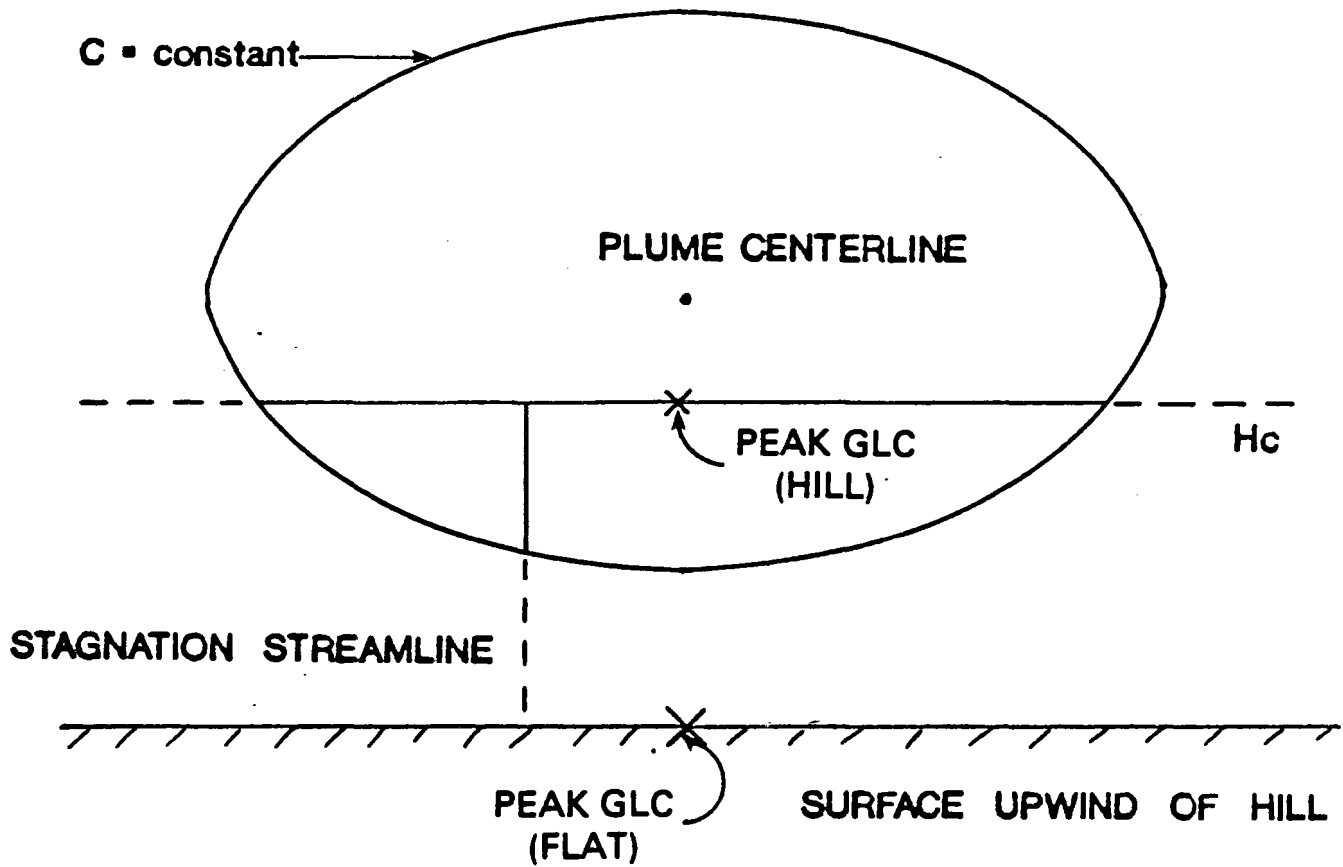


Figure 2-1. Idealized picture of how the dividing-streamline H_c plane and the plane of stagnation streamlines "cut" into a plume, allowing material nearer the center of a plume to contact the surface of a hill.

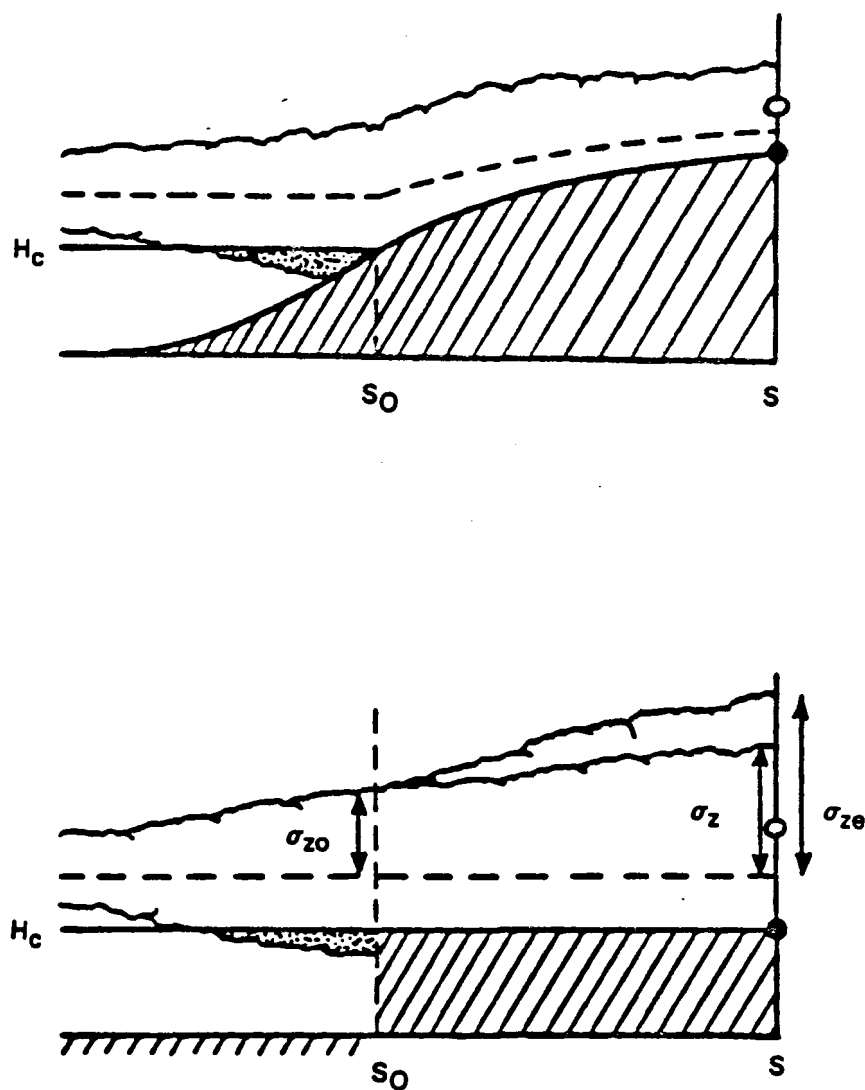


Figure 2-2. Depiction of plume behavior as it passes over a hill as seen from the side: upper figure shows actual plume path, bottom figure shows treatment within CTDMPPLUS with all ground-level receptors placed upon a flat surface of height H_c above stack base and the plume with an effective $\sigma_z = \sigma_{ze}$.

amount of additional growth of the plume caused by changes to the rate of diffusion. The lower portion of Figure 2-2 illustrates how the model actually treats the plume. Reflection of plume material from the surface ($z = 0$) is allowed from the source to s_0 , and reflection of plume material above H_c is allowed from the surface $z = H_c$ beyond s_0 . Furthermore, the distortion in the flow (and the plume) beyond s_0 is scaled out, leaving only the effect of the distortion on the diffusivity in what is termed the effective sigma-z (σ_{ze}). As illustrated, σ_{ze} exceeds σ_z , the plume size in the absence of the hill, because the diffusion in the vertical across streamlines is increased by the contraction in the vertical spacing of the streamlines.

Figure 2-3 addresses plume material below H_c . The diagram on the left illustrates the plume in horizontal cross-section as it splits and flows around a hill. In this case, some plume material has crossed the stagnation streamline before the hill is encountered, so plume material is found on both sides of the hill. Once the plume wraps around the leading edge of the hill, the stagnation streamline (which forms the boundary of the hill) becomes a reflecting surface in addition to the plane $z = 0$, and material cannot diffuse from the segment of the plume on one side of the hill to the segment on the opposite side. The diagram on the right side of Figure 2-3 illustrates how the model treats this flow. The actual surface of the hill is replaced by a line in the plume which corresponds to the stagnation streamline cut in Figure 2-1. All distortion is scaled out as was done for the flow above H_c , and the effect of the distortion on lateral diffusion is ignored as a second order effect. The lateral position of all receptors below H_c essentially collapses onto the stagnation streamline, as depicted by the points labeled A and B, so that each is the same distance from the plume centerline. However, concentrations along one side of the line differ from those on the other side because diffusion through the line is not allowed.

Adjusting receptor positions while keeping the trajectory of the plume a straight line simplifies the mathematics of CTDMPPLUS a great deal. Rather than keeping track of the actual boundary of a hill and the deformed trajectory of each of the segments of the plume as in the left portion of Figure 2-3, concentrations are computed at receptor points A and B for a plume geometry like that of the right portion of Figure 2-3, which is only slightly more complicated than that for flat terrain. A similar adjustment of receptor positions is employed for receptors above H_c , as illustrated in Figure 2-4. The upper portion of the figure shows how a plume in the flow above H_c distorts over a hill as viewed from above. Three streamlines are marked, the centerline of the plume, and streamlines passing through receptors A and B. When the deflection of each streamline is removed, and the distortion in the plume is scaled out, an equivalent plume-receptor geometry is obtained, as illustrated in the lower portion of the figure.

2.1.2 Pollutant Releases into Unstable Layers (An Overview)

The methodologies employed in CTDMPPLUS for modeling releases into unstable layers (where the Monin-Obukhov length is negative) are designed to take advantage of our recent understanding of turbu-

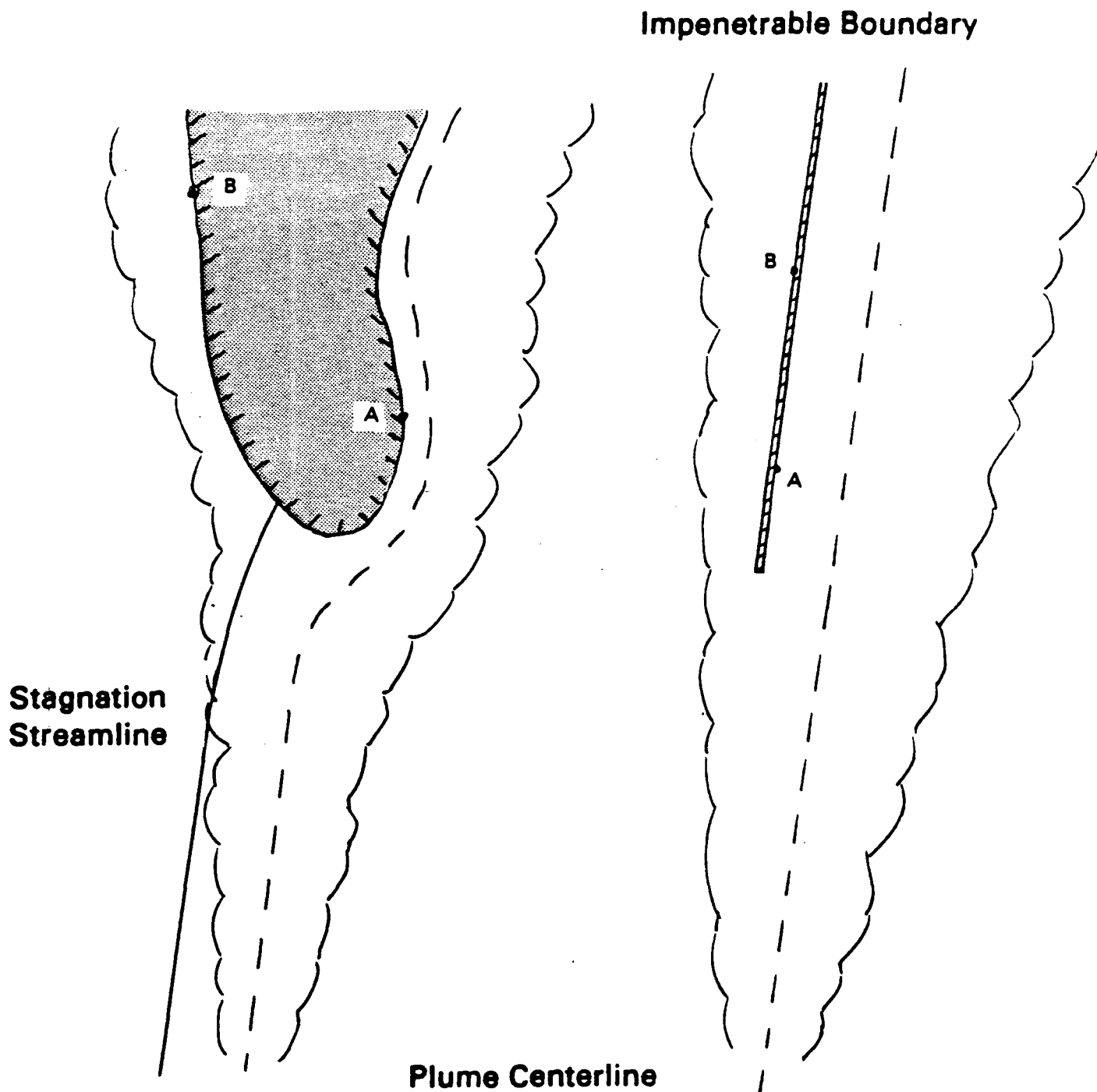


Figure 2-3. Depiction of plume behavior as it is deflected around a hill as seen from above: the stagnation streamline in the left figure separates flow going around the right and left sides of the hill. In CTDMPPLUS, the hill is treated as being collapsed into an impenetrable wall (right figure) that separates the flow and plume material going on either side of the hill, with an effective crosswind distance and σ_y .

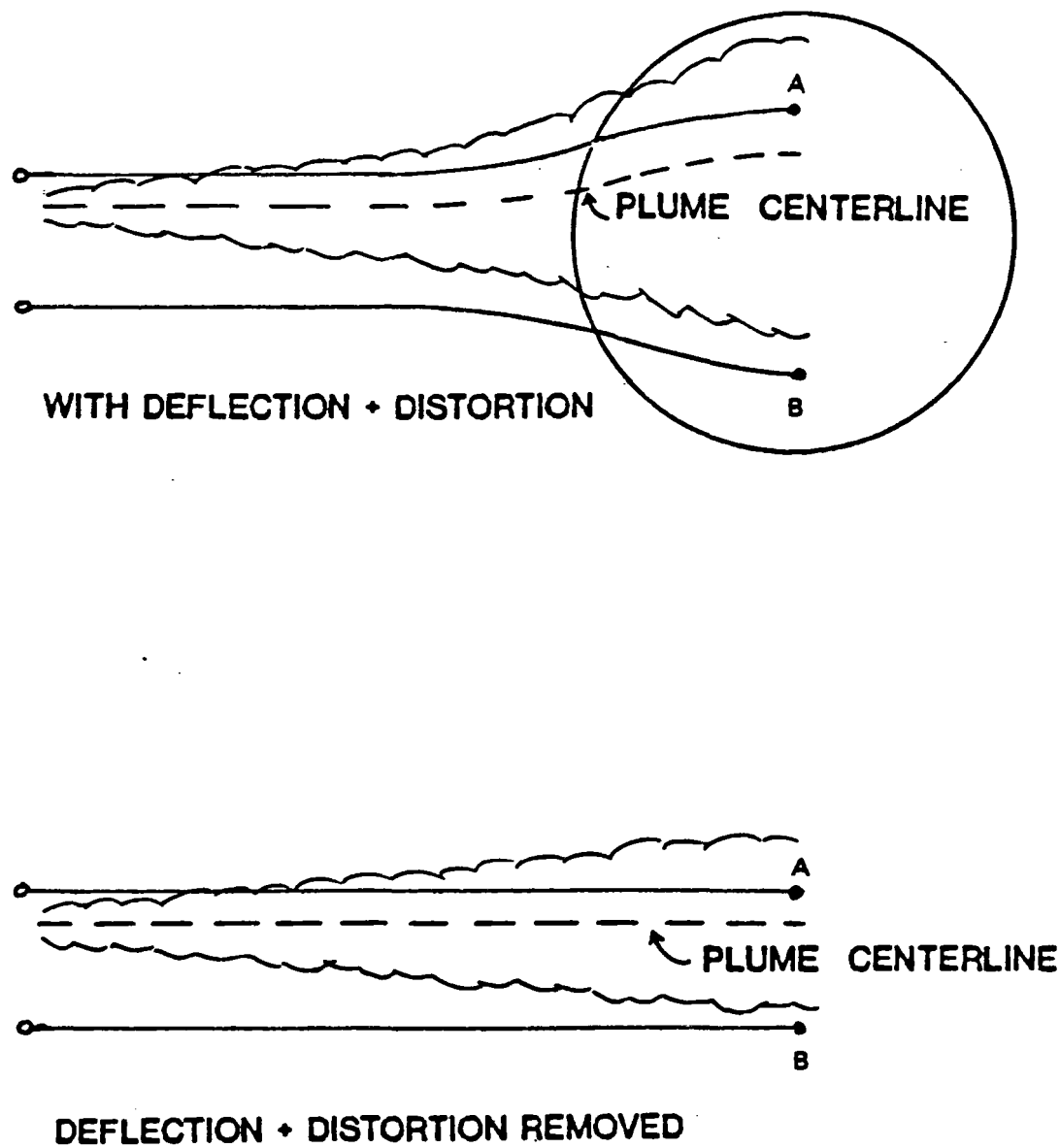


Figure 2-4. Depiction of plume behavior in CTDMPLUS as it passes over a hill as seen from above: upper figure shows actual deflection and distortion of the plume, bottom figure shows treatment within CTDMPLUS with source-receptor spacing equal to spacing between streamlines upwind of hill and appropriate adjustment of effective σ_y .

lence and diffusion in convective boundary layers as outlined in the literature over the past two decades. At the same time, compatibility with the original CTDM is maintained in order to utilize that existing technology and to minimize additional user input requirements.

The CTDMPLUS algorithms for unstable conditions focus on the following areas: 1) plume rise in unstable conditions; 2) buoyant plume penetration into an elevated stable layer; 3) application of a probability density function (PDF) approach to define the vertical pollutant distribution with use of the original CTDM flow module to calculate flow distortion by terrain; 4) terrain adjustments to the mixed-layer depth (based on recent fluid modeling studies) and associated effects on the flow in the mixed layer; and 5) lateral dispersion parameters based on convective scaling concepts.

Unstable plume rise in CTDMPLUS is calculated with methods suggested by Briggs (1975) with modifications to account for the relationship of the risen plume to the mixed layer lid and for transitional plume rise. CTDMPLUS uses interpolated or extrapolated vertical profiles of the meteorology to estimate plume rise in an iterative fashion.

An important consideration in determining the amount of the pollutant that is available to impact the surface is plume penetration into the stable layer above the mixed layer. For a steady-state condition (no significant mixed-layer growth during the modeling period) the portion of the plume that penetrates aloft can be considered unlikely to affect ground level concentrations. CTDMPLUS uses an algorithm proposed and tested by Briggs (1984) for estimating the fraction of a buoyant plume that escapes the mixed layer. Plume penetration in this algorithm is dependent on the strength of the stratification aloft, wind speed, the mixed layer height, and the buoyancy flux of the plume. CTDMPLUS uses the estimated fraction of penetrated plume material to adjust the mass in that portion of the plume that remains in the mixed layer and impacts on the receptors.

With the exception of cloudy or windy conditions or with very moist surface conditions, daytime boundary layers are dominated by convection that is driven by surface heating. The strength of the convection and the depth of the mixed layer are primarily functions of sun angle and surface conditions. In contrast to that in stable or neutral layers, the vertical distribution of pollutants released from elevated sources into a convectively-driven mixed layer is not Gaussian. Distinctly non-Gaussian vertical distributions have been repeatedly observed in convective tank studies (Willis and Deardorff, 1976, 1978, 1981), numerical modeling studies (Lamb, 1979, 1981), and field studies (Briggs and McDonald, 1978, Briggs, 1985, 1986).

Pollutant distributions reflect the distributions of vertical velocities which, due to the nature of convection, are not symmetric for updrafts and downdrafts. Although the average vertical velocity may be zero, updraft velocities tend to be "stronger" and downdrafts cover more horizontal area. This area dominance by downdrafts results in a negative value for the mode of the velocity distribution. Consequently, the vertical

pollutant distribution from an elevated source exhibits a descending mode of highest concentration (the region of highest concentration tends toward the surface) as the plume moves downwind (as observed in the aforementioned studies). This contrasts with the mode (centerline) of a Gaussian distribution which remains elevated.

To model the vertical distribution, CTDMPLUS employs a probability density function (PDF) approach which is based on a PDF suggested by Li and Briggs (1988). PDF models assume that, with convective turbulence, the Lagrangian time scale is sufficiently large and that particles released into the flow will remain approximately on their initial trajectory until the surface or the mixed layer top are reached. Therefore, particles initially released into a downdraft will remain in a downdraft and those released into an updraft will remain in an updraft until a boundary is reached.

Additionally it is assumed that the initial particle trajectories are linear and have a slope of w/U (w is vertical velocity and U is mean wind speed). For steady state conditions ($U = \text{constant}$), the trajectory of the particle is controlled by the vertical velocity at the time and point of release. In other words, the vertical distribution of pollutant material will be controlled by the probability density function of vertical velocities at the source.

Li and Briggs have proposed an asymmetrical bi-Gaussian form of the PDF which produces pollutant distributions very similar to those observed experimentally (Willis and Deardorff, 1981). CTDMPLUS utilizes the Li and Briggs PDF; modifications to the particle trajectories for terrain influences have been added.

When terrain is present, the trajectories become curved as the flow is deflected by the terrain. The flow field is computed by the flow module (already present in CTDM) and is used to construct the paths linking a receptor to the source position. An algorithm was developed which calculates the correct path by an iterative process and determines the initial vertical velocity that will send the particle down that curved path. This, in conjunction with the PDF, determines the probability of particles reaching the receptor and thus the associated concentration.

Another important consideration in modeling unstable conditions is the effect of terrain on the mixed layer depth, z_i . This variable has been established as the dominant length scale for parameterizing mixed layer variables and serves as the height that separates the layer dominated by surface effects from that which is influenced little by the surface. Consequently, pollutant that finds itself above z_i will not generally impact surface receptors. However, the generally stable stratification above z_i has a strong influence on the adjustment of the mixed layer depth as the layer flows over terrain. This in turn has an effect on the terrain distortion of that portion of the plume that resides in this restricted mixed layer.

CTDMPLUS accounts for the effects of the elevated stable layer on restricting the lifting of the mixed layer (and thus the plume) over the terrain. Based on results of a recent fluid modeling study (Perry and Snyder, 1989), CTDMPLUS estimates the deflections of z_i over the terrain feature in question as a function of the hill Froude number (itself a function of flow speed, hill height, and strength of the elevated stratified layer). It then uses this estimate to calibrate the flow model so that it yields equivalent deflections for the z_i streamline. By using a bulk calibration such as this, deflections of the pollutant trajectories calculated in the PDF approach reflect the restrictions on the mixed layer created by the stable layer aloft.

Finally, there is the question of the distribution of material in the horizontal. Since significantly non-Gaussian plume shapes have not been observed in the daytime mixed layer, analytical diffusion models have retained the usual Gaussian form (Briggs, 1985). CTDMPLUS also adopts a Gaussian horizontal distribution function which depends on receptor crosswind distance and a lateral dispersion coefficient.

The lateral (crosswind) distance between the streamlines passing through the source and receptor is determined with the flow model. Because of the deflection and distortion of the flow around and over the terrain, the effective crosswind distance can be significantly different than the geometric lateral distance between source and receptor.

The form of the lateral dispersion coefficient, σ_y , is based on convective scaling concepts and analyses of various data bases. Hanna (1986) correctly points out that there are about as many σ_y formulations as there are data sets to analyze. The one chosen for CTDMPLUS was suggested by Briggs (1985) and Hanna (1986) after analyses of power plant data. For passive plumes, σ_y is dependent on the height of the mixed layer and a non-dimensional downwind distance. For highly buoyant plumes, σ_y is dependent on those two variables plus the buoyancy flux of the release.

More detailed discussions of the algorithms for unstable conditions are contained in subsections 2.8 through 2.11. Users of CTDMPLUS who are familiar with the original CTDM users manual will find that the technical discussions of the algorithms for stable and neutral conditions have changed very little. A primary consideration in the development of the unstable algorithms was to be compatible with and complementary to the original CTDM. Therefore, users will find that concentrations estimated with CTDMPLUS will be identical to those of CTDM for those cases where CTDM is applicable. For this reason, results of existing evaluations of CTDM with stable and neutral hours are valid also for CTDMPLUS.

2.2 CALCULATION OF METEOROLOGICAL VARIABLES

CTDMPLUS reads two files of hourly meteorological data:

- SURFACE, a file passed from the meteorological preprocessor (METPRO) that contains derived surface boundary layer parameters such as the Monin-Obukhov length (L), friction velocity (u_*), surface roughness length (z_0), and mixed layer height (h or z_i).
- PROFILE, a user-created file of on-site measurements of wind direction, wind speed, temperature, σ_θ (or σ_v), and σ_w taken at one or more (no more than 50) heights.

In addition, for the unstable hours, CTDMPPLUS requires the daily RAWIN file (already required by METPRO) in order to estimate the temperature profile above the mixed layer.

CTDMPLUS computes values of wind direction, wind speed, vertical potential temperature gradient (VPTG), σ_v , and σ_w at the height of the plume. If on-site measurements of these variables are provided both above and below the plume height, linear interpolation is used to calculate the values at plume height. If interpolation cannot be used and the plume is within the surface layer, values of meteorological parameters are estimated at plume height using surface layer profile equations (described in more detail in this section). If the plume is above the surface layer and no measurements are available, CTDMPPLUS uses constant values above either the top of the surface layer or the uppermost measurement height, whichever is higher. The user should note that the surface layer is defined here as the stable mixed layer height, h , (either as defined in eqn (1) or as measured) or during unstable conditions as the greater of $|2L|$ and $0.1 z_i$. Also, σ_θ and σ_w are not needed for computations during unstable conditions.

2.2.1 Mixed Layer Height

Two values of mixed layer heights are available from the meteorological preprocessor: a measured value (if available) and a calculated value. The calculated value is always provided by METPRO for stable or neutral surface layers ($L > 0$ or $|L| \geq 100$ m), but is provided for unstable surface layers only for execution mode 3 of METPRO.

If both observed and calculated mixed layer height values are available, the CTDMPPLUS user has an option (via a model parameter switch) to use one or the other for each hour. If only one value is available, that one is used in spite of the user's preference. If both values are missing, in stable/neutral conditions, an "unlimited" value (99999 m) is used. Because of the importance of mixing height for scaling in convective conditions, CTDMPPLUS will not provide concentration estimates for unstable conditions when both z_i values are missing.

As documented in the user's guide for METPRO (Paine, 1987), the following formula is used to calculate mixing heights, h , in stable conditions (Nieuwstadt, 1981):

$$(h/L) = \frac{0.3 u_* / (fL)}{1 + 1.9 h/L} \quad (1)$$

where u_* = friction velocity

L = Monin-Obukov length

and f = Coriolis parameter

For unstable conditions, the Carson (1973) prognostic formulation is used, as modified by Weil and Brower (1983) to estimate the daytime mixed layer height, z_i . This formulation is also described in the METPRO manual. Note the distinction in notation between stable mixed layer height, h , and convective (daytime) mixed layer height, z_i .

2.2.2 Wind Speed

Both scalar and vector wind speed observations can be read by CTDMPLUS. If the vector wind speed, u_v , is not available, it is calculated from the scalar wind speed, u , and σ_θ (or σ_u) after Yamartino (1984):

$$u_v = u(1 - \epsilon^2)^{1/2} \quad (2)$$

where $\epsilon = \sin \sigma_\theta (1 - G \sigma_\theta)$ and $G = 0.073864$

If σ_u is provided instead of σ_θ , then σ_θ is approximated by σ_u/u for use in equation 2, where u is the scalar wind speed.

The CTDMPLUS user may elect to set measured wind speeds that are less than 1.0 m/sec to 1.0 m/sec, as recommended in EPA's Guideline on Air Quality Models, Revised (1986). If the user selects this option, proportional corrections are made to the vector wind speed (u_v) and the standard deviations of the crosswind and vertical wind speeds, σ_v and σ_w , in order to preserve the turbulence intensity values: $i_y = \sigma_v/u_v$ and $i_z = \sigma_w/u_v$.

The assignment of the wind speed (either vector or scalar) at plume height is done by either:

- interpolating between observations above and below the plume height, or
- extrapolating from the nearest measurement height to plume height.

When extrapolation is necessary, CTDMPLUS checks the position of plume height relative to the surface layer. For plumes within the surface layer, the model extrapolates by using surface layer profiling equations to be described below. For plumes above the surface layer, CTDMPLUS extrapolates the wind speed to the top of the layer using profile equations; this speed is used aloft if the uppermost measurement height lies within the surface layer. If the uppermost measurement height is outside the layer, then that measurement is used for all heights above the measurement height.

The profiling equations that are used for wind speed are listed below (Lumley and Panofsky, 1964; Businger, 1973).

$$u = \frac{u_*}{k} \left[\ln \left(\frac{z}{z_0} \right) - \Psi_m \right] \quad (3)$$

where, for unstable conditions, the stability correction denoted as Ψ_m is as follows:

$$\Psi_m = 2 \ln \left[\frac{(1 + \Phi_m^{-1})}{2} \right] + \ln \left[\frac{(1 + \Phi_m^{-2})}{2} \right] - 2 \arctan(\Phi_m^{-1}) + \frac{\pi}{2} \quad (4)$$

and

$$\Phi_m = \left(1 - 15 \frac{z}{L} \right)^{-1/4} \quad (5)$$

For stable conditions, the stability correction Ψ_m is given by:

$$\Psi_m = -4.7 \frac{z}{L} \quad (6)$$

If the scalar wind speed is missing at all observation heights, CTDMPLUS does not predict concentrations for that hour.

2.2.3 Wind Direction

The assignment of wind direction at plume height is handled similarly to that of wind speed. The preferable method involves interpolation between observations both above and below the plume height. If extrapolation beyond the uppermost measurement height to plume height is necessary, then the method used depends upon the relationship of the plume height to the depth of the surface layer. If the plume is within the surface layer (as is the uppermost measurement height), then the wind direction is scaled with height if the user elects to have this calculation performed (controllable via a model parameter switch). No

attempt is made to calculate the turning of the wind with height above the surface layer, as there is no definite trend that can be relied upon (Hanna et al., 1986). Therefore, the wind direction used for plumes above the surface layer is either:

- the direction calculated at the top of the layer from scaling (if the uppermost measurement height is within the surface layer), or
- the direction measured at the uppermost sensor.

The Tennekes (1981) wind direction adjustment is used for the computation of the change in direction within the surface layer:

$$\Delta\alpha = \arctan\left(\frac{B}{0.4} \frac{u_*}{u_g}\right) \quad (7)$$

where u_g is the geostrophic wind speed (here assumed to be the wind speed at the top of the surface layer) and B is obtained as a function of h/L using graphs from Melgarjo and Deardorff (1974).

If the wind direction is missing at all heights, CTDMPLUS does not attempt to predict concentrations for that hour.

2.2.4 Potential Temperature Gradient

CTDMPLUS calculates the vertical potential temperature gradient, $d\theta/dz$ (or VPTG), from temperature data contained in the "PROFILE" file. Temperature at various heights should be obtained from measurements of temperature differences so that the temperature gradients are calculated accurately. The height assigned to a calculated $d\theta/dz$ value is the midpoint of the interval bounded by the two temperature measurements. Linear interpolation of $d\theta/dz$ values is used for heights between these midpoint heights.

If the plume is above the uppermost height at which a value of $d\theta/dz$ is available, the last available value is used. No attempt is made to scale $d\theta/dz$ with height, even within the surface layer (such as by the use of a method like Stull, 1983). The scaling methods were found during the development of CTDM to give worse performance (values of $d\theta/dz$ that were too low) than using the uppermost measurement, so the latter method is used.

If observed temperature gradients are not available, a default value is chosen:

- a stability class-dependent default value if the plume is within the surface layer, or

- the greater of the stability class default value and the value for stability E (slightly stable) if the plume is above the surface layer.

The default values are 0.0 K/m for stability classes A-D, 0.02 K/m for stability class E, and 0.035 K/m for stability class F. These default values are consistent with the complex terrain screening models. Stability class is determined by the method of Golder (1972) using u_* and L .

2.2.5 Turbulence Intensities

Values of σ_v (or σ_θ) and σ_w are related to horizontal and vertical turbulence intensities (i_y and i_z , respectively) as follows:

$$i_y = \frac{\sigma_v}{u_v} \approx \sigma_\theta \quad (8)$$

$$i_z = \frac{\sigma_w}{u_v} \quad (9)$$

The values of σ_v and σ_w are used to calculate the plume σ_y and σ_z in stable/neutral conditions (see Section 2.4.1).

Values of σ_v and σ_w at the elevation of the plume are obtained by interpolation if measurements exist both below and above the plume height. If the plume lies outside the range of the measurement heights, the nearest available observation of σ_v or σ_w is used. If no measurements are available for either σ_v or σ_w , CTDMPPLUS will not produce concentration estimates for hours in which the plume is released into a stable or neutral layer. Neither σ_v (σ_θ) nor σ_w is needed for hours during which all plumes are released into unstable layers.

A minimum value for σ_v of 0.2 m/sec is used. This choice is consistent with the data obtained at Cinder Cone Butte, Hogback Ridge, and the Tracy Power Plant, where very few hours with σ_v less than 0.2 m/sec were found. This minimum value is also consistent with values reported by Hanna (1983).

A minimum value of 0.01 m/sec for σ_w was chosen to avoid division by zero. Actual values of σ_w (other than in perfectly calm conditions, which are not modeled by CTDMPPLUS) are expected to be at least 0.01 m/sec.

2.3 PLUME RISE CALCULATIONS

2.3.1 Momentum Rise

Momentum rise is used only if the buoyancy flux is zero (stack temperature not greater than ambient). The following formulas are used (Briggs, 1975) for momentum rise:

$$\Delta h = 3 \frac{dw_s}{u_s} \quad (10a)$$

$$\Delta h = 1.5 \left(\frac{w_s^2 d^2 T_a}{4 T_s u_s} \right)^{1/3} s^{-1/6} \quad (10b)$$

where d = stack diameter

w_s = stack gas exit velocity

u_s = stack top wind speed

T_a = ambient temperature

T_s = stack gas temperature

$s = (g/T_a)(d\theta/dz)$.

If $L > 0$ (stable/neutral), the minimum plume rise from Equations 10a and 10b is used; if $L < 0$ and $L > -100$ (unstable/neutral) Equation 10a is used.

2.3.2 Neutral/Unstable Buoyant Final Rise

These formulas from Briggs (1975) apply for plumes within the mixed layer:

Final or transitional ($x_f = x$) rise:

$$\Delta h = 1.6 (F x_f^2)^{1/3} / u \quad (11a)$$

where

$$x_f = 119 F^{0.4} \quad \text{for } F > 55 m^4 s^{-3} \quad \text{and} \quad (11b)$$

$$x_f = 49 F^{0.625} \quad \text{for } F \leq 55 m^4 s^{-3} \quad (11c)$$

Unstable breakup rise:

$$\Delta h = 4.3 (F/u)^{3/5} H^{-2/5} \quad (12)$$

Touchdown plume rise:

$$\Delta h = 1.0 \frac{F}{uu_a^2} \left(1 + \frac{2h_s}{\Delta h} \right)^2 \quad (13)$$

Neutral breakup rise:

$$\Delta h = 1.3 \frac{F}{uu_s^2} \left(1 + \frac{h_s}{\Delta h} \right)^{2/3} \quad (14)$$

where u = wind speed at height $h_s + \Delta h/2$,

F = buoyancy flux, $0.25 w_s d^2 g (T_s - T_a) / T_s$,

$H = -u_s^3 (0.4 L)$ is the surface heat flux, and

$w_a = 0.4 w_s$.

Transitional plume rise is calculated using Equation 11a with x_f replaced by actual downwind distance. The neutral/unstable plume rise is the minimum of the transitional rise and the final rises of Equations 11 through 14.

An iterative technique is used for calculating plume rise in any of the buoyancy equations (11 through 14), since the plume rise is assumed to be a function of the wind speed and temperature gradient at a height halfway between the stack top and final plume height. For some plume rise formulas, this method does not converge for certain profiles of wind speed and/or $d\theta/dz$. Therefore, iteration is stopped after five tries at convergence (defined by less than 1% change between successive iterations). After each iteration (and the fifth one, if no convergence), the plume rise guess for the next iteration (or the final rise, if no convergence) is the average of the plume rise estimate for the previous two iterations.

2.3.3 Neutral/Stable Buoyant Final Rise

There are several final plume rise formulas available for stable conditions, depending on whether winds are nearly calm or not, and depending on whether conditions are close to neutrality. The final neutral/stable rise that is used in CTDMPLUS is the minimum of those calculated by means of Equations 11, 14, and the following equations 15 and 16 Briggs (1975):

Neutral high wind rise:

$$\Delta h = 1.54 [F/(uu_s^2)]^{2/3} h_s^{1/3} \quad (15)$$

Bent-over stable:

$$\Delta h = 2.6 (F/us)^{1/3} \quad (16a)$$

Calm stable:

$$\Delta H = 4 F^{1/4} s^{-3/8} \quad (16b)$$

In stable conditions, the distance to final rise, x_f , is given by

$$x_f = 2.07 u s^{-1/2} \quad (16c)$$

The iterative technique described in Section 2.3.2 is also used for neutral/stable conditions.

2.4 DISPERSION PARAMETERS FOR STABLE/NEUTRAL CONDITIONS

2.4.1 Plume Spread Due to Turbulence

The formulation for σ_z is described in Venkatram et al. (1984). It is based on the form of Taylor's (1921) theorem of diffusion for very short and very long times of travel:

$$\sigma_z = \sigma_w t \quad ; \quad t \ll T_L \quad (17a)$$

$$\sigma_z = (2K_z t)^{1/2} \quad ; \quad t \gg T_L \quad (17b)$$

where σ_w is the standard deviation of the vertical velocity fluctuations, t is the travel-time, T_L is the Lagrangian time-scale, and K_z is the eddy diffusivity. Using mixing-length arguments, K_z is defined as $\sigma_w l$, where $l = \sigma_w T_L$, so that in the limit $T \gg T_L$, Equation (17b) becomes

$$\sigma_z = \sigma_w (2t T_L)^{1/2} \quad (18)$$

An interpolation formula used by other authors (Deardorff and Willis, 1975) is employed to span the gap between small and large times-of-travel:

$$\sigma_z = \frac{\sigma_w t}{\left(1 + \frac{t}{2T_L}\right)^{1/2}} \quad (19)$$

In Equation (19), σ_w is measured directly, but T_L must be related to other measurements before σ_z can be calculated in the model. This is accomplished by using the empirical flux-profile relationships of surface similarity theory (Businger, 1973) to estimate the mixing length, l . The derivation relies on the appropriateness of surface similarity theory and on the assumption that σ_w is proportional to the friction velocity, u_* . If we assume that measured σ_w is due mainly to turbulent fluctuations, then the formulation is appropriate.

By introducing two new constants, γ and Γ , the length scale, l , can be expressed as

$$\frac{1}{l} = \frac{1}{2\Gamma z} + \left[\left(\frac{1}{2\Gamma z} \right)^2 + \left(\frac{N}{\gamma^2 \sigma_w} \right)^2 \right]^{1/2} \quad (20)$$

where N is the Brunt-Vaisala frequency given by

$$N^2 = \frac{g}{\Theta} \frac{d\Theta}{dz} \quad (21)$$

and

$$\gamma^2 = \frac{1}{(\alpha^2 \sqrt{\beta})} \cong .27$$

$$\Gamma = \frac{k}{(\alpha \alpha)} \cong .36$$

$$\alpha \cong \frac{\sigma_w}{u_*} = 1.3$$

and α and β are parameters in the surface similarity profiles (.74 and 4.7, respectively).

The resulting expression for l has two distinct limiting forms. When z is very large, for non-zero N , stratification dominates the scale of the mixing process and

$$l = \frac{\gamma^2 \sigma_w}{N} = l_s \quad (22)$$

When N is nearly zero and z is finite, the length scale for the mixing process is proportional to height above the surface:

$$l = \Gamma z = l_n \quad (23)$$

The quantities l_s and l_n are introduced to distinguish the mixing lengths for the stable and neutral limits.

Equation 22 states that the length scale for turbulent mixing in the stable limit is proportional to σ_w/N , where γ^2 is the constant of proportionality. This is consistent with the notion that a fluid element in this limit must overcome a stable potential temperature gradient in order to be displaced vertically. Given

that the velocity scale for vertical dispersion is σ_w , the length scale that naturally follows is proportional to σ_w/N . In the neutral limit, the size of the turbulent eddies is restricted by the height above the surface, so that the mixing length should be proportional to z , where Γ is the constant of proportionality.

A simple weighting function is used to obtain a length scale between the neutral and stable limits:

$$\frac{1}{l} = \frac{1}{l_n} + \frac{1}{l_s} \quad (24)$$

With this expression for l , T_L is computed as

$$T_L = \frac{l}{\sigma_w} \quad (25)$$

and σ_z is computed from Equation 19 as a function of the time-of-travel, including source effects (see Section 2.4.2).

An equation similar to that used for σ_z is used to compute σ_y as a function of the time-of-travel and the turbulence velocity scale for lateral fluctuations, σ_v :

$$\sigma_y = \frac{\sigma_v t}{\left(1 + \frac{t}{2T_L}\right)^{1/2}} \quad (26)$$

The departure of this expression from that for σ_z arises in specifying the functional form of T_L , which is the Lagrangian time-scale of the transverse correlogram. In this case, T_L cannot be derived from measurements of the mean flow and its statistics. Instead, T_L is set equal to the time-of-travel required to cover a distance of 10 km, which has the effect of reducing σ_y by about 18% from the value that would be obtained using a linear growth law at a distance of 10 km.

All of the Complex Terrain Model Development field experiments included sampler locations within 10 km of the source, so that the growth in σ_y beyond 10 km was not documented. Nearly linear growth in σ_y over the first 5 km was typical of many of the experiments. The use of the 10 km length scale is meant to underscore the uncertainty of using linear growth beyond 10 km, while allowing nearly linear growth within 5 km of a source. Note that the scale used by Briggs (1973) for dispersion in open country corresponds to 5 km, which would reduce σ_y at 10 km by about 29%. Because CTDMPLUS is intended for use in complex terrain, the use of a larger scale for T_L was judged appropriate in that lateral fluctuations in the flow which are induced by complex topography would promote greater meandering of the plume.

In summary, the following equations are used to calculate the plume spread parameters σ_z and σ_y :

$$\sigma_z = \frac{\sigma_w t}{\left[1 + \sigma_w t \left(\frac{1}{.72z} + \frac{N}{.54\sigma_w} \right) \right]^{1/2}} \quad (27a)$$

$$\sigma_y = \frac{\sigma_v t}{[1 + ut/20,000]^{1/2}} \quad (27b)$$

2.4.2 Allowance for Source-Induced Effects

A virtual time-of-travel is introduced to account for increases in σ_y and σ_z caused by how the plume is released into the atmosphere. For buoyant releases in stable conditions, the initial growth during plume rise is characteristically much greater than the growth caused by ambient turbulence alone. Therefore, once the plume reaches its equilibrium height and ambient turbulence becomes dominant, the plume evolves as if it had experienced a greater time-of-travel.

Write the general form for σ_z or σ_y as:

$$\sigma_t = \frac{\sigma t}{\left(1 + \frac{t}{2T_L} \right)^{1/2}} \quad (28)$$

and solve for t :

$$t = \frac{1 + \left[1 + 4 \left(\frac{2T_L \sigma}{\sigma_t} \right)^2 \right]^{1/2}}{T_L \left(\frac{2\sigma}{\sigma_t} \right)^2} \quad (29)$$

The virtual time-of-travel (t_v) is found by setting σ_t equal to the plume size caused by source-induced effects (σ_{ts}) and setting t equal to $t_s + t_v$, where t_s is the time-of-travel to the point where ambient turbulence dominates source-induced turbulence:

$$t_v = -t_s + \frac{1 + \left[1 + 4 \left(\frac{2T_L \sigma}{\sigma_{ts}} \right)^2 \right]^{1/2}}{T_L \left(\frac{2\sigma}{\sigma_{ts}} \right)^2} \quad (30)$$

Ambient turbulence is assumed to dominate source-induced turbulence quickly for neutral and unstable conditions, and t_s is set to zero for these cases. As implemented, σ_{ts} is just the size of the plume resulting from buoyant rise (buoyancy-enhanced dispersion, Pasquill, 1976):

$$\sigma_{ts} = \sigma_{tb} = \frac{\Delta H}{3.5} \quad (31)$$

where ΔH is the plume rise. Similarly, t_s is the time-of-travel to final rise. Depending on the relative values of σ (ambient turbulence) and σ_{ts} for the time t_s , t_v can become negative in Equation 30. Physically, this indicates that the growth of the plume due to ambient turbulence exceeds that due to source effects. In the case of σ_y , this frequently happens when meandering is great. Consequently, t_v is never allowed to be less than zero, so that buoyancy enhancement is active only when it exceeds the growth rate due to the ambient turbulence. In fact, T_z is always greater than zero, as it has a minimum value corresponding to the time it takes for the plume (σ_y, σ_z) to grow to the size of the stack radius. Once t_v is calculated for both the lateral and vertical scale of the plume, it is added to the actual time-of-travel in Equation 27.

2.5 THE LIFT COMPONENT

2.5.1 Overview of LIFT

The flow above H_c is considered to be weakly stratified. That is, the stratification is strong enough to influence the flow pattern (e.g., lee waves), but not strong enough to inhibit significant vertical motion. To simplify the modeling task, H_c is assumed to be a level surface, and the flow above H_c is only affected by that portion of the hill that lies above H_c .

H_c is computed for each hill from profiles of wind speed, $u(z)$, and temperature (Brunt-Vaisala frequency, $N(z)$) by locating the lowest height at which the kinetic energy (K.E.) of the approach flow just balances the potential energy (P.E.) attained by elevating a fluid parcel from this height to the top of the hill, H . The statement that defines that point of balance is:

$$\frac{1}{2}u^2(H_c) = \int_{H_c}^H N^2(z) (H - z) dz \quad (32)$$

In practice, the value of H_c for which the equality in Equation 32 is attained is found by rewriting the integral as a series of sums over layers of constant N . For each layer, starting with the one that includes the top of the hill, the bottom and the top of the layer are tested to see if the K.E. (left-hand side) has decreased below the P.E. (right-hand side). The lowest layer in which the K.E. exceeds the P.E. at the

top, but not at the bottom, is the layer that contains H_c . H_c is then computed from Equation 32 by assuming a linear velocity gradient within that layer, and constant N within each of the layers to the top of the hill.

The plume is allowed to diffuse as if the terrain were perfectly flat until it reaches the point where its trajectory crosses the height contour equal to H_c in elevation (say, at a distance s_0 from the source, see Figure 2-5). If H_c is zero, then this zone extends from the source to the base of the hill, although conceptually it could extend to any point where the hill is thought to exert a significant influence on the flow. Beyond s_0 , the plume material below H_c is disregarded by the LIFT component, and the evolution of the remaining material is modeled as if the terrain were flat, and the lower boundary were H_c (with full reflection). However, the rate of plume spread and the position of the plume centerline relative to the receptor are modified to reflect the net alternation of these properties between s_0 and s (where s is the distance from the source to the receptor) induced by the presence of the hill. The simplicity of the Gaussian plume solution is retained in this way, while the full dilution of the plume from the source to the hill (s_0) as well as the effects of the hill on both flow and diffusion beyond s_0 are explicitly incorporated.

Aside from the obvious distinction of incorporating the primary influence of H_c on the plume-terrain interaction, this approach notably differs from the current regulatory modeling approach (at least as embodied in Valley, COMPLEX I, and II) in that the terrain influence for a receptor on a hill only affects the diffusion of the plume once it is over the terrain. The mathematical formulation of the "partial plume height correction" approach of COMPLEX I and similar models actually "lowers" the plume at the source. If this technique were engineered to produce the "correct" hill-influenced ground-level concentrations, the terrain correction factor for a particular receptor would need to be a function of downwind distance, terrain shape, and distance between source and terrain. As employed in regulatory modeling, however, the terrain correction factor depends only on the stability class, so that its use has led to problems of interpreting "surface reflection" from sloping terrain, as well as to problems in justifying values chosen for the terrain correction factor.

2.5.1.1 LIFT Structure

The terrain effect as modeled in LIFT includes re-initializing the flow at a distance s_0 downwind of the release. This re-initialization can be illustrated first for flat terrain and uniform flow. The concentration at a receptor downwind of s_0 is composed of contributions from the entire concentration distribution at s_0 .

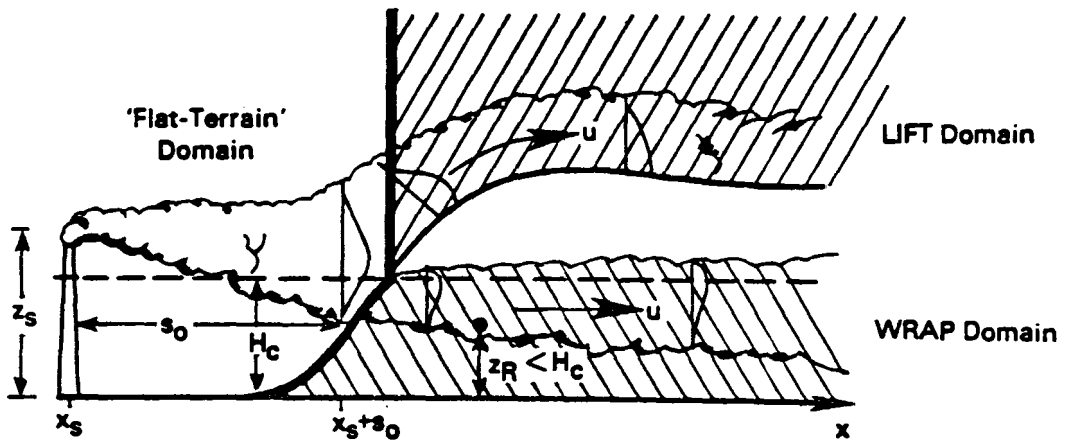
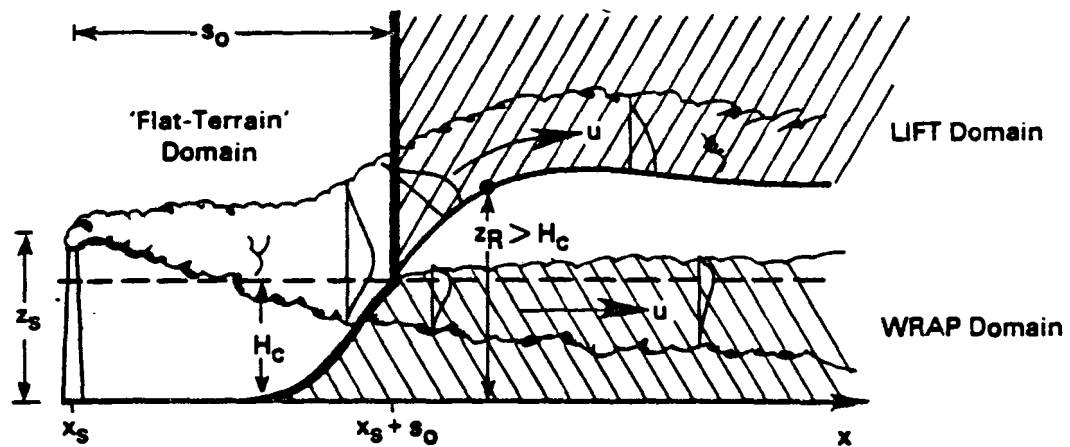
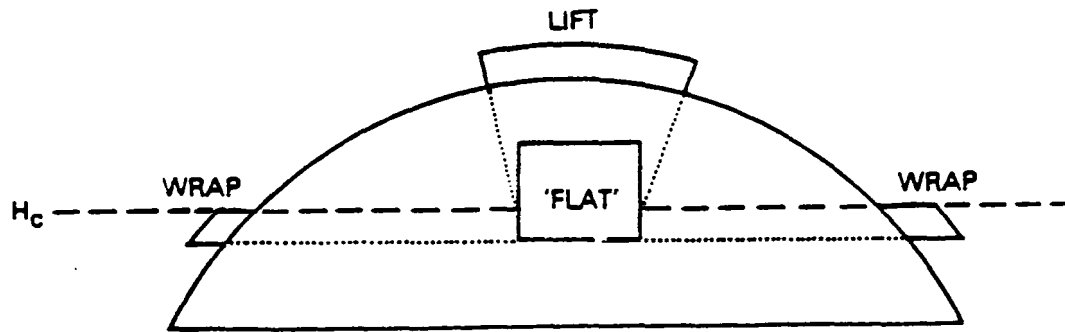


Figure 2-5. Idealized stratified flow about hills indicating domain of individual CTDMPLUS component algorithms. The distance s_0 is the distance from the source to the intersection of H_c with the hill surface for receptors above H_c (the LIFT domain), and it is the distance from the source to the terrain-height contour equal in height to the receptor elevation for receptors below H_c (the WRAP domain). Note that in the upper figure the flow is into the page.

Conceptually, the flux of plume material through the plane $x = x_s + s_0$ (note that the x-axis lies along the flow direction, and the plume is released at x_s, y_s, z_s) can be thought of as a distribution of point sources. If we track the plume material in terms of the distance downwind of the source, $s = x - x_s$, then the source strength of one of these point source elements located at the point (s_0, y, z) is given by:

$$dQ(s_0, y, z) = C(s_0, y, z) u \, dy \, dz \quad (33)$$

Because the flow beyond s_0 is considered to be uniform, the influence of each of these sources follows the Gaussian plume solution to the advective diffusion equation so that the contribution of the source element at the point (s_0, y, z) to the concentration at the point (s, l, h) is:

$$dC(s, l, h; s_0) = \frac{dQ(s_0, y, z)}{2\pi\sigma_y^*\sigma_z^*u} e^{-0.5\left(\frac{y-l}{\sigma_y^*}\right)^2} \left(e^{-0.5\left(\frac{z-h}{\sigma_z^*}\right)^2} + e^{-0.5\left(\frac{z+h}{\sigma_z^*}\right)^2} \right) \quad (34)$$

where σ_y^*, σ_z^* denote the plume spread statistics for each point source element over the interval $s - s_0$ (see Figure 2-6). The total concentration at (s, l, h) is found by integrating Equation 34 over all point source elements, so that

$$C(s, l, h; s_0) = \int_0^\infty \int_{-\infty}^\infty \frac{C(s_0, y, z)}{2\pi\sigma_y^*\sigma_z^*} e^{-0.5\left(\frac{y-l}{\sigma_y^*}\right)^2} \cdot \left(e^{-0.5\left(\frac{z-h}{\sigma_z^*}\right)^2} + e^{-0.5\left(\frac{z+h}{\sigma_z^*}\right)^2} \right) dy \, dz \quad (35)$$

The plume spread statistics σ_y^* and σ_z^* for the interval $s - s_0$ are specified by the requirement that Equation 35 for flat terrain reduces to the expression obtained for the original point source located at $s = 0$ (i.e., Equation 34 with $s_0 = 0$ and $\sigma^* = \sigma(s)$). Equating these two expressions for C , with $h = 0$, we obtain

$$\sigma_z^{*2} = \sigma_z^2(s) - \sigma_z^2(s_0) = \sigma_z^2 - \sigma_{z0}^2 \quad (36a)$$

$$\sigma_y^{*2} = \sigma_y^2(s) - \sigma_y^2(s_0) = \sigma_y^2 - \sigma_{y0}^2 \quad (36b)$$

Equations 35 and 36 illustrate the re-initialization technique for the limiting case of flat terrain and uniform flow. Terrain influences are incorporated by altering the rate of diffusion within the interval $s - s_0$, and by changing the position of the receptor relative to the centerline of the deflected plume. Furthermore, because no plume material below H_c travels over the hill and because H_c defines the lower

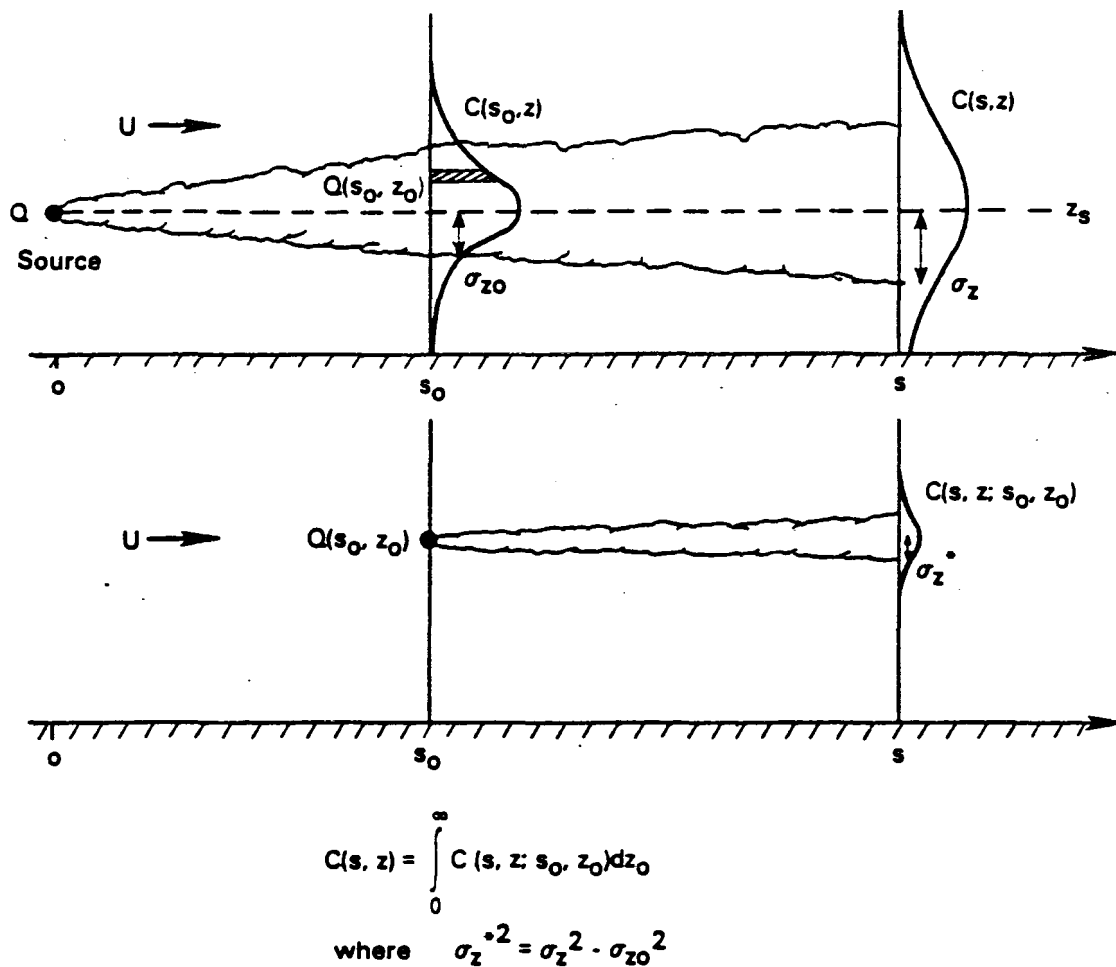


Figure 2-6. Illustration of the relationship between the crosswind-average concentration profiles at s_0 and s , and the plume from one of many point-source elements representing the flux of material across the plane at s_0 . The total concentration at a particular point $C(s, z)$ is constructed by summing the contribution $c(s, z; s_0, z_0)$ from each point-source element $Q(s_0, z_0)$.

boundary over the hill beyond s_0 (see Figure 2-7), the integration in the vertical in Equation 35 is performed over the domain $z = H_c$ to $z = \infty$ and material from each point source element is reflected from the boundary $z = H_c$ rather than $z = 0$.

Denote the receptor height above ground relative to the terrain-altered plume as h_R' (see the lower part of Figure 2-7). Denote its lateral position relative to the terrain-altered plume centerline as y_R' . Denote the altered growth rates of the plume as σ_z^* and σ_y^* and define terrain-effect factors T_z and T_y so that

$$\begin{aligned}\sigma_z^* &= \frac{\sigma_z}{T_z} \\ \sigma_y^* &= \frac{\sigma_y}{T_y}\end{aligned}\quad (37)$$

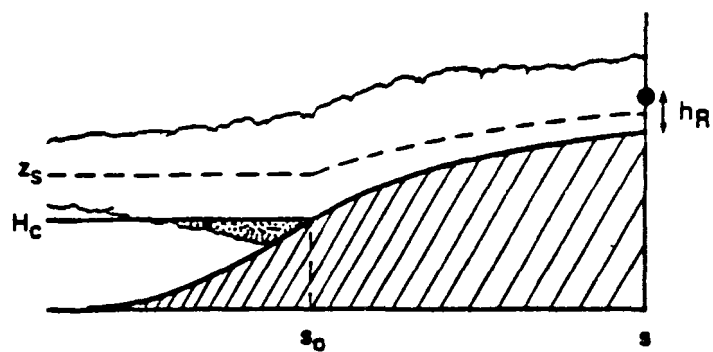
Then, the effective plume spread, accounting for the effect of strain in the flow on the rate at which material diffuses across streamlines, is defined as

$$\begin{aligned}\sigma_{ze}^2 &= \sigma_{zo}^2 + \left(\frac{\sigma_z^*}{T_z}\right)^2 \\ \sigma_{ye}^2 &= \sigma_{yo}^2 + \left(\frac{\sigma_y^*}{T_y}\right)^2\end{aligned}\quad (38)$$

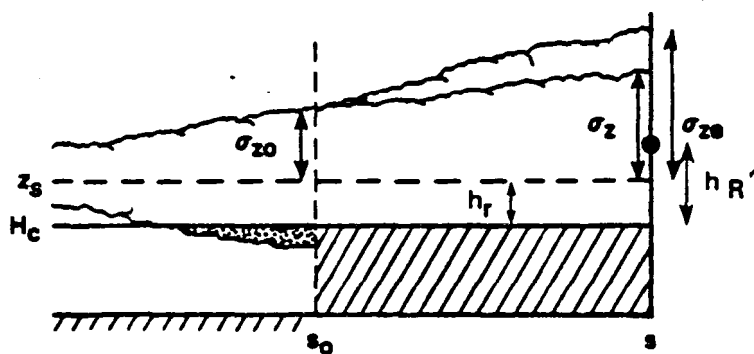
With these definitions, the concentration at the receptor is:

$$C(s, y_R', h_R'; s_0) = \frac{Q e^{-0.5 \left(\frac{y_R' - y_s}{\sigma_{ye}} \right)^2}}{4 \pi u \sigma_{ye} \sigma_{ze}} F_z \quad (39a)$$

where



PHYSICAL PICTURE: material above H_c rides up and over hill in a distorted flow. Material below H_c passes round the side.



LIFT CALCULATION: net effect of flow distortion is to increase the effective rate of plume growth (σ_{zs}) over that in the absence of the hill (σ_z)

Figure 2-7. Illustration of terrain effect on the vertical distribution of plume material above H_c as modeled in LIFT.

$$\begin{aligned}
F_z = & e^{-0.5 \left(\frac{h_R' - z_s + H_c}{\sigma_{ze}} \right)^2} \left\{ 1 + \text{ERF } A_z \left[(z_s - H_c) \left(\frac{\sigma_z^*}{T_z} \right)^2 + h_r' \sigma_{zo}^2 \right] \right\} \\
& + e^{-0.5 \left(\frac{h_R' + z_s - H_c}{\sigma_{ze}} \right)^2} \left\{ 1 + \text{ERF } A_z \left[(z_s - H_c) \left(\frac{\sigma_z^*}{T_z} \right)^2 - h_r' \sigma_{zo}^2 \right] \right\} \\
& + e^{-0.5 \left(\frac{h_R' + z_s + H_c}{\sigma_{ze}} \right)^2} \left\{ 1 - \text{ERF } A_z \left[(z_s + H_c) \left(\frac{\sigma_z^*}{T_z} \right)^2 - h_r' \sigma_{zo}^2 \right] \right\} \\
& + e^{-0.5 \left(\frac{h_R' - z_s - H_c}{\sigma_{ze}} \right)^2} \left\{ 1 - \text{ERF } A_z \left[(z_s + H_c) \left(\frac{\sigma_z^*}{T_z} \right)^2 + h_r' \sigma_{zo}^2 \right] \right\} \quad (39b)
\end{aligned}$$

and

$$A_z = \left(\sqrt{2} \sigma_{zo} \sigma_{ze} \frac{\sigma_z^*}{T_z} \right)^{-1} \quad (39c)$$

Equation 39 provides the framework for estimating concentrations due to plume material that travels up and over a hill. It shows how the influence of the terrain affects the magnitude and the distribution of GLCs. The most complicated part of Equation 39 is the expression for F_z , the vertical distribution factor. It contains four terms because it applies to an elevated receptor, so the image source contribution is not equal to the contribution from the primary source (hence two terms are needed rather than one). And it also applies to a plume segment above H_c rather than an entire plume profile, so that an image source contribution at s_0 must be explicitly maintained (hence, two more terms). The error functions also arise from treating only the portion of plume material that lies above H_c at s_0 . If H_c is zero, then Equation 39 becomes:

$$C(s, y_R', h_R'; s_0) = \frac{Q e^{-0.5 \left(\frac{y_R' - y_s}{\sigma_{ye}} \right)^2}}{2\pi u \sigma_{ye} \sigma_{ze}} \left[e^{-0.5 \left(\frac{h_R' - z_s}{\sigma_{ze}} \right)^2} + e^{-0.5 \left(\frac{h_R' + z_s}{\sigma_{ze}} \right)^2} \right] \quad (40)$$

which, with the exception of alterations in the plume size and in the distance between the plume centerline and the receptor, is the familiar Gaussian plume equation for the concentration at an elevated receptor.

The key quantities that need to be evaluated in order to apply Equation 39 are the effective receptor coordinates (y_R' and h_R'), and the terrain-effect factors (T_z and T_y). The factors T_z and T_y are obtained from the results of Hunt and Mulhearn (1973), and require a model of the flow field over a hill as does the receptor position relative to the deflected plume centerline. These features of LIFT are described in Appendix A.

2.6 THE WRAP COMPONENT

2.6.1 Overview of WRAP

A particle in a steady two-dimensional flow around an obstacle will experience both accelerations and decelerations as it passes by. The magnitude of these changes in speed depends upon how close the particle is to the stagnation streamline of the flow. Maximum changes occur for particles on the stagnation streamline. Furthermore, the spacing between adjacent streamlines varies in inverse proportion to these changes in the speed along streamlines. Figure 2-8 is a representation of a typical streamline pattern for flow around an ellipse when the incident flow is at an angle to the axes of the ellipse.

A plume in this steady flow (with some small-scale turbulence) will follow the streamline patterns, spreading slowly across adjacent streamlines. However, as streamlines spread apart (or contract) the plume size in the horizontal will expand (or shrink) to the same extent. In the absence of diffusion, these kinematic changes in the horizontal size of the plume will not alter the concentration of material within the plume. Changes to the horizontal scale of the plume are balanced by changes in the flow speed so that the flux of material is unchanged. With the addition of small-scale diffusion, the rate of plume growth in the horizontal can be altered by changes in streamline spacing (Hunt and Mulhearn, 1973). However, based on the observations at CCB and Tracy field sites we choose to ignore the effects of small-scale diffusion on concentrations in the WRAP component. The observations suggest that low frequency turbulence--meanders--control crosswind plume growth over hourly averaging times.

2.6.2 WRAP Structure

To simulate ground-level concentrations due to dispersion of releases below H_c in complex terrain settings, CTDMPPLUS must approximate the key features of steady two-dimensional flow around an ellipse that were described above. Two key approximations in the WRAP component are (1) lateral diffusion is insensitive to accelerations in the flow (i.e., the kinematic deformation of the plume has no effect on the diffusion rate), and (2) the mean flow for the averaging period (one hour) is considered steady, while all of the variability in the flow over the period, including that due to meandering, is considered "turbulence."

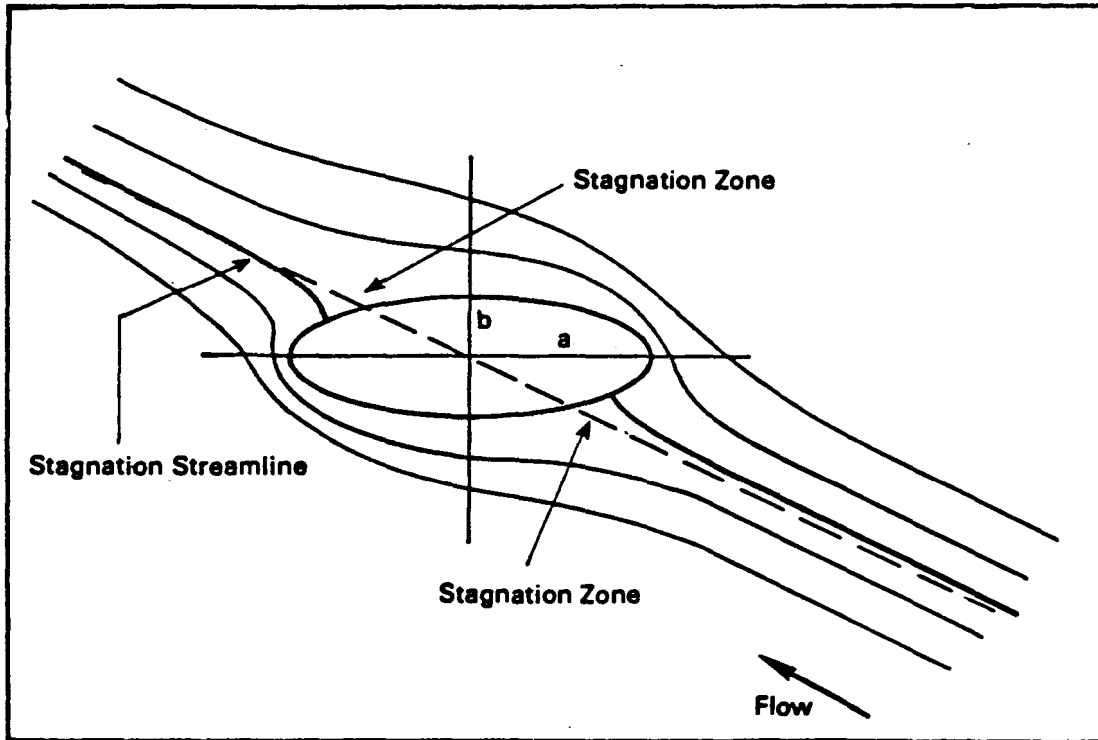


Figure 2-8. Typical streamline patterns in two-dimensional flow around an elliptical cylinder.

A primary difference between WRAP and LIFT formulations arises from the location of solid boundaries and the relationship between the position of these boundaries and the wind direction fluctuations. The terrain effect is modeled in WRAP by re-initializing the flow at the distance s_0 downwind of the source (see Figure 2-5). The concentration at a receptor downwind of s_0 is composed of concentrations from that part of the concentration distribution at s_0 that lies below H_c , and that also lies on the same side of the stagnation streamline as the receptor (see Figure 2-9). Reflection of plume material in the vertical is allowed from the plane $z = 0$ over the entire distance s , and reflection in the horizontal is also allowed from the hillside beyond s_0 . Note that the stagnation streamline forms the boundary of the hill surface in horizontal cross section.

For a receptor located on the hillside at a distance s (see Figure 2-9) and a height z_R above the plane $z = 0$, the concentration due to one elemental point source located at (s_0, y, z) in the plume is given by

$$dC(s, 0, z_R; s_0) = \frac{dQ(s_0, y, z)}{2\pi u \sigma_y^* \sigma_z^*} 2e^{-0.5\left(\frac{y}{\sigma_y^*}\right)^2} \left(e^{-0.5\left(\frac{z-z_R}{\sigma_z^*}\right)^2} + e^{-0.5\left(\frac{z+z_R}{\sigma_z^*}\right)^2} \right) \quad (41)$$

In Equation 41, we assume that the x-axis of the coordinate system points along the stagnation streamline, and that the source is located at (x_s, y_s, z_s) . The total concentration at the receptor contains contributions from those elements below H_c and on the same side of the stagnation streamline as y_s :

$$C(s, 0, z_R; s_0) = \int_0^{H_c} \int_{(s_0)}^{\infty} \frac{C(s_0, y, z)}{2\pi \sigma_y^* \sigma_z^*} 2e^{-0.5\left(\frac{y}{\sigma_y^*}\right)^2} \cdot \left(e^{-0.5\left(\frac{z-z_R}{\sigma_z^*}\right)^2} + e^{-0.5\left(\frac{z+z_R}{\sigma_z^*}\right)^2} \right) dy dz \quad (42)$$

where

$$C(s_0, y, z) = \frac{Q}{2\pi u \sigma_{y_0} \sigma_{z_0}} e^{-0.5\left(\frac{y-y_s}{\sigma_{y_0}}\right)^2} \left[e^{-0.5\left(\frac{z-z_s}{\sigma_{z_0}}\right)^2} + e^{-0.5\left(\frac{z+z_s}{\sigma_{z_0}}\right)^2} \right] \quad (43)$$

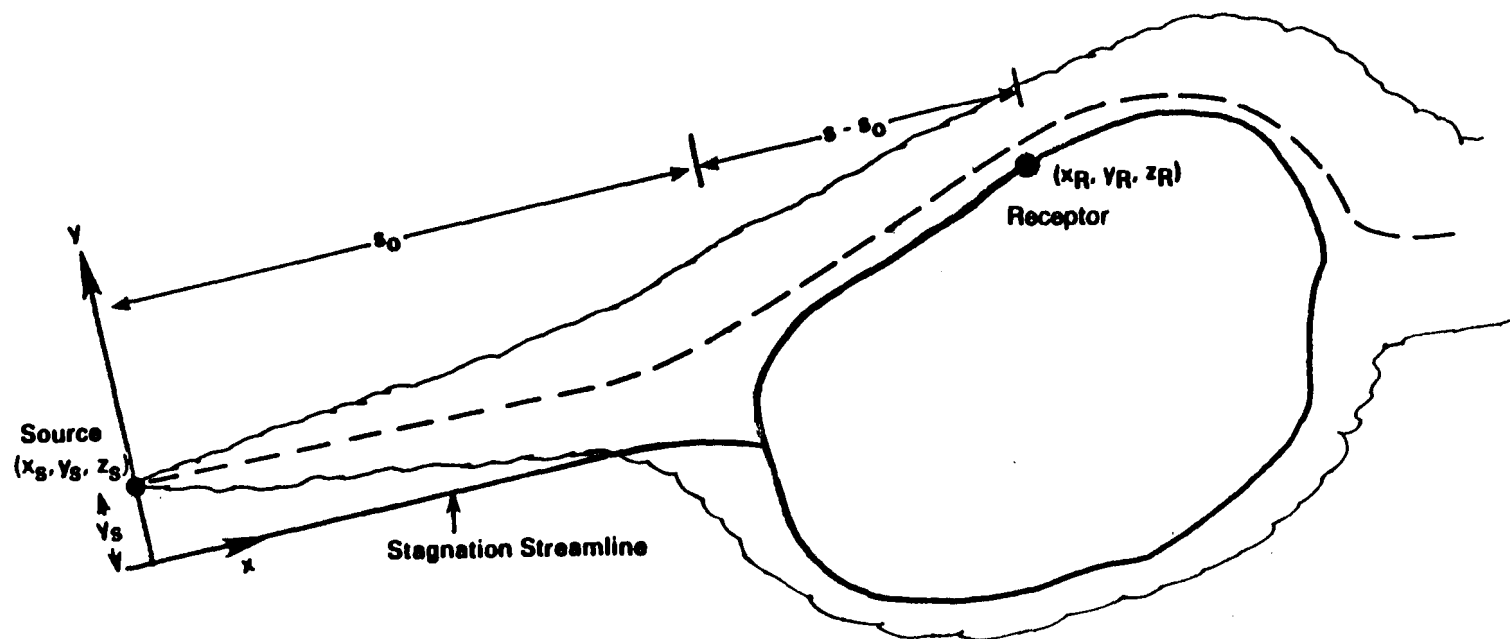


Figure 2-9. Top view of a plume in two-dimensional flow around a hill. The shape of the hill in cross-section at the receptor height is assumed to be invariant with height so that the deformation of the entire plume around the hill is a function of the receptor location.

These expressions are analogous to Equations 34 and 35 of the LIFT component. The integral for dy has the limits (0) and (∞). This is meant to denote integration from 0 to $+\infty$ if the receptor lies on the "positive" side of the stagnation streamline, and integration from $-\infty$ to 0 if the receptor lies on the "negative" side. Note that material is allowed to diffuse upwards through H_c so that receptors which lie above H_c , and which are downwind of s_o , can receive a contribution from the elemental point-sources below H_c at s_o . The total concentration at such receptors is the sum of both the LIFT and WRAP contributions.

The integrals in Equation 42 are evaluated to obtain:

$$C(s, O, z_R; s_o) = \frac{Q}{4\pi u \sigma_y \sigma_z} e^{-0.5\left(\frac{d}{\sigma_y}\right)^2} \left[1 + \text{sign}(y_R) \text{ERF} \left(\frac{d\sigma_y^*}{\sqrt{2}\sigma_{y_o}\sigma_y} \right) \right] \cdot \left(B_1 e^{-0.5\left(\frac{z_s - z_R}{\sigma_z}\right)^2} + B_2 e^{-0.5\left(\frac{z_s + z_R}{\sigma_z}\right)^2} \right) \quad (44)$$

Most of the notation here has already been encountered in Section 2.5. The factor 'sign (y_R)' denotes the sign of the receptor position in the coordinate system with x-axis aligned with the flow, and it results from the choice of integrating over the "positive" or "negative" portion of the flow in Equation 42. The factors B_1 and B_2 are given by

$$B_1 = \text{ERF} \left(\frac{b_1 - b_2 - b_3}{b_o} \right) + \text{ERF} \left(\frac{b_1 + b_2 + b_3}{b_o} \right)$$

$$B_2 = \text{ERF} \left(\frac{b_1 - b_2 + b_3}{b_o} \right) + \text{ERF} \left(\frac{b_1 + b_2 - b_3}{b_o} \right) \quad (45)$$

where

$$b_o = \sqrt{2}\sigma_z\sigma_{z_o}\sigma_z^*$$

$$b_1 = H_c\sigma_z^2$$

$$b_2 = z_R\sigma_{z_o}^2$$

$$b_3 = z_s\sigma_z^{*2}$$

The subscript R denotes the receptor location, and the subscript s denotes the source location (see Figure 2-10). The distance from the stagnation streamline associated with the mean wind direction to the centerline of the plume is denoted as d ; the total σ_y indicates the horizontal spread of the mean plume,

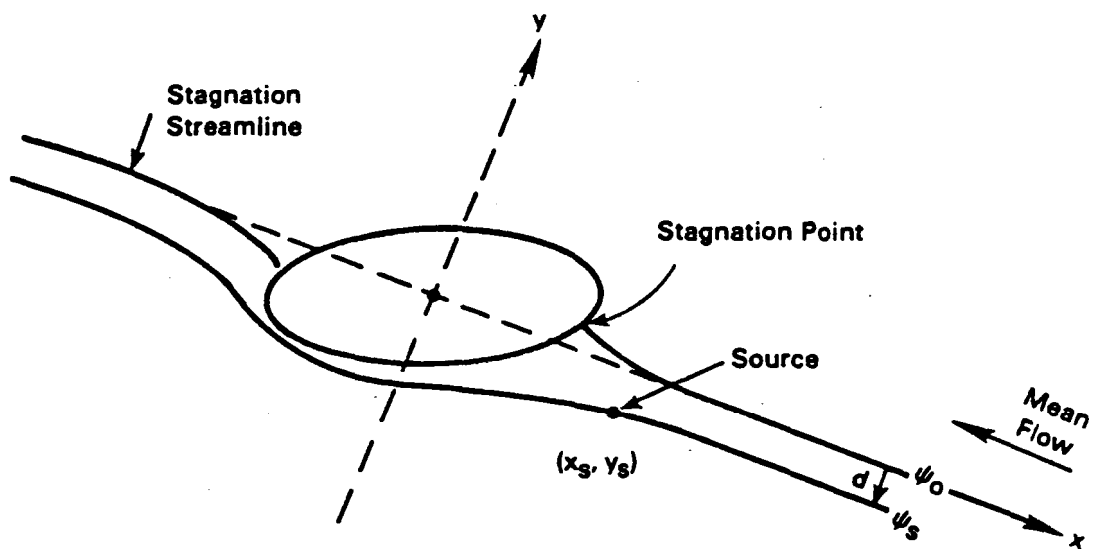


Figure 2-10. Sketch of the flow around an ideal cylinder of elliptical cross- section. The section shown is taken either at the elevation of the centerline of the plume (z_s), or at H_c , depending on which is smaller, and it indicates the relationship between the streamline through the source (ψ_s), the stagnation streamline ($\psi_o = 0$), and the coordinate system with x-axis aligned with the mean wind direction.

and the total σ_z indicates the vertical spread. The amount of plume spread experienced over the distance to the stagnation point is denoted as σ_{z_o} and σ_{y_o} , and the rate of plume growth beyond the stagnation point to the receptor is denoted as σ_z^* and σ_y^* , where

$$\begin{aligned}\sigma_z^{*2} &= \sigma_z^2 - \sigma_{z_o}^2 \quad \text{and} \\ \sigma_y^{*2} &= \sigma_y^2 - \sigma_{y_o}^2\end{aligned}\quad (46)$$

The ellipse that is used to estimate the flow below H_c is taken from the horizontal cross-section of the hill at the minimum of the following two elevations: either the elevation of the centerline of the plume, or the elevation of H_c . In this way, the shape of the hill selected is associated with the peak concentration of plume material found within the layer of fluid below H_c .

Concentrations at receptors located on the hillside just upwind of the stagnation point are estimated as if the receptor sits on a pole of height equal to the receptor elevation above the base of the stack. Furthermore, the lateral distance between the plume centerline and the receptor is set equal to d , so that concentrations at all of these receptors are controlled by the amount of material on the stagnation streamline. In this way, plume material below H_c follows streamlines around the hill, and only material which diffuses onto the stagnation streamline impinges on the hill. The equation for estimating these concentrations is:

$$\begin{aligned}C &= \frac{Q}{2\pi u \sigma_y \sigma_z} \exp\left(-0.5\left(\frac{d}{\sigma_y}\right)^2\right) \\ &\cdot \left[\exp\left(-0.5\left(\frac{z_R - z_s}{\sigma_z}\right)^2\right) + \exp\left(-0.5\left(\frac{z_R + z_s}{\sigma_z}\right)^2\right) \right] \quad (47)\end{aligned}$$

Equations 47 and 44 provide estimates of ground-level concentrations of plume material before and after plume material above H_c is "removed," respectively. That is, the upper and lower portions of the flow do not become distinct until the impingement or stagnation point is reached.

2.7 RECEPTORS NOT TREATED BY LIFT OR WRAP

The LIFT and WRAP segments of CTDMPLUS compute concentrations at receptors that are located on hills beyond the impingement point. Receptors that are upwind of the impingement point, or those that are not associated with any of the hills in the modeling domain require separate treatment. This treatment is described in the following two sections.

2.7.1 Receptors Not Influenced by Hills

In theory (for stable/neutral conditions), the main subroutines of CTDMPLUS produce results which are identical to flat-terrain results in the limit that the hill height goes to zero. However, the LIFT and WRAP code is not designed to check for hill height of zero before executing statements that may require division by the hill height; and if it were, many extensive calculations would be needlessly executed, with the model returning no terrain-effects. Furthermore, the structure of these sections of the model requires that receptors be associated with specific hills wherein each hill requires extensive information. A flat terrain algorithm is included in the model to avoid such numerical problems and extra input requirements.

The flat terrain algorithm simply performs a Gaussian plume computation which assumes that there is no mixing lid, that all receptors lie on a single ground-plane, and that plumes travel in straight lines. All plume rise and growth algorithms match those used in the other sections of the model.

To invoke this algorithm, the user must select a hill number of zero for this receptor. Guidance on which receptors should receive this treatment may be found in Section 3.

2.7.2 Receptors Upwind of the Impingement Point

All receptors on a hill that lie upwind of the impingement point sample a plume that is diffusing as if all terrain were absent with respect to reflection from the lower boundary of the flow. That is, reflection is allowed only from the surface $z = 0$ (the reference plane for the terrain features), and no changes are made to the rates of diffusion. However, the sampling point is altered relative to the centerline of the plume.

Several possible receptor locations are sketched in Figure 2-11. The actual terrain surface can depart significantly from the simple terrain shape used in the model, and this leads to the situation illustrated. Not all of the receptors upwind of the impingement point may lie at elevations below H_c . The surface of the terrain beneath receptors 1 and 2 is below H_c , but because elevated receptors are allowed in the model, receptor 2 actually lies above H_c . At receptor 3, the surface of the terrain exceeds H_c , so that this receptor lies above H_c regardless of whether it is elevated or not. Each of these receptors is treated differently.

Receptor 1 lies within the two-dimensional flow below H_c that is deflected around the terrain. Therefore, the lateral position of the receptor is defined by the location of the stagnation streamline, as described in the WRAP component. The vertical position of the receptor is given by z_1 in the figure. Essentially, a standard WRAP-like computation is done for this receptor, except that plume material is allowed to diffuse across the stagnation streamline, and plume material above H_c has not been removed. (The removal of material above H_c and the imposition of a reflecting surface along the stagnation streamline is initiated once the flow has reached the impingement point.)

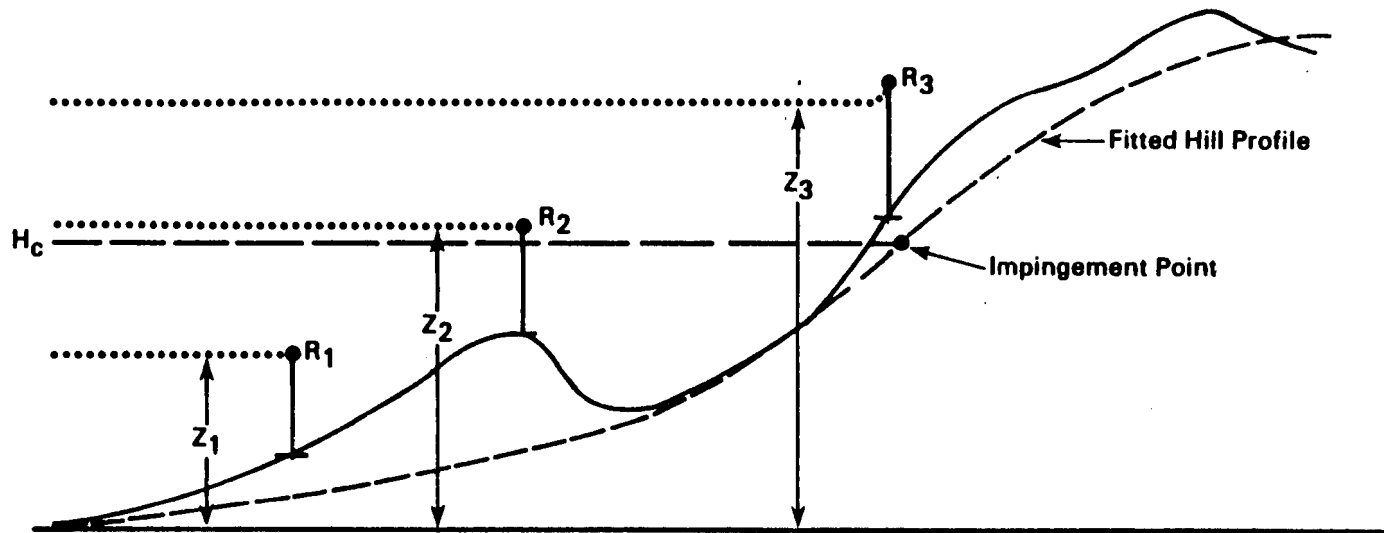


Figure 2-11. Treatment of receptors upwind of the impingement point. Receptors 1 and 2 sit above terrain that lies below H_c . Both are modeled as "receptors-on-poles", preserving their actual height (Z_1 and Z_2) above the reference plane. Receptor 3 is above terrain that exceeds H_c in elevation, so that the flow above H_c follows the surface of the hill. Therefore, the height of the "pole" Z_3 is less than the actual elevation of the receptor above the plane.

Receptor 2 lies in the flow that travels over rather than around the hill. Because it lies upwind of the impingement point, it is assumed to be upwind of the cut-off hill as well. The concentration is obtained at receptor 2 by assuming that terrain-effects are totally absent. Hence, the flat-terrain algorithm is used in combination with a "pole" height of z_2 as illustrated in the figure.

Receptor 3 is treated in nearly the same way. But because the terrain exceeds H_c at this location, the flow above H_c is assumed to rise. Therefore, without accounting for terrain effects on dispersion or streamline spacing, the streamline that passes through receptor 3 had originally been at an elevation of z_3 in the figure. The "pole" height, z_3 , for this flat-terrain calculation is the sum of the actual receptor elevation above the surface of the terrain and H_c .

2.8 PLUME PENETRATION INTO ELEVATED STABLE LAYERS

In modeling daytime unstable conditions, it is important to consider the interactions of elevated plumes with the top of the mixing layer. In particular, buoyant plumes are capable of partially or wholly exiting the mixed layer by penetrating into the stable layer aloft and thus becoming unavailable (except when re-entrainment occurs) for impact on receptors within the mixed layer and particular those at the surface. CTDMPLUS estimates the effects of plume penetration in the following way. Based on the integration of the buoyancy flux equation for a bent over buoyant plume and the assumption that the vertical plume distribution is rectangular ("top hat"), Briggs (1975) first defined a factor for estimating the fraction of the plume that will penetrate into the stable layer above a well mixed layer. This formulation has received some use in currently available models (in particular, the Rough Terrain Dispersion Model, Paine and Egan, 1987). However, Briggs (1984) points out that his 1975 penetration factor overpredicts penetration data measured by lidar at the Keystone power plant (Johnson and Uthe, 1969) and thus proposes a more conservative approach where the stratification of the elevated layer is assumed constant throughout the entire layer of rise. Then that portion of the plume above the mixing height, z_i , is assumed to penetrate and that below does not. In this way, the penetration factor becomes:

$$P = \frac{3.9 - z_b / (F_b / US)^{1/3}}{2.6} \quad (48)$$

where

$S = (g/\theta)(d\theta/dz)$ = the stability parameter,

$d\theta/dz$ = the potential temperature gradient above z_i

$z_b = z_i$ - stack height.

and F_b = plume buoyancy flux.

For the majority of the Keystone data, equation 48 provides a superior fit in comparison to the Briggs (1975) formulation and has been incorporated into CTDMPPLUS for plume penetration calculations.

Note that the use of this formulation requires an estimate or measurement of vertical potential temperature gradient in the stable layer aloft. A simple procedure for estimating this gradient from normally available meteorological data will be discussed in section 2.10.1.

Once the penetration factor, P , has been determined, the remaining plume material is defined by an adjustment of $(1 - P)$ to the original source strength and plume buoyancy flux. For example, if 30% of the plume penetrates into the stable layer then $P = 0.3$ and the source strength and buoyancy flux of the remaining plume becomes $0.7Q$ and $0.7F_b$, respectively. These adjusted values are then used in any subsequent calculations in the model.

2.9 THE VERTICAL DISTRIBUTION FUNCTION

CTDMPLUS calculates the vertical pollutant distribution separately from the horizontal distribution (discussed in section 2.11) and then combines the two to obtain the receptor dependent concentration. Section 2.9.1 contains a discussion of the probability density function approach used to obtain the vertical distributions and section 2.9.2 contains a description of the adjustments made to the PDF for terrain induced distortions in the flow.

2.9.1 The Probability Density Function (PDF)

The vertical distribution of pollutants (as discussed in Section 2.1.2) in a convective mixed layer has been observed to be strongly non-Gaussian. These observations are clearly reflecting the skewed distribution of vertical velocities that are present in a convective mixed layer and which are responsible for the distribution of passive pollutants. One approach to modeling this skewed distribution is with a probability density function (PDF) of the vertical velocities based on the observations available. Several PDF models are described in the literature (e.g. Weil and Furth, 1981, Misra, 1982, and Venkatram, 1983, and a review by Briggs, 1985).

CTDMPLUS employs a recently suggested (Li and Briggs, 1988) PDF approach which assumes (as do other PDF models) that the Lagrangian time scale is sufficiently large such that particles released into the flow maintain their initial trajectories until a boundary is reached. With the assumption that these particle trajectories are linear and have the slope w/U (w is vertical velocity and U is mean wind speed) as the air flows past the release point, a steady wind, time-averaged, crosswind-integrated concentration is given by

$$CWIC = \int \chi dy = (Q/x) P_w(w_z | z_s) \quad (49)$$

where Q is the release rate (source strength), P_w is the probability of $w_z = U(z - z_s)/x$, z_s is the effective source height, z is the receptor height, and x is the downwind distance. w_z is the convective vertical velocity that will take the particle from source to receptor.

For the direct path between source and receptor, z_s and z are the actual source and receptor heights. For particles that reach the receptor through one or more reflections from the surface or mixing height, z_s and z must be adjusted based on source/receptor/surface/mixing lid geometry. Assuming perfect reflections from the surface and mixing lid, the contribution to the total CWIC due to trajectory reflections can be calculated by applying equations 49 with virtual sources that are located vertically from the real source so that virtual trajectories intercept the receptor. Figure 2-12 illustrates the relationship between "image" sources and the paths (including one or more reflections) from the source to the receptor. The total CWIC as a result of direct path and reflected paths is the sum of values calculated by equation 49 for each path.

Calculating the crosswind integrated concentration (CWIC) removes lateral diffusion as an issue for the moment. In section 2.11 the horizontal distribution function (which is independent of the way in which the vertical diffusion is handled in CTDMPLUS) will be discussed as will the method for coupling it to the CWIC to obtain the concentration at a given receptor.

Li and Briggs (1988) examined a number of previously proposed PDF models and concluded that the CWIC was most impacted by the form of P_w chosen; assumptions that these models make about the reflections of the particles from the surface and mixing lid were found to be of minor concern. Therefore they elected to keep the reflection assumptions simple (perfect reflections assumed) and focus on developing forms of P_w that best described laboratory and field observations.

The PDF formulation of Li and Briggs (1988) which is contained in CTDMPLUS is an asymmetrical bi-Gaussian form that produces pollutant distributions very similar to those observed experimentally (Willis and Deardorff, 1981). The bi-Gaussian form of P_w (equation 4 in Li and Briggs) is

$$\begin{aligned} P_w &= G_m \exp[-w'^2/(2\sigma_{w+}^2)] & \text{for } w' > 0 \\ &= G_m \exp[-w'^2/(2\sigma_{w-}^2)] & \text{for } w' < 0 \end{aligned} \quad (50)$$

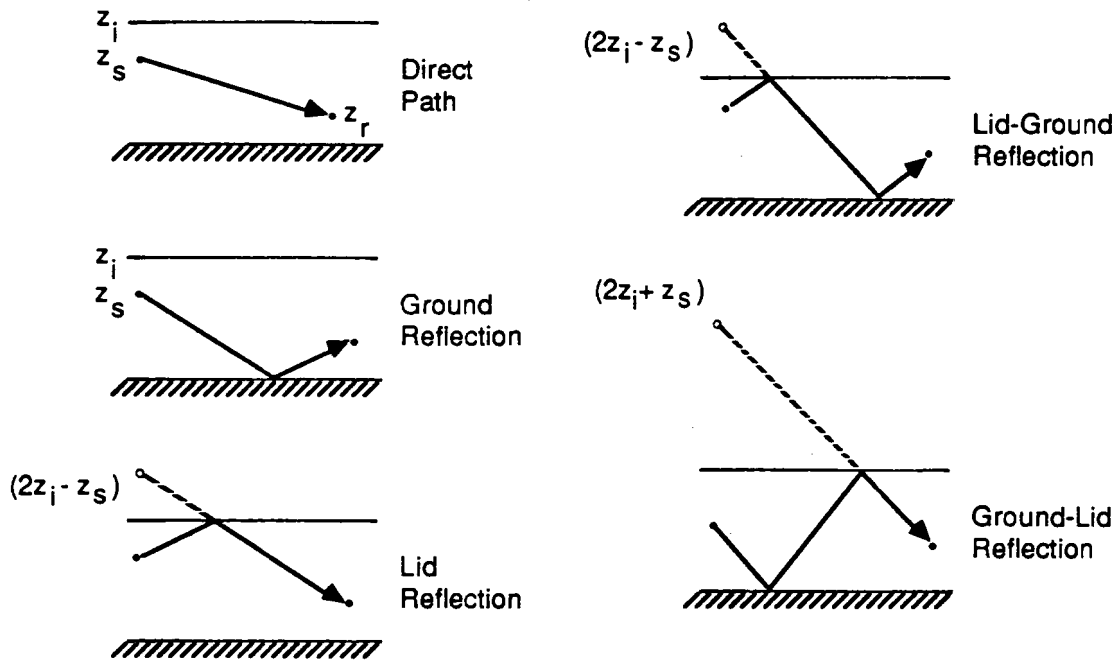


Figure 2-12. Illustration of the use of image sources to model possible paths between the point (x_s, z_s) and the point (x_r, z_r) .

where G_m is the maximum probability, $w' = (w - \hat{w})$, and \hat{w} is the mode of the vertical velocity. The standard deviation of the velocities above and below the mode are denoted by σ_{w+} and σ_{w-} respectively. The distribution in equation 50 is illustrated in Figure 2.13. The bi-Gaussian P_w is different from the standard Gaussian P_w in that for the bi-Gaussian \hat{w} is generally less than zero ($\hat{w} = \bar{w} = 0$ for Gaussian) and the distribution is skewed ($\sigma_{w+} = \sigma_{w-}$ for the Gaussian).

The bi-Gaussian skewed distribution is obtained by introducing an asymmetry (skewness) factor $\beta = [(\sigma_{w+}/\bar{\sigma}_w) - 1] = (1 - \sigma_{w-}/\bar{\sigma}_w)$ where $\bar{\sigma}_w = (\sigma_{w+} + \sigma_{w-})/2$. With these definitions, equation 50 can be evaluated with the following relationships (Appendix A of Li and Briggs, 1988):

$$G_m = 1/[\bar{\sigma}_w \sqrt{2\pi}] \quad (51)$$

$$\hat{w} = -\bar{\sigma}_w \beta \sqrt{8/\pi} \quad (52)$$

$$\sigma_{w+} = \bar{\sigma}_w (1 + \beta) \quad (53)$$

$$\sigma_{w-} = \bar{\sigma}_w (1 - \beta) \quad (54)$$

$$\bar{\sigma}_w = \sigma_w / (1 + (3 - 8/\pi)\beta^2)^{1/2} \quad (55)$$

Based on observations, Li and Briggs suggest approximating σ_w (in equation 55) as $0.5w_*$, where w_* is the convective scaling velocity. This approximation is used in CTDMPPLUS.

The asymmetry factor, β , ranges from 0 to 1.0 with a value of zero yielding the standard Gaussian distribution. A β value of 0.7 yields results very similar to the experimental distributions of Willis and Deardorff (1981). $\beta = 0.7$ is used in CTDMPPLUS. Further refinement of β (perhaps making it a function of release height) may be practical after further study. For further details concerning the bi-Gaussian PDF, the user is referred to the Li and Briggs paper.

A comparison of the vertical pollutant distribution based on the Gaussian PDF, the bi-Gaussian (BG) PDF, and the tank experiments of Willis and Deardorff (1981) is seen in Fig. 2.14. The BG model reproduces the tank results very well with the maximum surface CWIC occurring with about the same magnitude and at about the same location. The standard Gaussian results where the mode remains elevated do not compare as favorably.

The PDF model, as described, gives no consideration to alterations to the vertical pollutant distribution by terrain distortion to the flow. The following section describes the use of the flow model (already present in the original CTDM code) to alter the trajectories of the pollutant particles in order to correctly

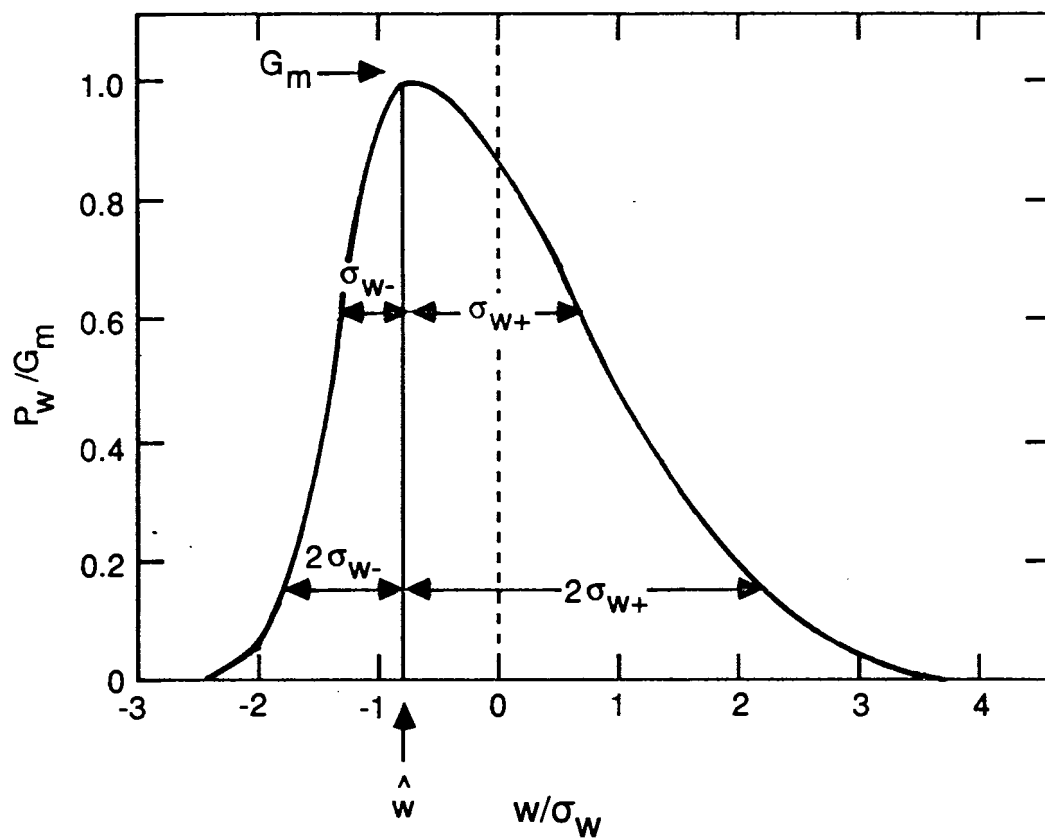


Figure 2-13. Illustration of the bi-Gaussian distribution of P_w .

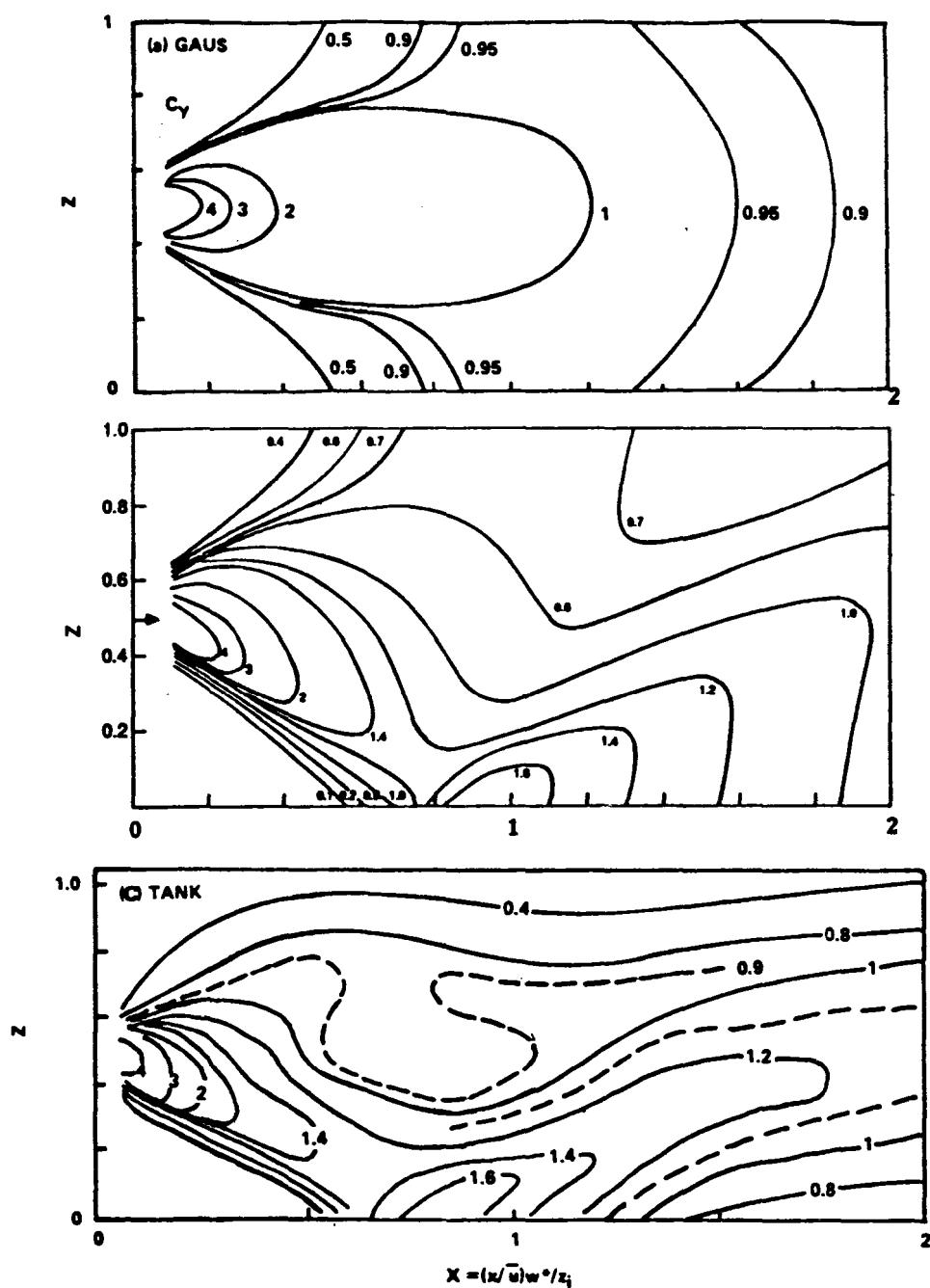


Figure 2-14. Comparison of normalized crosswind integrated concentration contours as a function of $Z = z/z_i$ and X for a) Gaussian model, b) bi-Gaussian PDF model (revised from Li and Briggs, 1988), and c) Willis and Deardorff (1981) tank data. Note the slightly expanded abscissa of figure c), but each figure has X ranging from 0 to 2.

connect the release points with the receptor points through a terrain distorted flow field. Since the convective vertical velocity producing a trajectory from the source to a receptor on a hill is different from that in the absence of the hill, the probability (equation 50) and the crosswind integrated concentration (equation 49) will differ for the receptor on the terrain.

2.9.2 Terrain Influences on the PDF

A primary assumption in the PDF approach is that a particle is given an initial convective vertical velocity at the source (or effective source) height which it "remembers" throughout its trajectory. When complex terrain is not present and straight line flow is assumed, the flat terrain PDF described in section 2.9.1 is adequate to describe the CWIC distribution. When complex terrain is present, it is necessary to account for the effect of perturbations in the flow field on the particle trajectories.

We know the positions of the source and the receptor but we do not know the convective vertical velocity which, when added to the terrain-perturbed flow will result in a trajectory from source to receptor. This must be found with an iterative approach. In each iteration a backwards trajectory is calculated from the receptor toward the source based on the terrain-perturbed flow and the superimposed convective vertical velocity. This trajectory is taken backwards until the x coordinate of the source is reached. A revised estimate of the vertical velocity is based on how far the end point of the backwards trajectory is displaced from the source position in the x-z plane. The iterations continue until a vertical velocity is found that connects the source to the receptor through the disturbed flow.

Before beginning the iterative process, a first and second guess of the vertical velocity must be obtained. A first guess for the vertical velocity, w_1 , is computed as the average of the unperturbed (no hill) vertical velocities needed to reach receptors if they were placed at $z = 0$ and on a pole at $z = z_r$ (the height of the receptor above base elevation). Defining receptor variables with subscript r and source variables with subscript s , these vertical velocities are calculated as:

$$w = Uz_s/(x_s - x_r) \quad \text{for receptor at } z = 0 \quad (56a)$$

$$w = U(z_s - z_r)/(x_s - x_r) \quad \text{for receptor at } z = z_r \quad (56b)$$

The first guess for the convective vertical velocity becomes the average of estimates in equations 56a and 56b such that:

$$w_1 = U(2z_s - z_r)/2(x_s - x_r) \quad (57)$$

w_1 is then used to estimate the second guess, w_2 . w_1 is used to calculate a back trajectory through the perturbed flow from the receptor point (x_r, z_r) to the point (x, z) where the flow first becomes unperturbed (assuming that the source is upwind of the terrain perturbations). If the source is within the perturbed flow region, the backward trajectory is calculated to the point (x_s, z) where the trajectory crosses the y-z plane containing the source, and the point (x_s, z) should be used in place of (x, z) in the following discussion.

Having determined the point (x, z) , the second estimate of the convective vertical velocity, w_2 , is made in one of two ways. The first is an intercept method, illustrated in Figure 2-15. m is defined as the slope of the line tangent to the trajectory at the point (x, z) where flow perturbations become negligible. Since both U and w_1 are constant in the unperturbed flow region, $m = w_1/U$. This tangent line crosses the x-axis at x_i where $x_i = x - z/m$. The second estimate of vertical velocity is based on the slope (m') of the line from the source to x_i where $m' = z_s/(x_s - x_i)$ such that:

$$\begin{aligned} w_2 &= U m' = U \left[\frac{z_s}{x_s - x_i} \right] \\ &= U \left[\frac{z_s}{(x_s - x_i) + z/m} \right] \end{aligned} \quad (58)$$

When the slope m is small, causing numerical problems in equation 58, the intercept method is replaced with a weighted average approach for estimating w_2 . This approach is illustrated in Figure 2-16. Again, m is the slope of the line tangent to the trajectory at the point (x, z) ; m'' is the slope of the line connecting the source (x_s, z_s) to the point (x, y) . Then an average of m and m'' , each weighted by the x distance over which it applies, is used to estimate w_2 :

$$w_2 = \frac{U[m''(x - x_s) + m(x_r - x)]}{x_r - x_s} \quad (59)$$

These first two estimates of vertical velocity are used to begin an iterative process in which each subsequent estimate is found, using a linear interpolation method (regula falsi technique).

Starting with w_1 and w_2 , the procedure begins by calculating backward trajectories from the receptor to points (x_1, z_1) and (x_2, z_2) respectively (refer to Figure 2-17). Using the slope of the tangent to the trajectory at each of these points, the trajectories are continued backward until they intersect the x-y plane of the source. (If the source is in the perturbed flow region, the points (x_1, z_1) and (x_2, z_2) will

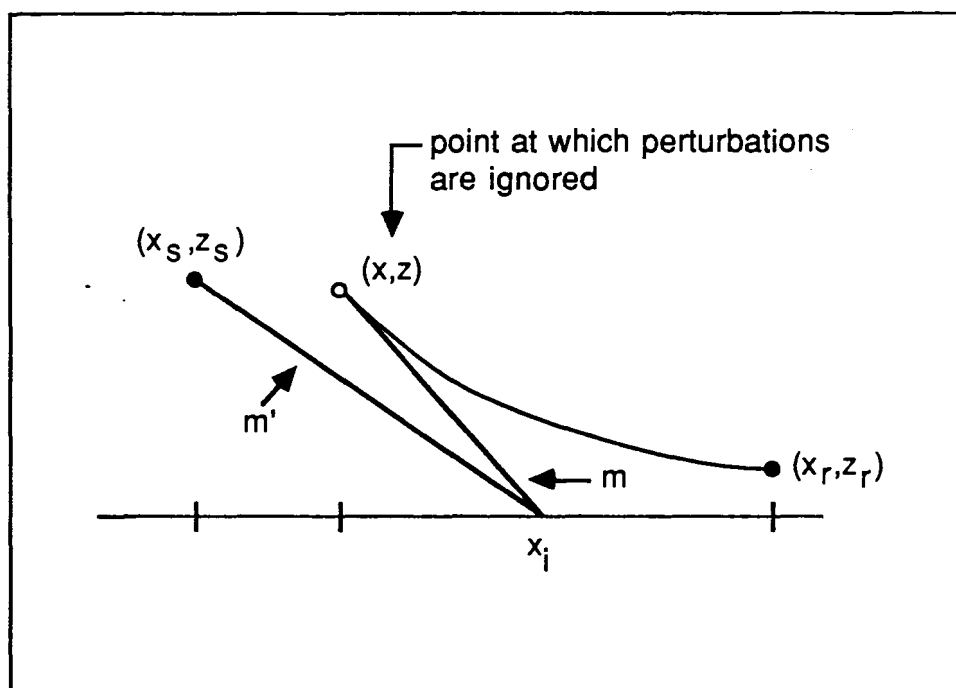


Figure 2-15. Illustration of the intercept method used for finding a second estimate of the vertical velocity (w) that carries a parcel from (x_s, z_s) to the point (x_r, z_r) in a deformed flow over a hill.

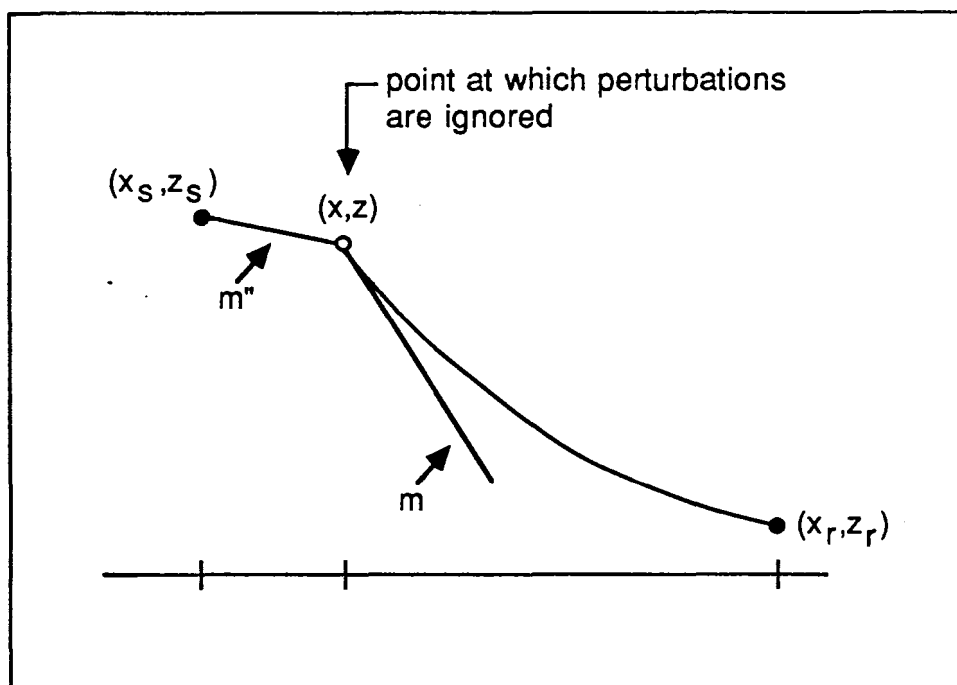


Figure 2-16. Illustration of the weighted average approach used for finding a second estimate of the vertical velocity (w) that carries a parcel from (x_s, z_s) to the point (x_r, z_r) in a deformed flow over a hill.

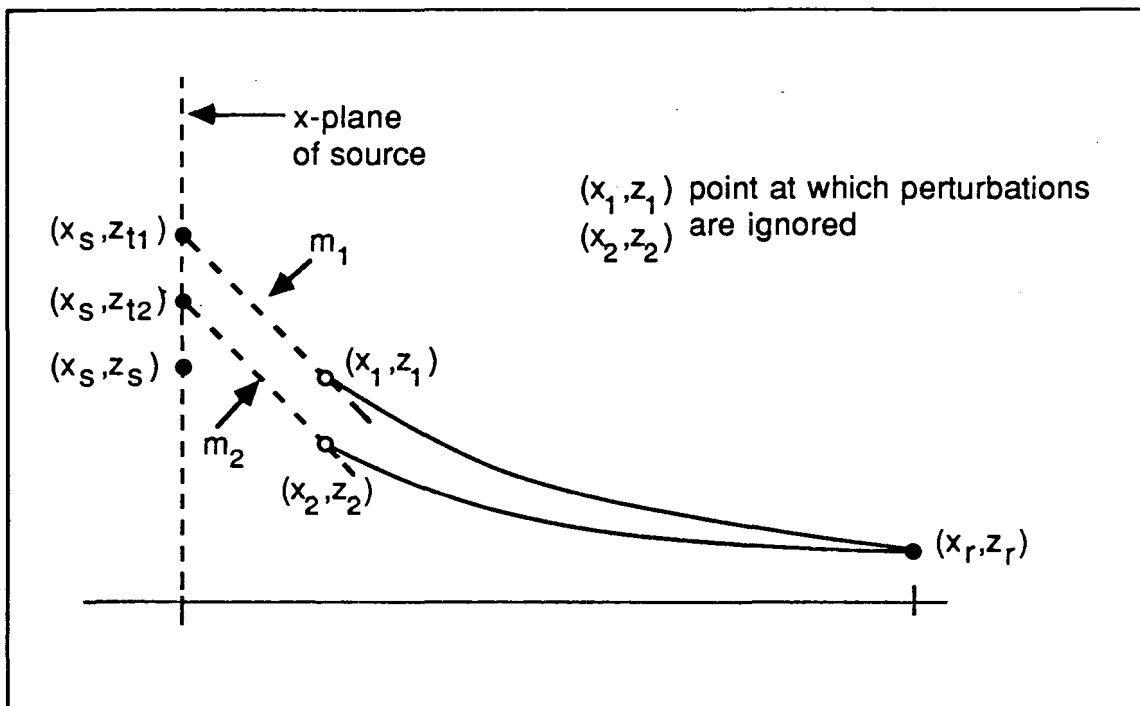


Figure 2-17. Illustration of the linear interpolation method used iteratively to determine estimates of the vertical velocity (w) that carries a parcel from (x_s, z_s) to the point (x_r, z_r) in a deformed flow over a hill.

already be in the x-y plane of the source). These points of intersection are denoted as (x_s, z_{i1}) and (x_s, z_{i2}) in Figure 2-17. The vertical difference between each of these points and the source point is calculated and defined as:

$$f_1 = z_{i1} - z_s$$

$$f_2 = z_{i2} - z_s$$

These values of f_1 and f_2 measure how close the corresponding w_1 and w_2 are to the true value producing a trajectory from source to receptor. The new estimate of vertical velocity, w_3 , is found by interpolating between w_1 and w_2 such that:

$$w_3 = (f_1 w_2 - f_2 w_1) / (f_1 - f_2) \quad (60a)$$

With this new estimate of w the iterations continue by calculating a third backward trajectory and proceeding as above, so that, in general, subsequent estimates are made using the following expression:

$$w_N = (f_{N-2} w_{N-1} - f_{N-1} w_{N-2}) / (f_{N-2} - f_{N-1}) \quad (60b)$$

As the correct value of w is approached in these iterations, the value of f is minimized; the iterations continue until f_N is negligible. Then w_N will be the vertical velocity that will "send" the particle along a trajectory through the disturbed flow to the receptor. It is this vertical velocity that is then used in equation 49 to obtain the probability estimate for equation 50.

If the elevated terrain is removed or if a particular receptor is not associated with a terrain feature, CTDMPPLUS will return a flat terrain PDF result (as found in Li and Briggs, 1988).

In a convective boundary layer, there is a distance (travel time) downwind from the source where the pollutant released from a point source will be sufficiently well mixed through the vertical layer that no significant vertical gradient of concentrations will exist. This distance will be proportional to the time scale associated with the largest convective eddies, w_e / z_i , and the horizontal wind speed. Beyond the point where the pollutant is thought to be uniformly mixed, the effect of terrain is only important in terms of the

horizontal distribution function. Therefore, for receptor downwind distance where $X > 4$, CTDMPLUS calculates the CWIC as if the terrain is flat and the pollutant uniformly mixed in the vertical. Terrain effects on the lateral separation of source and receptor are maintained at all downwind distances.

2.10 TERRAIN INFLUENCE ON MIXING HEIGHT

Current formulations for models in regulatory use provide, if any, a constant type of correction factor which results in z_i adjustments ranging from no change to values of z_i that follow the terrain. Some, for example, apply a "half-height" correction to both the plume and to z_i in unstable conditions. This approach has merit in that it is based upon typical potential flow solutions for distortions of streamlines over a two-dimensional ridge. However, consideration should be given to variations in controlling meteorology and terrain shape. In addition, the constant correction factor approach has the effect of correcting the mixing height over the entire distance from source to receptor even though the distortion may only occur over a small portion of that distance.

For CTDMPLUS, we selected a somewhat different approach to modeling adjustments to the vertical pollutant distribution caused by terrain induced distortions in the mixing height. This approach is based upon a recent fluid modeling study (Perry and Snyder, 1989) of deflections of z_i over terrain as functions of terrain shape, upstream z_i , and hill Froude number. The study results indicated that these parameters are important for scaling the dynamic response of the mixed layer depth to changes in topography.

To simulate the mean flow in a daytime well-mixed layer beneath a deep stable layer, Perry and Snyder used the large towing tank at the EPA Fluid Modeling Facility to measure vertical deflections of streamlines over the crest of the model hills. They identified four significant dimensional parameters: z_i , H (the hill height), U (the tow speed), and N (the Brunt-Vaisala frequency related to the elevated stable layer). From these they established two dimensionless products, $F_r = U/NH$ and z_i/H , which were used to scale their results.

They used two terrain features to obtain some appreciation for the degree to which terrain shape affects mixing height distortions. One feature (labeled ACCB) was an axisymmetric, polynomial-shaped hill with a center height, H , of approximately 15% of the total depth of the tank and a half-height radial dimension of $2.5H$. The second feature was an elongated (in the crossflow direction) version of the first, with a half-height radial dimension of $5.0H$.

A summary of the study is shown in figure 2-18. Figure 2-18a shows the deflection of z_i as a function of both initial z_i and hill Froude number for the axisymmetric hill. As the upstream height of the mixed layer is increased, the influence of the hill is decreased and the deflections in the z_i -streamline are reduced. For example, when $F_r = 1.54$, a doubling of the upstream z_i from one to two hill heights

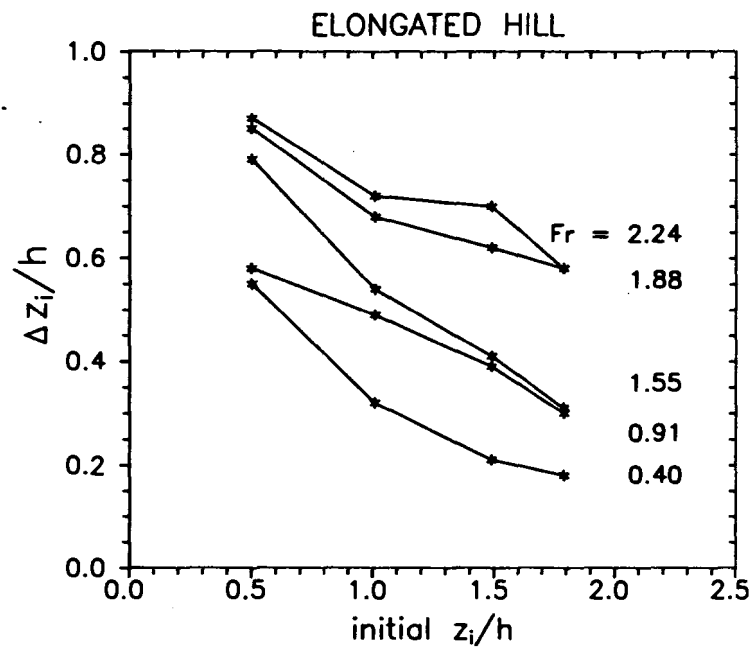
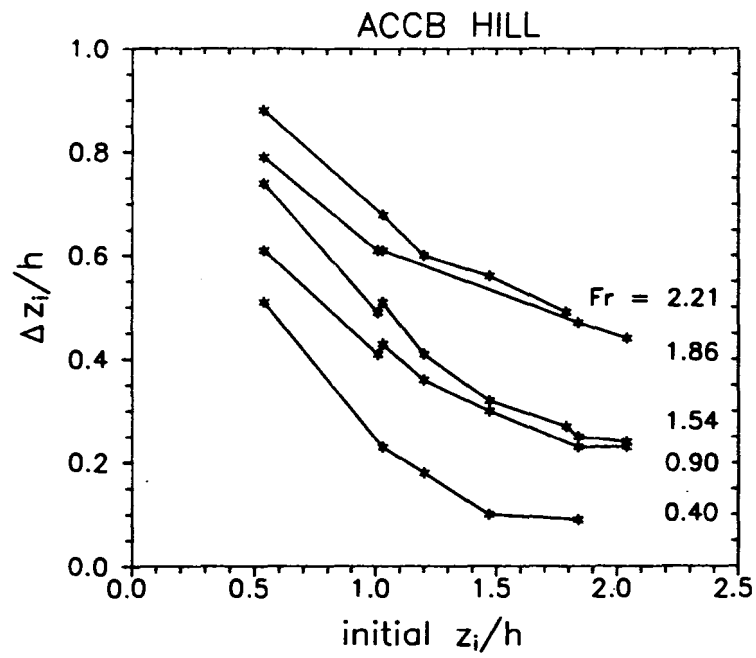


Figure 2-18. Fluid modeling results from Perry and Snyder (1989) showing deflections in the z_i streamline as a function of the initial z_i height and the hill Froude number for an (a) axisymmetric hill and (b) elongated hill.

results in a 52% decrease in the deflection over the hill top. For a given mixing height, an increase in the Froude number is associated with an increase in streamline deflections, signifying an increased ability of the flow to overcome the elevated stratification and push up over the hill top.

Figure 2-18b shows results for the elongated terrain feature where, in contrast, the magnitude of the deflections for any given F_r and z_i is greater than that for the symmetric hill. Since the elongated hill "appears" more like a ridge to the flow than does the ACCB, there is less lateral spreading of the streamlines over the crest and an increase in the vertical deflections.

In contrast to the half-height correction factor approach where the deflection in z_i is always a constant 0.5, figure 2-18 shows that, in fact, the amount of deflection is very much a function of meteorological variables. Over the range of F_r and z_i/H contained in their experiments, Perry and Snyder found the "correction factor" ranging from about 0.1 to 0.9. To account for these variations, CTDMPPLUS uses the results of Perry and Snyder (1989) to estimate the appropriate deflection to apply to the mixing height at the hill crest. Where necessary, interpolation between values is accomplished. In the present version of CTDMPPLUS, the study results are contained in a lookup table. Analytical fits to the data may be added at a later time.

To account for the effects of the z_i deflection on the flow within the mixed layer below z_i , CTDMPPLUS adjusts the flow model's stratification factor (Froude number) in order that the z_i -streamline deflection at the hill crest matches the fluid modeling results. Then, this adjusted flow model is used in the flow distortion corrections to the PDF model of the vertical distribution function. This prevents the flow model from calculating particle trajectories (based on streamline distortions) that might otherwise escape the mixing layer. This type of bulk correction to the flow model calculations accounts for the influence that the elevated stable layer has on the vertical extent of the flow in a mixed layer over terrain.

In order to calculate the hill Froude number and thus apply the corrections described above, the Brunt-Vaisala frequency, N , for the layer above z_i must be calculated. This requires an estimate of the potential temperature gradient in that layer. The following section describes the simple method used in CTDMPPLUS to estimate that gradient.

2.10.1 Estimate of the Elevated Temperature Gradient

The gradient of potential temperature in the stable layer above the mixed layer is an important factor in determining the potential for plume penetration and for estimating the magnitude of the deflection in z_i . In most cases, measurements of the gradient in this elevated layer are not available for any given hour of the

day since tower measurements are normally limited to heights of 100 meters or so. Therefore CTDMPLUS is designed to store the morning temperature profile (provided in the RAWIN input file) and to use it throughout the day for estimating the gradient above z_i . The following approach is used.

Consider the morning temperature profile depicted in figure 2-19. As the sun rises and begins to heat the surface, a convectively well mixed (uniform temperature) layer develops near the surface and "grows" throughout the day. However, the temperature profile in a layer above z_i changes relatively little from that in the morning sounding. Of course this assumes that there is neither significant subsidence nor cold or warm air advection occurring in the upper layer. Having stored the morning sounding, for a given hour of the day the model can call for the temperature gradient that is appropriate for the layer just above z_i (model currently uses a layer from z_i to $z_i + 500m$).

Field measurements (e.g. the Wangara experiment, Clark et al., 1971) of observed profiles throughout the day lend support to this concept of using the the morning sounding throughout the day for upper level temperature gradient estimates. These data point out the relative invariance of upper level temperature data even during periods of intense heating at the surface.

2.11 THE HORIZONTAL DISTRIBUTION FUNCTION

Since significantly non-Gaussian plume shapes are not generally observed in relation to lateral diffusion, analytical diffusion models have retained the usual Gaussian form (Briggs, 1985). Therefore, CTDMPLUS uses the standard Gaussian form for the horizontal distribution function (HDF)

$$HDF = \frac{1}{(2\pi)^{1/2}\sigma_y} \exp[-0.5(y/\sigma_y)^2] \quad (61)$$

where y is the effective crosswind distance from plume centerline and σ_y is the lateral dispersion coefficient. Equation 61 can be combined with the crosswind integrated concentration, CWIC (discussed in section 2.9) to extract the field of concentrations as a function of downwind and crosswind distance. The concentration at any receptor (x_r, y_r, z_r) is then

$$C(x_r, y_r, z_r) = \frac{CWIC}{(2\pi)^{1/2}\sigma_y} \exp\left[-0.5\left(\frac{y}{\sigma_y}\right)^2\right] \quad (62)$$

The flow model used to calculate the trajectories for the PDF submodel (section 2.9) also provides the lateral distance $(y, -y')$ between the source and the trajectory passing through the receptor because the endpoint of the trajectory returned by the submodel is at (x, y', z) . This distance $(y, -y')$ differs

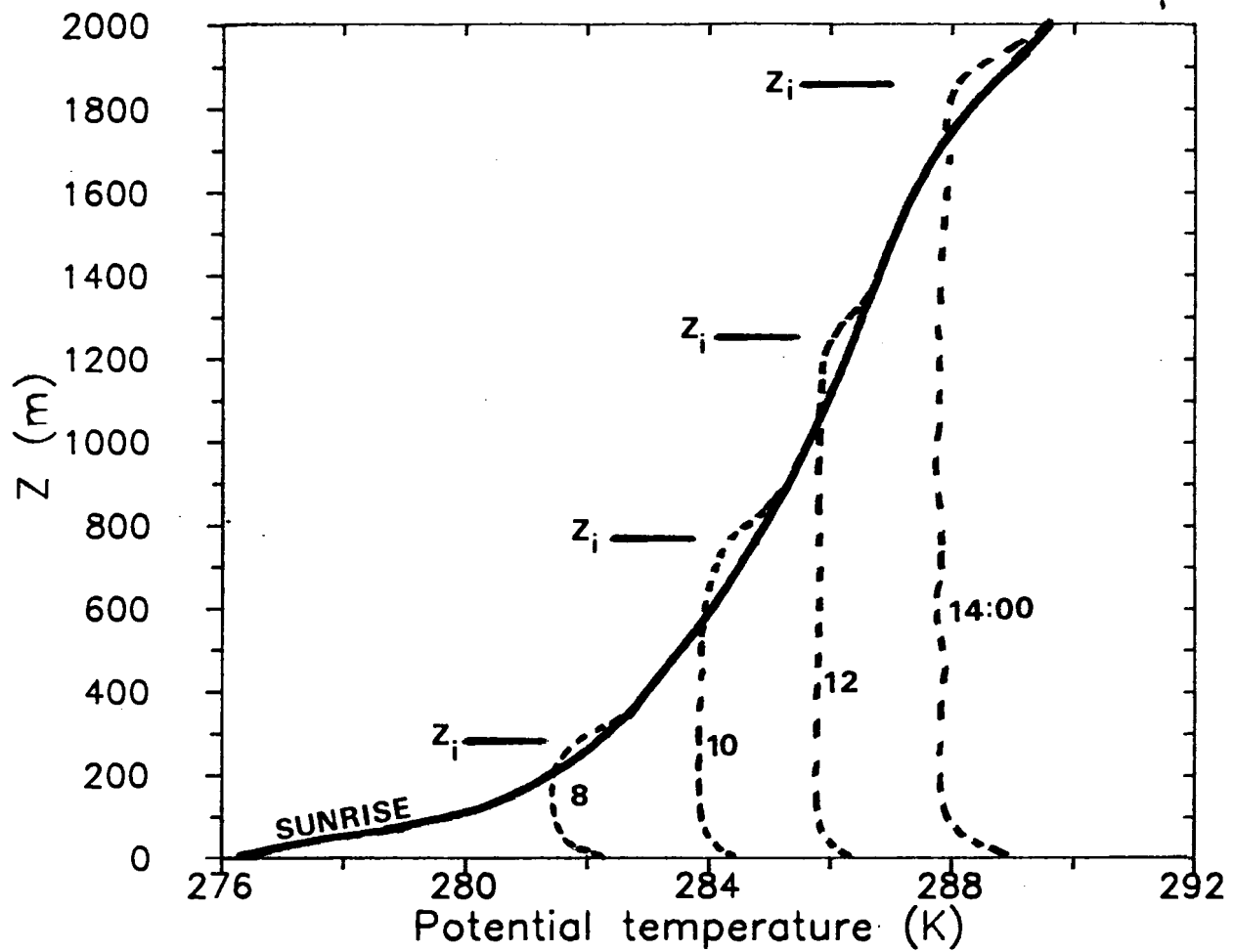


Figure 2-19. Typical profile of mean potential temperature showing the growth of the well mixed layer throughout the day. At each time of the day, the potential temperature gradient above z_i does not differ significantly from the gradient of that level in the morning sounding.

from the geometric source-receptor separation $(y_s - y_r)$ because the deflection of the flow around the terrain alters the relative position of the receptor within the streamlines of the flow. Therefore y of equation 62 is set equal to $(y_s - y')$ remembering that y' is related to y through the flow model calculations. For flat terrain (no flow distortion) y reduces to the expected $(y_s - y_r)$.

The remaining parameter to specify in equation 62 is the lateral dispersion coefficient, σ_y . Recent literature has been generous with parameterizations of σ_y applicable to daytime convective boundary layers which are primarily based on convective scaling concepts and on analyses of available data (field, fluid modeling, and numerical). Hanna (1986) points out, quite correctly, that there are about as many σ_y parameterizations as there are data sets. Briggs (1985) reviewed a number of formulations for σ_y each of which has its own merits compared to particular data sets. The formulation chosen for CTDMPLUS was one suggested by Briggs (1985) after an analysis of Weil's (1977) power plant data and which was also recommended by Hanna (1986) after an analysis of other power plant data. This parameterization, for highly buoyant plumes ($F_b > 0.10$), is:

$$\sigma_y = 1.6 z_i X^{2/3} F_b^{1/3} \quad (63)$$

where

z_i = mixing height

$X = \frac{v \cdot x}{u z_i}$ = non-dimensional downwind distance

$w_* = u_* \left(\frac{z_i}{-0.4L} \right)^{1/3}$ = convective scaling velocity

L = Monin-Obukov length

u_* = friction velocity

$F_b = F_b / (U w_*^2 Z_i)$

and

F_b = plume buoyancy flux.

Briggs found that equation 63 fits the data reasonably well except for very light wind conditions where $U/w_* < 1.5$ (these conditions may need to be handled separately but are not currently so in CTDMPPLUS). In addition, Hanna found that at certain distances downwind (where perhaps the buoyancy is no longer important) the data better supported a linear growth with non-dimensional distance of the form

$$\sigma_y = 0.6 z_i X \quad (64)$$

Therefore, for buoyant plumes in a convective layer, the lateral dispersion coefficient is modeled in CTDMPPLUS with equation 63 except when $X > 1$ (or $X/F_* > 17$) where equation 64 is used.

For the case of passive plumes ($F_* < 0.10$), the choice of σ_y is based on the results of studies concerned primarily with non-buoyant, elevated releases. Briggs (1985) accumulated data from a number of field studies including Prairie Grass (Barad, 1958), Cabauw (Agterburg et al., 1983), and Condors (Kaimal et al., 1986), laboratory results of Willis and Deardorff (1976, 1978, 1981), and numerical modeling by Lamb (1979). Briggs suggested a reasonable fit to the bulk of the data to be

$$\sigma_y = \frac{0.6 z_i X}{(1 + 2X)^{1/2}} \quad (65)$$

Others (e.g. Venkatram and Vet, 1981) have observed the slow departure of σ_y from a linear growth with X and have proposed simple linear formulas. The scatter in the data is such that any number of possible formulas could be justified. However equation 65 is an adequate fit to a majority of the data with the added attraction of being a particularly good fit to the convective tank data; thus it is used as the passive plume lateral dispersion coefficient for CTDMPPLUS.

SECTION 3

USER INSTRUCTIONS FOR RUNNING CTDMPLUS

3.1 OVERVIEW

CTDMPLUS is a refined model designed for complex terrain applications. Accordingly, a considerable amount of data preparation needs to be done prior to running the model, especially for terrain and meteorological data. Figure 3-1, a schematic of the system flow, shows the input files for each of the programs.

CTDMPLUS requires a mathematical depiction of the shape of each terrain feature (hill) that is associated with at least one model receptor. The terrain preprocessor programs must be run to generate the terrain input to CTDMPLUS unless the required hill shape functions are already known. The terrain preprocessor user's guide (Mills et al., 1987) gives a complete description of the procedure for generating the required terrain input file. A brief summary is given here.

The user first obtains a topographic map of the area of interest and selects the specific features (isolated hills or distinct portions of "complex" hills) that are to be modeled. Then, several contours must be digitized; that is, (x, y) points along the contour are determined with enough resolution so that the line segments connecting the points are a good representation of the actual map contour. The vertical spacing between contours that are digitized should be small enough so that detailed information about the shape of the hill is retained. However, unnecessary detail and work could result if every contour were digitized. In general, at least 5-10 contours for each hill is desirable. A maximum of 21 contours is imposed by the terrain preprocessor. The actual digitization can be done on a graphics board or can be done by an outside vendor, as long as the format specifications required by the terrain preprocessor are followed.

The terrain preprocessor programs FITCON and HCRIT should be run first. Both FITCON and HCRIT require an options file, "FOPTIONS" and "HOPTIONS", respectively. The formats of these options files are shown in Table 3-1 and Table 3-2. Once FITCON has been run to read and process the digitized contours, the user has the terrain information necessary to run the receptor generator program, RECGEN, if desired (RECGEN is described further in Section 4.1). The output file from HCRIT contains the mathematical hill descriptions in the correct format for input to CTDMPLUS. CTDMPLUS requires that the lowest critical elevation be at or below the common stack base (the lowest base elevation of the meteorological tower and stacks). If the defined hill does not extend to the common base, HCRIT can be used to extrapolate the hill downward to that level by using mode 2 (modes are discussed in the terrain preprocessor user's guide). The mathematical fit to the actual contours can be plotted by running a third program, PLOTCON.

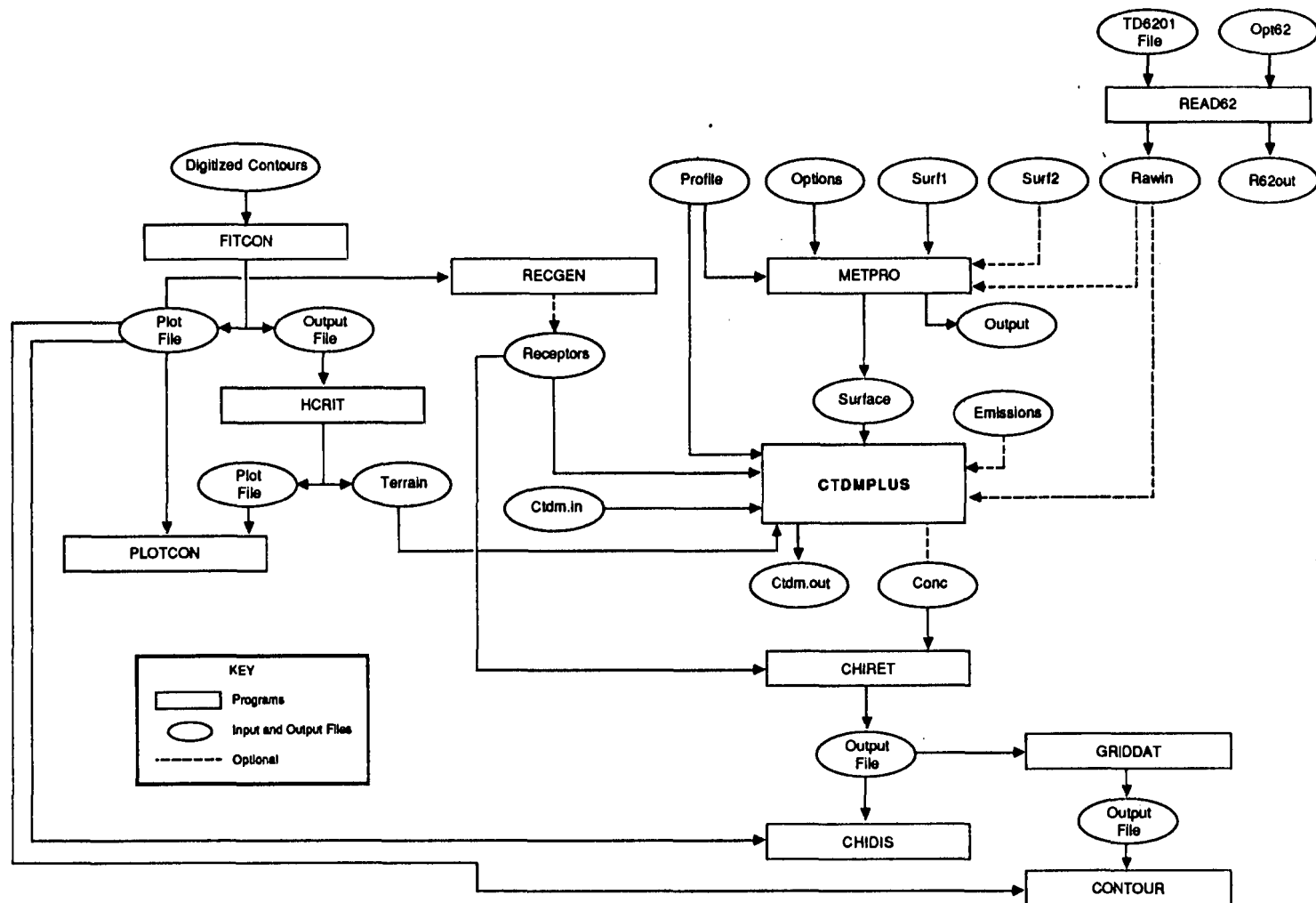


Figure 3-1. Interaction among components of the CTDMPPLUS system.

TABLE 3-1. FORMAT OF THE "FOPTIONS" FITCON OPTIONS FILE

Record Group	Format	Description
1	A12	Contour master file name
2	A12	Diagnostic output file name
3	I2	Hill identification number
4	A8	Hill name
5	F10.4	Hill top elevation (user units)
6	F10.4	Hill center x-coordinate (user units)
7	F10.4	Hill center y-coordinate (user units)
8	A1	Angular filtering option (y or n)
9*	A4.1	Angular filtering size
10	I1	Contour selection mode
11**	I4	Lower bound of contour identification numbers
12**	I4	Upper bound of contour identification numbers
13***	A12	Contour identification number file name
14	A1	Plot file option (y or n)
15*	A12	Plot file name
16	A12	Fitted output file name

Input value required only:

*If this option is selected

**If selection mode = 2

***If selection mode = 3

TABLE 3-2. FORMAT OF THE "HOPTIONS" HCRIT OPTIONS FILE

Record Group	Format	Description
1	A12	FITCON output file name
2	A12	HCRIT output file name
3	A1	Plot file option (y or n)
4*	A12	Plot file name
5	A1	Selection mode for critical elevations
6**	A3	Number of critical elevations
7**	F10.4	Lowest critical elevation (user units)

Input value required only:

*If this option is selected

**If selection mode = 2

Meteorological data is input to CTDMPLUS from three separate files. The first of these files, "PRO-FILE", is created by the user and should represent user-validated and quality-assured meteorological data consisting of conventionally available measurements of

- wind direction;
- wind speed [scalar, vector (optional)];
- air temperature;
- standard deviation of the horizontal wind direction (σ_θ) or of lateral wind speed (σ_v); and
- standard deviation of the vertical wind speed (σ_w).

These measurements can be provided at a number of levels (CTDMPLUS can accept up to 50 levels) and should extend upward into the region typically occupied by the plumes to be modeled.

The second meteorological data file, "RAWIN", consists of rawinsonde data created from a National Climatic Data Center TD6201 file by using the READ62 preprocessor [discussed in the meteorological preprocessor user's guide (Paine, 1987)]. The "RAWIN" file is required by CTDMPLUS only if the model is being run for unstable hours. The "RAWIN" file contains upper air measurements of

- air pressure,
- height above local ground,
- air temperature,
- wind direction, and
- wind speed.

CTDMPLUS uses this pressure and temperature information to determine the stability above the mixing height during daytime conditions. The meteorological preprocessor, METPRO, also uses the "RAWIN" data for calculating daytime mixed layer heights.

A third file required by CTDMPLUS, "SURFACE", consists of the following processed meteorological variables:

- Monin-Obukhov length (L),
- friction velocity (u_*),
- nighttime surface layer height (h), or daytime mixed layer height (z_i), and

- surface roughness length (z_0).

METPRO produces the "SURFACE" variables from the meteorological data in "PROFILE" and "RAWIN" and from additional radiation information (net or total incoming radiation or cloud cover) and surface characteristics [see METPRO user's manual (Paine,1987) for details].

The file "CTDM.IN" contains model switches, meteorological tower coordinates, and source information. Receptor information is supplied to CTDMPLUS in a file named "RECEPTOR". This file can be created with RECGEN, the receptor generator program, or with a text editor.

There is an optional input file to CTDMPLUS containing hourly emissions data ("EMISSION"). If the emissions do not vary, then this file is not necessary and the constant emissions data are read from "CTDM.IN".

CTDMPLUS executes for as many hours as are contained in the input meteorological data files. It can be run for a period as short as a single hour. Data in multiple-hour runs must be sequential. Information in the data files "SURFACE", "PROFILE", "EMISSION", and "RAWIN" must be chronologically consistent.

When CTDMPLUS is run, it produces a concentration file, in either binary or text format (user's choice), and a list file containing a verification of model inputs and case study output (also at the user's option). Another option is to print a table listing the contribution from each source to the total concentration at a receptor for each hour. A summary of the top four one-hour concentrations at each receptor for the entire run is included at the end of the list file if that display option is selected. The concentrations can be plotted onto a display of terrain contours by the CHIDIS postprocessor (see Section 4.3). Concentration isopleths can be displayed using the CONTOUR program available through the menu driver system (see Section 5.2.8).

The input files required for CTDMPLUS are described in detail in Section 3.2. A menu driver program that can be used to run the system using pre-existing files is described in detail in Section 5. An interactive program (SETUP) exists to aid users (especially new users) in constructing these files for short runs of CTDMPLUS. The SETUP program is described in Section 4.2.

3.2 INPUT DATA REQUIREMENTS

There are five required input files and two optional input files for CTDMPLUS. The five required files consist of:

- a general file of program specifications, which consist of program switches, source data, meteorological tower coordinates and hill surface roughness lengths ("CTDM.IN");

- a terrain data file which is obtained directly from the HCRIT terrain preprocessor ("TERRAIN");
- a file containing receptor names, locations, and the associated hill numbers ("RECEPTOR");
- a surface meteorological data file which is obtained directly from the METPRO meteorological preprocessor program ("SURFACE");
- a user-created meteorological profile data file which contains conventional meteorological data measured at multiple levels ("PROFILE");

The optional input data files consist of:

- a file of hourly emissions parameters ("EMISSION");
- a file containing upper air data from rawinsonde data which is obtained from the READ62 preprocessor ("RAWIN").

The input files are discussed in more detail in Sections 3.2.1 through 3.2.7. CTDMPPLUS output files are discussed in Section 3.3.

3.2.1 General Program Specifications

The input file "CTDM.IN" contains program options, meteorological tower coordinates, source data, and surface roughness lengths for each hill. The inputs and file formats are listed in Table 3-3 (a sample input file is shown in Figure B-1). Some program options control the amount of model output in the following areas:

- case-study printout (if used, a voluminous output results; use this only for short runs)
- summary table for the current run (if called, a table of the top four one-hour concentrations at each receptor is printed)
- file (either text or binary) of predicted concentrations for postprocessing
- hourly source contribution table.

Other program options, which control the use of input or output data, tell CTDMPPLUS to:

- choose which mixed layer height value to use if both measured or calculated mixed layer heights are provided (case-specific; in general, measured values should be used if available and of good quality)
- set the minimum scalar wind speed to 1 m/s (recommended for most applications)

TABLE 3-3. CONTENTS OF THE "CTDM.IN" FILE

Line Group #	Variable Name	Columns	Format	Description
1	Title	1-80	A80	80 Character header
2	ICASE	*	*	Case study printout option. 0=No, 1=Stable hours only, 2 = Unstable hours only, 3 = All hours
	ITOPN			Create a top 4 table at the end of the run. 0=NO, 1=YES
	ICONC	*	*	Concentration output file option. 0=NO, 1=BINARY, 2=TEXT, 3=TEXT with receptor information
	IMIX	*	*	0=use calculated mixing heights as first priority, 1=use observed mixing heights as first priority
	IWSI			Set minimum wind speed = 1.0 m/s. 0=NO, 1=YES
	ISIGV	*	*	Assume σ_0 input if 0; σ_v input if 1
	IWD	*	*	Scale wind direction with height. 0=NO, 1=YES
	ICHIQ	*	*	0=output concentrations ($\mu\text{ g}/\text{m}^3$) 1=output chi/Q ($\mu\text{ s}/\text{m}^3$)
	ISOR	*	*	Create a source contribution table at the end of the run. 0 = No, 1 = Yes
	IUNSTA	*	*	1 = Model unstable hours (RAWIN file required) and stable hours 0 = Model only stable hours
3	HORIZ	*	*	Horizontal scale factor, converts user units to meters
	VERT	*	*	Vertical scale factor, converts user units to meters
	RLAT	*	*	Site latitude (degrees)
	RLON	*	*	Site longitude (degrees)
	TZONE	*	*	Site time zone (hours behind GMT)
	IPOL	*	*	Pollutant Code (1-4)
4	LABEL	1-20	A20	Meteorological tower name
	XT	21-30	F10.0	X-coordinate of tower (user horizontal units)
	YT	31-40	F10.0	Y-coordinate of tower (user horizontal units)
	ZT	41-50	F10.0	Z-coordinate (user vertical units) of tower base
5**	SNAME	1-16	A16	16 character source name
	XS	17-23	F7.0	X-coordinate of source, (user horizontal units)
	YS	24-30	F7.0	Y-coordinate of source (user horizontal units)
	ZS	31-37	F7.0	Source base elevation (user vertical units)
	HS	38-44	F7.0	Stack height (m)
	DS	45-51	F7.0	Stack diameter (m)
	TS***	52-58	F7.0	Stack gas temperature (K)
	VS***	59-65	F7.0	Stack gas exit velocity (m/s)
	Q***	66-72	F7.0	Emission rate (g/s)
	IQ	80	I1	Variable emission rate flag for this stack (0=constant, 1-variable)
6	ENDS	1-4	A4	'ENDS'. Flag for end of source data.
7	ZOH	*	*	Surface roughness length (m) for each hill in the order that the hills appear in the TERRAIN file.

*Free format

**One line per source, maximum of 40 sources (maximum number can be changed)

***These values are replaced if hourly emissions data are provided for this stack.

- indicate which variable (either σ_θ or σ_v) is provided in "PROFILE" for the stable/neutral crosswind turbulence measurements
- scale wind direction with height (recommended unless the user is trying to "aim" the plume at a hill in a test run)
- display concentrations in units of mass per volume (chi) or chi divided by the emission rate (χ/Q)
- model all hours: stable, unstable, and neutral

The user is also asked to provide other program constants, such as:

- factors by which to multiply user units to obtain meters for both vertical and horizontal coordinates;
- site latitude, longitude, and time zone;
- pollutant code number for hourly emissions (1-4).

"CTDM.IN" includes the position (x,y,z) of the meteorological tower for the data contained in "PROFILE". The horizontal position, if on or near a hill modeled by CTDMPLUS, is used by the model to determine the upwind wind direction and speed. The vertical (tower base) information is used to reference the meteorological measurements relative to the common stack base; "PROFILE" contains the measurement heights relative to the local ground surface at the tower site.

Point source information (in "CTDM.IN") includes stack name, horizontal and vertical coordinates, stack height and diameter at the outlet, stack gas temperature, and exit velocity. Variable emissions for any subset of the total number of stacks is allowed. Emission rates for up to four pollutants may be included in the variable emissions file ("EMISSION"). The specific emission rate used for a given run is chosen via a pollutant code number. CTDMPLUS does not require stacks to be co-located, but a common stack base is retained for convenience; this is calculated to be the minimum of the tower base and the lowest stack base among those input. The lowest "critical elevation" specified in the terrain preprocessor HCRIT run for each hill must be at or below the common stack base to avoid a CTDMPLUS runtime error. The elevation of each stack top is preserved by adjusting the stack height if the base elevation is changed. Up to 40 sources can be input; this number can be altered by changing the code in the INCLUDE file "PARAMS.INC".

Surface roughness lengths for the local surface characteristics of each hill are given in "CTDM.IN". The values of these roughness lengths vary according to vegetative cover and season of the year. See Table 3-4 for guidance.

TABLE 3-4. EXAMPLE SURFACE ROUGHNESS LENGTHS,
FOR LAND USE TYPES AND SEASONS (METERS)

Land Use Type	Spring	Summer	Autumn	Winter
1. WATER (FRESH WATER AND SEA WATER)	0.0001	0.0001	0.0001	0.0001
2. DECIDUOUS FOREST	1.00	1.30	0.80	0.50
3. CONIFEROUS FOREST	1.30	1.30	1.30	1.30
4. SWAMP	0.20	0.20	0.20	0.05
5. CULTIVATED LAND	0.03	0.20	0.05	0.01
6. GRASSLAND	0.05	0.10	0.01	0.001
7. URBAN	1.00	1.00	1.00	1.00
8. DESERT SHRUBLAND	0.30	0.30	0.30	0.15

DEFINITIONS OF SEASONS:

"Spring" refers to periods when vegetation is emerging or partially green. This is a transitional situation that applies for 1-2 months after the last killing frost in spring.

"Summer" applies to the period when vegetation is lush and healthy, typical of midsummer, but also of other seasons in locations where frost is less common.

"Autumn" refers to a period when freezing conditions are common, deciduous trees are leafless, crops are not yet planted or are already harvested (bare soil exposed), grass surfaces are brown, and no snow is present.

"Winter" conditions apply for snow-covered surfaces and subfreezing temperatures.

3.2.2 Terrain Data

The terrain data file is created by the terrain preprocessor program and is used by CTDMPLUS without modification. This file contains the hill center, hill height, major axis orientation, ellipse major and minor axis lengths, and inverse polynomial lengths and exponents which are used to define the hill used by the WRAP and LIFT components of CTDMPLUS. The base of each hill must be at or below the common stack base. HCRIT, when run in mode 2, allows the user to select a range of elevations between which critical elevations will be spaced. This option allows the hill to effectively be extrapolated down to the common stack base. Table 3-5 shows the format of the "TERRAIN" input file; an example is shown in Figure B-2.

3.2.3 Receptor Data

The file "RECEPTOR", containing receptor names, coordinates, and hill number, is read by CTDMPLUS. This file can be used directly from the output of the receptor generator, RECGEN (see Section 4.1) or can be altered or created using a text editor. The format of this file is shown in Table 3-6 (an example is shown in Figure B-3). Up to 400 receptors can be input to CTDMPLUS; this number can be altered by changing the code in "PARAMS.INC".

Each receptor must have a hill number assigned. Those receptors which are beyond a digitized hill region (outside the "skirt" of any hill) should be assigned a hill number of 0; they will be modeled as if in flat terrain.

3.2.4 Meteorological Profile Data

The meteorological data file, "PROFILE", consists of hourly averaged values of wind, temperature, and turbulence data. This file must be provided by the user. Each record represents measurements at a single height. The data for each hour are grouped together with the highest level for any hour indicated by setting a flag from 0 to 1. There is no restriction on the number of hours, nor need they be contiguous; however, the dates/hours of the data must be sequential. The input records for each hour must be in order of increasing height. The heights do not have to be the same from hour to hour.

The data in the "PROFILE" data file are read in free format. Missing data values are indicated by -999. There must be at least one non-missing value for each variable for each hour [although σ_v (σ_θ) and σ_w values are not needed for hours in which all plumes are released into unstable layers]. The order of the variables in "PROFILE" is given in Table 3-7; a sample file is shown in Figure B-4.

TABLE 3-5. FORMAT OF THE "TERRAIN" INPUT DATA FILE
(FROM THE TERRAIN PREPROCESSOR)

Record Group	Parameter Name	Columns	Format	Description
1**	NH***	6-7	I2	Hill identification number
1	NZ****	9-10	I2	Number of critical elevations
1	HTP	21-30	E10.4	Hill top elevation (user units)
1	HNAME	31-45	A15	Hill name
2*	ZH	1-10	F10.3	Critical elevations (user units)
2	XHW,YHW	11-30	2F10.3	x,y-coordinates of the ellipse centroid for the critical elevation
2	MAJORW	31-40	F10.3	Orientation (degrees) of the ellipse major axis with respect to north
2	MAJAXW MINAXW	41-60	2F10.3	Semi-major and semi-minor axes lengths for the ellipse at the critical elevation
3*	ZH	1-10	F10.3	Critical elevation (must match critical elevations in Record Group 2)
3	L	10-30	2E10.4	x,y-coordinates for the fitted cutoff hill centroid
3	MAJORL	31-40	F10.3	Orientation of the fitted cut off hill major axis with respect to north (degrees)
3	EXPOMA EXPOMI	41-60	2F10.3	Inverse polynomial exponent parameters for the major and minor fitted hill axes
3	SCALMA SCALMI	61-80	2F10.3	Inverse polynomial length scale parameters for the major and minor fitted hill axes

*There are NZ records for group 2 followed by NZ records for group 3

**Record groups 1-3 are repeated for each hill

***There is a maximum of 25 hills

****There is a maximum of 21 hill contours

TABLE 3-6: FORMAT OF THE "RECEPTOR" INPUT DATA FILE*

Record Group	Variable Name	Columns	Format	Description
1**	RNAME	1-16	A16	16-character receptor name
	XR	21-30	F10.0	x-coordinate of receptor (user horizontal units)
	YR	31-40	F10.0	y-coordinate of receptor (user horizontal units)
	ZR	41-50	F10.0	Height of receptor above local ground surface (user vertical units)
	GE	51-60	F10.0	Ground-level elevation (user vertical units)
	NH***	61-65	I5	Hill number of this receptor

*No special line is required to signify the end of receptor input; this is signified by the end of the file

**One line per receptor, maximum of 400 receptors

***Hill number 0 is used to indicate flat terrain algorithm to be used for this receptor

TABLE 3-7. FORMAT OF USER-CREATED "PROFILE" FILE

Variable* Name	Description
JYR	Year (two digits)
JMO	Month (1-12)
JDY	Day of month (1-31)
JHR	Hour at the end of the period (1-24)
HT**	Height of this observation above the tower base (m)
IEND	0 if not the highest (last) level; otherwise 1
WD***	Wind direction (deg)
WS***	Scalar wind speed (m/s)
TA***	Ambient dry bulb temperature K
SIGTH***	Sigma-theta (deg) or sigma-v (m/sec), determined by a switch in "CTDM.IN"
SW***	Sigma-w (m/s)
UV***	Vector wind speed (m/s)

*All variables are read free format; one line per height level

**There is a maximum of 50 heights for each hour; heights must be in ascending order.

***Missing value is indicated by -999.

3.2.5 Meteorological Surface Data

The meteorological surface data file, "SURFACE", is created by the meteorological preprocessor and is input directly to CTDMPPLUS. It contains hourly values of mixed layer heights, surface friction velocity, Monin-Obukhov length, and surface roughness length. The chronological sequence of the hourly data must match the "PROFILE" data sequence. The format of the "SURFACE" file is given in Table 3-8; a sample is shown in Figure B-5.

3.2.6 Meteorological Rawinsonde Data

The meteorological rawinsonde data file, "RAWIN", is created by the meteorological preprocessor, READ62, from an NCDC TD-6201 file. It contains upper air measurements of pressure, temperature, wind direction, and wind speed. If IUNSTA = 1 in "CTDM.IN", then (for unstable conditions) the temperature values are read from the "RAWIN" file by CTDMPPLUS to calculate the potential temperature profile above the daytime mixing height. The sequence of daily 12Z soundings must match the date sequence of the "SURFACE" file data. If no unstable hours are included in the data, the user sets IUNSTA equal to zero and the RAWIN file is not required by CTDMPPLUS. The format of the "RAWIN" file is given in Table 3-9; a sample is shown in Figure B-6.

3.2.7 Hourly Emissions Data

Hourly source emission values (emission rate, stack gas exit velocity, and stack gas temperature) can be input to the model for any subset of the modeled sources via the file "EMISSION". There is one line per hour for each source with varying emissions. The sources with variable emissions must be in the same order as originally input in line group 5 of the program specifications file "CTDM.IN" (Table 3-3). CTDMPPLUS will check for time inconsistencies between the meteorological data and the hourly emissions data. Table 3-10 gives the format of the hourly emissions file.

3.3 CTDMPPLUS OUTPUT FILES

3.3.1 CTDMPPLUS Output Listing

An output listing is always created by the model; the content is determined by the case-study printout option. If the case-study printout option is not selected, then the listing is limited to a verification of input data from "CTDM.IN", a line printer map showing the relative locations of sources and receptors, and the information contained in the "TERRAIN" input file.

The case-study-mode output listing also includes:

- input meteorological data from "SURFACE" and "PROFILE"

TABLE 3-8. FORMAT OF "SURFACE" FILE (FROM THE METEOROLOGICAL PREPROCESSOR)

Variable* Name	Description
IYR**	Two-digit year
MO**	Month (1-12)
IDY**	Day of month (1-31)
JDAY	Julian day (1-366)
IHR**	Hour (at end of period, 1-24)
ZIOBS	Observed mixing height (m) from on-site measurement
ZIPRE	Calculated mixing height (m)
USTAR	Surface friction velocity (m/s)
EL	Monin-Obukhov length (m)
ZO	Hourly surface roughness length (m)

*All variables free format

**Date and times must match time variables in PROFILE data file.

NOTE: Negative values are written to "SURFACE" for missing mixed layer heights.

TABLE 3-9. FORMAT OF THE "RAWIN" FILE (FROM READ62 PROGRAM)

Record Group	Format	Description
1*	(A4) "6201"	Series "6201" label
	A5	Station identification number
	I2	Year of sounding
	I2	Month of sounding
	I2	Day of sounding
	I2	Hour of sounding (GMT)
	I2	Number of data levels in sounding
	I2	Number of data levels extracted
2**	F6.1	Pressure (mb)
	F5.0	Geopotential height (m)
	F5.1	Temperature (K)
	I3	Wind direction (deg)
	I3	Wind speed

*Repeated each hour

**Repeated for each level

TABLE 3-10. VARIABLE EMISSIONS INPUT FORMAT*

Line #	Variable	Description
For each hour, the user should provide one line of data for each source having variable emissions.	JYR	Year
	JMO	Month
	JDY	Day
	JHR	Hour (ending time for the hour)
	IS	Stack number
	TS	Stack gas temperature for this hour, K
	VS	Stack gas exit velocity for this hour, m/s
	QS(1)	Emission rates for up to four pollutants
	QS(2)	for the hour, g/s (ordering of pollutant
	QS(3)	emission rates should be consistent with
	QS(4)	pollutant code number, which is an input parameter to CTDM)

*Each line is read in free format.

- stack data for each source
- meteorological variables at plume height
- geometrical relationships between the source and the hill
- plume characteristics at each receptor for stable hours:
 - distance in along-flow and cross-flow directions
 - effective plume-receptor height difference
 - effective σ_y , σ_z values, both for flat terrain and the hill-induced case (the difference shows the effect of the hill)
 - concentration components due to WRAP, LIFT, and FLAT
- plume characteristics at each receptor for unstable hours:
 - distance in along-flow and cross-flow directions
 - horizontal distribution function
 - σ_y
 - crosswind integrated concentration.

Two other tables may be printed in the output file depending on the selection of options in "CTDM.IN". The user may select the ISOR option, which will print a source contribution table for every hour. If the user selects the TOPN option, a summary table of the top four concentrations at each receptor is given (See Figure B-6 for an example). The ISOR and TOPN switches are independent from the ICASE (case study printout) switch. A sample of the complete CTDMPLUS output listing file is given in Figure B-8.

3.3.2 Concentration File

A separate disk file of predicted concentrations ("CONC") is written if the user chooses this option. Three forms of output are possible:

- 1) a binary file of concentrations, one value for each receptor in the hourly sequence as run (ICONC = 1 in CTDM.IN);
- 2) a text file of concentrations, one value for each receptor in the hourly sequence as run (ICONC = 2); or
- 3) a text file as described above, but with a listing of receptor information (names, positions, hill number) at the beginning of the file(ICONC = 3).

Hourly information provided to these files (besides the concentrations themselves) includes the year, month, day, hour, receptor number with the highest concentration, the number of receptors, and the concentration units. The file formats are listed in Table 3-11 and a sample text file is shown in Figure B-7. The concentration file will have negative values at all receptors for hours in which CTDMPPLUS cannot calculate values. Only concentration files of the second type can be used with the CHIDIS and CONTOUR post-processors.

3.4 ADDITIONAL COMPUTER NOTES

The size of the CTDMPPLUS executable file on an IBM^R PC or compatible is approximately 360K bytes. This size is dependent upon the maximum number of sources, receptors, hills, etc., that are allowed. These maximum values can be changed by editing the file "PARAMS.INC" and then recompiling and relinking the CTDMPPLUS subroutines.

Default input/output unit numbers have been assigned for access to disk files:

"TERRAIN"	- unit 2
"EMISSION"	- unit 3
"RECEPTOR"	- unit 4
"CTDM.IN"	- unit 5
"CTDM.OUT"	- unit 6
"SURFACE"	- unit 7
"CONC"	- unit 9
"PROFILE"	- unit 11
"RAWIN"	- unit 14.

These assignments can be changed in the CTDMPPLUS main program.

Program execution will halt if any of several input problems is encountered:

- Time inconsistencies among data in files "SURFACE", "PROFILE", "RAWIN", and "EMISSION";
- Heights in the "PROFILE" file that are negative or not in increasing order;
- Read errors for various portions of the input;
- Too many sources or receptors; or
- Hill numbers out of sequence.

TABLE 3-11. FORMAT OF TEXT CONCENTRATION OUTPUT FILE

Line Group #	Columns	Format	Description
1* (appears only once, before the first hour's concentration values)	1-4	I4	Receptor number
	6-13	F8.0	Receptor x-coordinate (m)
	15-22	F8.0	Receptor y-coordinate (m)
	24-30	F7.1	Receptor height above local ground surface (m)
	32-37	F6.1	Receptor relief height above common stack base elevation (m)
2 (each hour)	39-42	I4	Hill number associated with this receptor
	1-5	I5	Year
	6-10	I5	Month
	11-15	I5	Day
	16-20	I5	Hour
	21-25	I5	Number of receptors with maximum concentration
	26-30	I5	Number of receptors
	31-46	A15	Units of concentration
3* (one line per receptor, each hour)	1-4	I5	Receptor number
	6-15	E10.4	Concentration ($\mu g/m^3$ or $\mu s/m^3$, depending on user option in "CTDM.IN")
4** (eight values per line until receptor list is exhausted, each hour)	1-10,11-20	8E10.3	Concentration ($\mu g/m^3$ or $\mu s/m^3$, depending on user option in "CTDM.IN")
	71-80		

*Used only if ICONC = 3 (receptor information written at beginning of file)

**Used only if ICONC = 2 (no receptor information written at beginning of file)

The messages associated with these errors are self-explanatory, and the user should be able to readily fix the problem and re-run the model.

Another group of program halts is attributable to potential, though rare, numerical convergence problems in the LIFT component. These problems for the most part have been solved, and thousands of test hours have been run without error. However, future users may encounter one of two possible problems:

- "ENDLESS LOOP IN PATH" (nonconvergence problem)
- "NO CONVERGENCE IN MIX ROUTINE".

These program halts may, in the future, be handled by having CTDMPPLUS not predict concentrations for the hour affected (negative concentrations being produced). Until more experience is gained with CTDMPPLUS, these program halts are being retained; our current experience indicates that they will be rarely encountered. If any of these program halts does occur, the case should be documented with input and output files and forwarded to the authors for analysis (MD-80, U.S. EPA, RTP, NC 27711).

3.5 CTDMPPLUS SUBROUTINE STRUCTURE

A brief overview of the structure of the major subroutines in CTDMPPLUS is presented in this section. It is designed to acquaint the user with how each of the subroutines "fits in".

The main program, which is named CTDMPPLUS, calls several subroutines which read in much of the preliminary data for a run and perform several setup operations, producing much of the printed output from the run. It then calls the major subroutine SEQMOD which actually performs all of the sequential computations. Figure 3-2 outlines the form of CTDMPPLUS (MAIN).

Each of the minor subroutines referred to in the figure performs a well-defined task:

- PAGE: Skips to a new page and writes a page header.
- INPAR: Reads and writes the input/output switches, conversion factors, and constants for the model. These values are passed through "PARAMS.CMN".
- INPSOR: Reads and writes all source data that remain fixed (constant) over the period of simulation. The source data are passed through "STACKS.CMN".
- INPREC: Reads and writes receptor data. These data are passed through "RECEPT.CMN".
- INPTOW: Reads and writes position of meteorological tower. The position is passed through "TOWER.CMN".

CTDMPLUS (MAIN)

- initializations
- Open: CTDM.IN, CTDM.OUT
- Call PAGE
- Call INPAR
- Call INPTOW
- Call INPSOR
- Open: EMISSION (if variable)
- Open RECEPTOR
- Call INPTER
- Close TERRAIN
- Open SURFACE, PROFILE, CONC
- Open RAWIN (if unstable hours)
- Call MAP
- Call SEQMOD
- Stop

Figure 3-2. Outline of the main program CTDMPLUS.

INPTER: Reads and writes the terrain information describing each hill. Data are passed through "HILL.CMN".

MAP: Creates a line-printer map of the relative locations of the sources and the receptors.

The major subroutine SEQMOD contains all of the dispersion computations, and the overall structure that controls the sequential loops over receptors, hills, and sources for each stable/neutral time period. SEQMOD calls another subroutine, DAYCALC, which performs these calculations and functions for the unstable hours ($HS < XMH$ and $-100 < L < 0$). Figure 3-3 outlines the form of SEQMOD, while Figure 3-4 outlines the form of DAYCALC.

Subroutines called by SEQMOD include the following:

RDSFC: Reads the SURFACE meteorological data for the current hour, computes w_* , and passes these data through "SFCMET.CMN".

SUN: Computes the hours of sunrise and sunset.

INPEMS: Reads the hourly emissions data from the "EMISSIONS" file, and passes these data through "STACKS.CMN".

HCRIT: Function that computes the dividing streamline height of the current hill. It calls the following: KLOSE, GETWS, GETTA, GETDTH.

BULKFR: Function that computes the bulk Froude number for the flow above H_c . It calls GETWS and GETTA.

GETWS: Function that returns the wind speed at a given height. It calls KLOSE.

GETWD: Function that returns the wind direction at a given height. It calls KLOSE.

GETTA: Function that returns the temperature (absolute) at a given height. It calls KLOSE.

GETDTH: Function that returns the vertical gradient of the potential temperature at a given height. It calls KLOSE.

KLOSE: Function that returns the position of the data value (in a given array) that lies nearest to a given value (but does not exceed the value).

SRISE: Computes height of final plume rise for the stable case (Monin-Obukhov length is positive). Calls GETWS, GETDTH, and PICK4.

URISE: Computes height of final plume rise for non-stable cases (Monin-Obukhov length is non-negative).

PICK4: Returns the minimum of four numbers.

PLAVG: Computes values of wind speed, wind direction, and potential temperature gradient at a given height. Calls GETWS, GETWD, and GETDTH.

SIGB: Computes the size of a buoyant plume that results from mixing associated with plume rise.

GETSW: Function returns a value of σ_w at a given height. It calls KLOSE.

GETSV: Function returns a value of σ_v at a given height. It also calls KLOSE.

PSRCE: Computes downwind and crosswind distances from the axis of the plume to a receptor.

XINTRP: Interpolation function.

MUNU: Computes the elliptical coordinates μ and ν for the point (x, y) , where the x-axis is aligned with the major axis of the ellipse.

WRAPIN: Computes the streamfunction through the source, the stagnation streamline, the impingement point, the distance between the plume centerline and the stagnation streamline, and the orientation of the β -coordinate system for use in WRAP.

TERAX: Computes the major and minor axis lengths of an ellipse that forms the shape of the hill above H_c in horizontal cross-section at a given elevation.

LIFTIN: Computes the factors T_y and T_z over the hill above H_c along a streamline that follows the surface of the cut-off hill if the plume centerline lies below H_c , or along a streamline half of the way between H_c and the center-of-mass of plume material above H_c . Calls TERAX, HILROT, and PATH.

HILROT: Computes a rotation factor and the length scales along the flow and perpendicular to the flow of a Gaussian hill oriented at an angle to the flow.

PATH: Computes the position of a given streamline over a Gaussian hill, at a given point along the flow, and returns the strain factors at that point. Calls FLOW and HILHGT.

- FLOW:** Computes deflections and wind perturbations experienced by a streamline that passes through a given point over a Gaussian hill, and computes the local strain factors at the given point. Calls SPEED.
- HILHGT:** Computes the local hill height (scaled by the height at its peak) at a point on a Gaussian hill.
- FLAT:** Computes the concentration at a given height above the ground for receptors that are not influenced by terrain.
- LIFT:** Computes concentrations at receptors above H_c resulting from plume material that lies above H_c . Calls FLAT (for receptors upwind of the cut-off hill), MIX, FLOW, HILHGT, and LVDF.
- MIX:** Computes the depth of an internal mixing layer that develops at the hill surface above H_c .
- LVDF:** Computes the vertical distribution factor for LIFT.
- WRAP:** Computes concentrations resulting from plume material that lies below H_c . Receptors upwind of the impingement point must be below H_c , but receptors downwind may be above H_c as well.
- WRITIT:** Writes hourly concentrations (all receptors) to a disk file in binary or text format.
- TOPN:** Initializes, updates, or prints out a top N table; N is defined by the parameter MAX-TOP in "PARAMS.INC".

Subroutines called by DAYCALC include the following:

- DTHDZ:** Returns vertical potential temperature gradient above the mixing height which is used in calculating the penetration factor.
- PENFCT:** Function calculates the partial plume penetration factor according to Briggs (1984).
- GETHIL:** Calculates hill dimensions and transforms coordinates to system with hill as center and x-axis parallel to the flow direction. These coordinates are used by the WPDF subroutine.
- TRANPR:** This subroutine calculates transitional plume rise for receptors downwind of final rise.
- WFLAT:** Provides vertical velocity and probability values for a receptor not influenced by terrain.

WPDF: Computes the vertical velocity needed to reach a receptor on a hill. Calls FLOWSP.

FLOWSP: Shortened version of FLOW, for use by WPDF. Computes the perturbation winds UP, VP, WP, at the point (x,y,z) above the surface of a rotated Gaussian hill.

SIGMAY: Computes σ_y and the horizontal distribution function.

SUBROUTINE SEQMOD

- initializations
- Hour Loop (top is line 100)

- ** RDSFC [return if EOF is found]
- ** SUN
- ** PAGE (icase > 0)
- read PROFILE data (loop over MAXLEV)
- ** INPEMS (hourly emissions)
- if z_0 , u^* , ws , wd , sv , or sw is bad: skip to
- write hourly met data (icase > 0)
- zero concentration array
- Preliminary Loop on Hills

- ** HCRIT
- ** BULKFR

- End Preliminary Loop on Hills
- Loop on Sources (do 300)

- initialize variables for current source
- if no emissions write source information: skip to
- ** GETWS
- ** SRISE (for stable)
- ** URISE (for non-unstable)
- if stack ht is in convective layer and $L < 0$, DAYCALC: skip to 300
- ** SIGB
- ** PLAVG
- ** GETSW
- ** GETSV
- rotate coordinate system
- compute virtual source, virtual time
- screen out hills upwind of source
- ** PSRCE
- Loop on Hills (do 270)

Figure 3-3. Outline of the subroutine SEQMOD.

SUBROUTINE DAYCALC

- if plume height > mixing height, correct plume height to be $.9 * \text{mixing height}$
- ** GETWD (gets wind direction at 1/2 plume rise height)
- get rotation factors from wind direction
- ** GETWS (gets wind speed at 1/2 plume rise height)
- ** DTHDZ
- ** PENFCT
- calculate source dependent variables
- if ica_{se} ≥ 2, write report
- check hills to see if they have any downwind receptors
- ** PSRCE
- Loop on Hills (do 270)
- if all receptors are upwind: skip to 270
- set up coordinate system for hill
- Loop on Receptors (do 260)
- get crosswind and downwind distances for receptor
- ** PSRCE
- if receptor is upwind: skip to 260
- rotate and translate receptor coordinates
- calculate transitional plume rise, if final rise > rise at receptor distance
- ** TRANPR
- get wind direction change over plume depth
- ** GETWD
- If hill # = 0
 - | ** WFLAT: skip to 268
- If hill # > 0
 - | ** WPDF
 - | — calculate probabilities for all paths
- calculate crosswind-integrated concentration
- if ica_{se} ≥ 2, write report
- calculate concentration (268)
- if ica_{se} ≥ 2, write report
- End Loop on Receptors (260)
- End Loop on Hill (270)
- Return

Figure 3-4. Outline of the subroutine DAYCALC.

SECTION 4

USER INSTRUCTIONS FOR AUXILIARY PROGRAMS

Three types of interactive computer programs that are associated with CTDMPLUS preprocessing or postprocessing functions are described in this section:

- a receptor generator program (RECGEN),
- an interactive file setup program for CTDMPLUS (SETUP), and
- graphical display programs for output concentrations from CTDMPLUS.

Each of these programs guides the user through execution and therefore does not require an extensive amount of documentation, compared with a batch program like CTDMPLUS. General user instructions and examples of runs are given in the subsections that follow.

4.1 RECEPTOR GENERATOR

Sensitivity tests on the representation of a single terrain feature in CTDMPLUS have shown that peak concentrations may change location (although the magnitude is not expected to change significantly) for different mathematical formulations of hill orientation and shape. It is important, therefore, to blanket a hill with receptors to assure that the peak concentration is captured. Obtaining x, y, and z input data for receptors in terrain has always been a laborious procedure. Fortunately, the availability of digitized terrain information allows the user to automate, to some extent, the selection of receptor input to CTDMPLUS.

RECGEN places receptors along digitized contours only. Since these contours are spaced to give an adequate representation of the shape of the hill, the receptor coverage resulting from RECGEN may be sufficient; if additional receptors are desired, they can be added using a text editor.

The CTDMPLUS receptor generator program, RECGEN, is an interactive program written in Pascal. RECGEN is designed to be compatible with the menu driver system and therefore uses the same naming conventions and directory setup as the menu driver. The user is first asked to select a plot file of terrain contours (generated by FITCON) from a list of available files. As each contour is displayed, the user is asked whether receptors on the contour are to have (1) a user-supplied spacing around the perimeter of the contour, or (2) a spacing calculated by dividing the total perimeter distance of the contour by a user-supplied number of points. The user then inputs the spacing or number of points, depending upon which option has been selected. In general, the number of receptors on contours should be decreased as the contour perimeters get smaller toward the top of the hill. Once the mode of point generation has been specified for all

contours, the locations of the generated receptors are plotted as filled circles upon a background of unedited hill contours. RECGEN produces a file of receptors that is written to the 'C:\CTDM\FILES' directory with an extension of '.RCT'.

Figure 4-1 shows a sample of a portion of the interactive session, while Figure 4-2 illustrates the display of receptors generated for an entire set of contours on a hill. An example of the resultant receptor file is shown in Figure 4-3.

4.2 INTERACTIVE SETUP PROGRAM

An interactive program (SETUP) has been developed to acquaint new users with the operation of CTDMPLUS. SETUP will create or modify files necessary to run the meteorological preprocessor, METPRO, in mode 0 only. It will also create or modify files necessary to run CTDMPLUS for constant-emission, stable/neutral cases. SETUP cannot be used to run METPRO for modes 1, 2, or 3; nor can it be used to run CTDMPLUS for variable emissions or unstable hours. For these cases, a text editor should be used to edit files.

SETUP first handles the input files to METPRO ("OPTIONS", "PROFILE", and "SURF1") if the user wishes to run METPRO. For each file, the user may elect to modify an existing file, copy from an existing file (by renaming it), or create a new file from scratch. Figures 4-4, 4-5, and 4-6 show the display of values that can be modified for the files "OPTIONS", "PROFILE", and "SURF1", respectively. The SETUP batch job then runs METPRO, creating an "OUTPUT" listing file and a "SURFACE" file.

The CTDMPLUS files that SETUP can modify (see Figure 4-7) include "CTDM.IN", "RECEPTOR", "SURFACE", and "TERRAIN", respectively. SETUP cannot create a "CTDM.IN" or "TERRAIN" file from scratch. Also, the "RAWIN" file must exist prior to starting SETUP for daytime hour runs. The SETUP batch job will then execute CTDMPLUS, creating the output listing file "CTDM.OUT" and "CONC" (if the user selects the concentration output). Additional runs of METPRO and CTDMPLUS can be easily made with small alterations in the input files by using the SETUP facility.

4.3 GRAPHICAL CONCENTRATION DISPLAYS

For short runs of CTDMPLUS, two programs, CHIDIS and CONTOUR, are available for displaying concentration values on a background of digitized terrain. The case-study printout from CTDMPLUS gives all of the numerical information required, but a spatial representation of the concentration distribution is also desirable. CHIRET, a FORTRAN program, reads the concentration and receptor information and creates a sorted concentration file that is used by both display programs. The "CONC" file must be in text format (created using ICONC = 2 in the "CTDM.IN" file) for the concentration display postprocessors to work correctly.

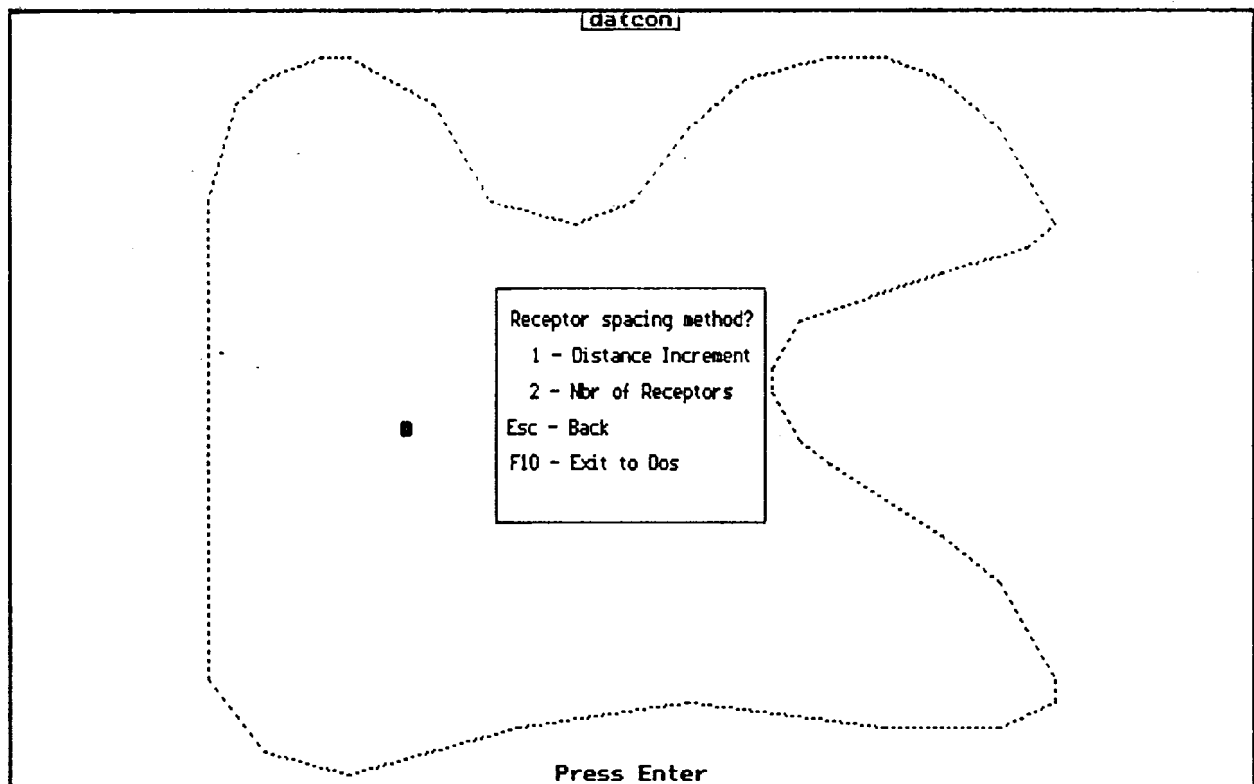


Figure 4-1. Portion of a sample interactive session from the RECGEN program.

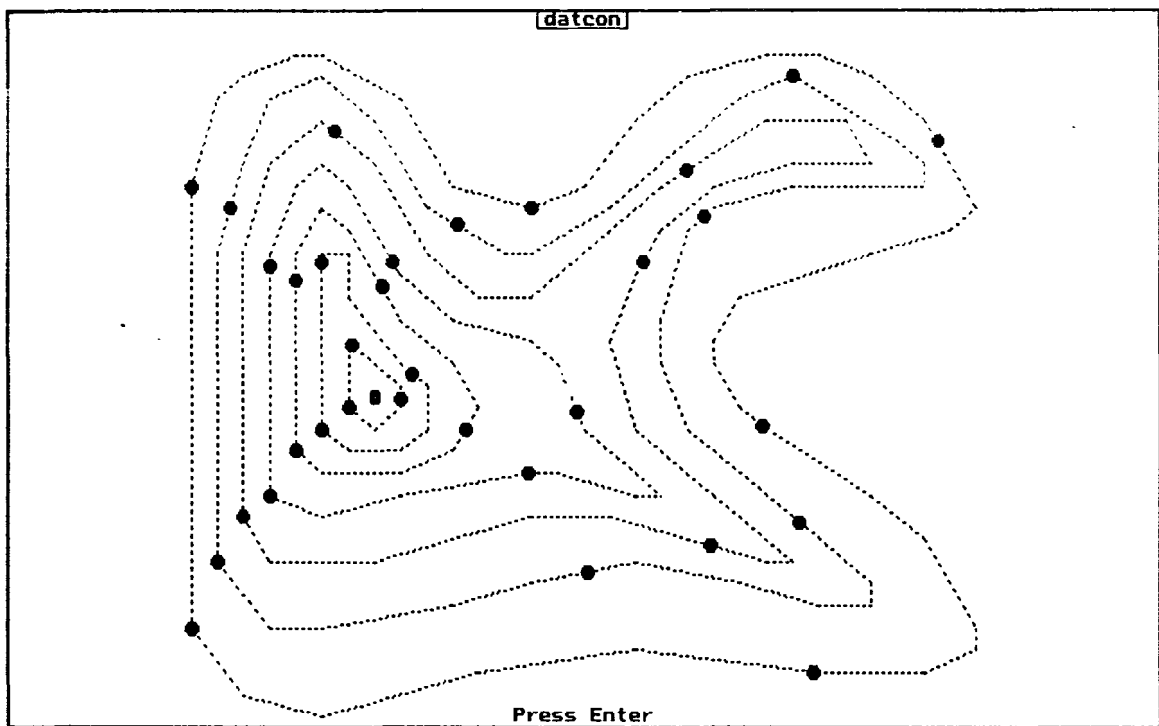


Figure 4-2. Receptor display from the RECGEN program.

datcon	1	0.000	4.000	0.000	10.000	1
datcon	2	0.000	12.401	0.000	10.000	1
datcon	3	0.000	20.802	0.000	10.000	1
datcon	4	1.763	28.763	0.000	10.000	1
datcon	5	8.548	26.905	0.000	10.000	1
datcon	6	14.781	23.890	0.000	10.000	1
datcon	7	20.634	29.545	0.000	10.000	1
datcon	8	27.926	27.074	0.000	10.000	1
datcon	9	26.713	21.238	0.000	10.000	1
datcon	10	20.000	16.972	0.000	10.000	1
datcon	11	25.023	10.733	0.000	10.000	1
datcon	12	29.946	4.108	0.000	10.000	1
datcon	13	22.967	2.148	0.000	10.000	1
datcon	14	14.659	2.610	0.000	10.000	1
datcon	15	6.549	0.516	0.000	10.000	1
datcon	16	1.000	7.000	0.000	20.000	1
datcon	17	1.000	18.279	0.000	20.000	1
datcon	18	4.138	28.569	0.000	20.000	1
datcon	19	11.509	21.327	0.000	20.000	1
datcon	20	20.302	27.302	0.000	20.000	1
datcon	21	27.359	24.000	0.000	20.000	1
datcon	22	18.432	19.726	0.000	20.000	1
datcon	23	22.067	9.933	0.000	20.000	1
datcon	24	21.422	5.859	0.000	20.000	1
datcon	25	10.545	5.182	0.000	20.000	1
datcon	26	2.000	9.000	0.000	30.000	1
datcon	27	2.069	21.275	0.000	30.000	1
datcon	28	8.247	22.507	0.000	30.000	1
datcon	29	17.081	23.081	0.000	30.000	1
datcon	30	25.253	25.000	0.000	30.000	1
datcon	31	16.429	18.288	0.000	30.000	1
datcon	32	21.810	8.190	0.000	30.000	1
datcon	33	12.737	8.912	0.000	30.000	1
datcon	34	3.000	10.000	0.000	40.000	1
datcon	35	3.000	18.655	0.000	40.000	1
datcon	36	6.143	23.714	0.000	40.000	1
datcon	37	11.589	17.470	0.000	40.000	1
datcon	38	16.832	11.168	0.000	40.000	1

Figure 4-3. Example receptor file generated by the RECGEN program.

datcon	39	11.194	10.639	0.000	40.000	1
datcon	40	4.000	12.000	0.000	50.000	1
datcon	41	4.000	19.768	0.000	50.000	1
datcon	42	7.291	19.418	0.000	50.000	1
datcon	43	10.500	13.000	0.000	50.000	1
datcon	44	5.000	13.000	0.000	60.000	1
datcon	45	5.000	18.712	0.000	60.000	1
datcon	46	6.235	18.647	0.000	60.000	1
datcon	47	9.000	13.884	0.000	60.000	1
datcon	48	6.000	14.000	0.000	70.000	1
datcon	49	6.155	16.845	0.000	70.000	1
datcon	50	8.000	14.391	0.000	70.000	1

Figure 4-3. (continued).

Modify OPTIONS file.

OPTIONS FILE - CASE STUDY MODE

Latitude: 57.000 [deg]
Longitude: 90.000 [deg]
Time Zone: 6
Surface Roughness Length: 0.30 [m]
Albedo: 0.20
Bowen Ratio: 1.00

Modify any of these values [Y/N]

Figure 4-4. Display from a sample interactive session of SETUP: "OPTIONS" input file for METPRO.

Meteorological Profile Data				12/4/80	Hour: 19		
Level	Wind	--Wind	Speed--	Ambient	Sigma	Sigma	
#	Height	Dir	Scalar	Vector	Temp	Theta	W
	[m]	[deg]	[m/s]	[m/s]	[deg-K]	[deg]	[m/s]
1	210.0	292.0	1.34	*****	*****	15.30	0.01
2	326.0	*****	*****	*****	273.71	*****	*****
3	366.0	69.0	0.13	*****	*****	35.00	0.00
4	416.0	90.0	0.40	*****	273.76	14.70	0.01

Modify (M), Insert (I), Append (A), Continue (RETURN)
Enter [M, I, A, RETURN]:

Figure 4-5. Display from a sample interactive session of SETUP: "PROFILE" input file for METPRO.

YR MO DY HR	TOTAL INCOMING SOLAR RADIATION [w/m2]	NET RADIATION [w/m2]	MIXING HEIGHT [m]	CEILING HEIGHT [ftx100]	CLOUD COVER
80 12 4 19	210.0	0.0	292.0	1	*

Modify (M), Continue (RETURN):

Figure 4-6. Display from a sample interactive session of SETUP: "SURF1" input file for METPRO.

Execute the CTDMPPLUS meteorological preprocessor program, METPRO ? (Y/N):n

CTDMPLUS requires the following input files

- CTDI.IN
- RECEPTOR
- PROFILE
- SURFACE
- TERRAIN

The status of these files is:

CTDI.IN file does not exist.
NOTE: This program cannot create one from scratch.
RECEPTOR file does not exist.
NOTE: This program cannot create one from scratch.
PROFILE file does not exist
SURFACE file does not exist
TERRAIN file does not exist
NOTE: This program cannot create one from scratch.

Hit RETURN to continue

Figure 4-7. Display from a sample interactive session of SETUP: listing of files required by CTDMPPLUS.

4.3.1 CHIRET

The program CHIRET reads the "RECEPTOR" and "CONC" files, sorts the data, and writes an output file ("CHIOUT"). The user is first asked to enter the identification number for the hill in question. Although more than one hill can be input to CTDMPLUS for a single run, only concentrations at receptors on a single hill can be displayed during a single run of either of the display programs. Next, the user must specify which of the following three methods is to be used for selecting hours from the concentration file for plotting concentrations:

- Only the first hour is selected, or
- All hours are selected, or
- All hours between user-specified starting and ending times are selected.

For each of the qualifying hours in the concentration file, the concentrations and receptor coordinates are sorted and written to the CHIRET output file, with only those receptors on the user-specified hill being included. Figure 4-8 shows an interactive session involving execution of the CHIRET program.

4.3.2 CHIDIS

The concentration display program, CHIDIS, is a menu driven program written in Pascal. The user is first asked to select the name of the plot file of digitized contours that was written by the program FITCON. The user is also asked to select the name of the file of sorted concentrations generated by the program CHIRET. For a given hour, the receptor with the highest concentration is displayed as a blinking filled circle. If the user presses the space bar, the receptor with the next highest concentration is displayed as a blinking filled circle. The date, receptor number, rank, and concentration for the current receptor can be displayed at the top of the plot by pressing the "C" key. Pressing the space bar then causes this text to be erased and the receptor with the next lowest concentration to be displayed as a blinking filled circle. If the key "N" is pressed at any time, the program begins the display of concentrations for the next hour. If all receptors have been displayed for a given hour, then pressing the space bar causes the display of receptors to be repeated, with the receptor having the highest concentration being displayed first. At any time, the user may press the **Esc** key to terminate execution of the program. Sample screen displays from CHIDIS are shown in Figures 4-9 and 4-10.

```
C:\CTDM\EXE>CD\CTDM\FILES
C:\CTDM\FILES>COPY CCB.CON CONC
1 File(s) copied
C:\CTDM\FILES>COPY CCB.RCT RECEPTOR
1 File(s) copied
C:\CTDM\FILES>C:\CTDM\EXE\CHIRET

ENTER THE HILL IDENTIFICATION NUMBER(1-99) -> 1

70 OUT OF 70 RECEPTORS WERE FOUND TO BE ON HILL 1

SPECIFY CONCENTRATION RECORD SELECTION MODE
1.) ONLY THE FIRST RECORD IS SELECTED
2.) ALL RECORDS SELECTED
3.) ALL RECORDS SELECTED BETWEEN A START AND END TIME
CHOICE?(1,2 OR 3) -> 1
```

Figure 4-8. Sample Interactive session for the program CHIRET.

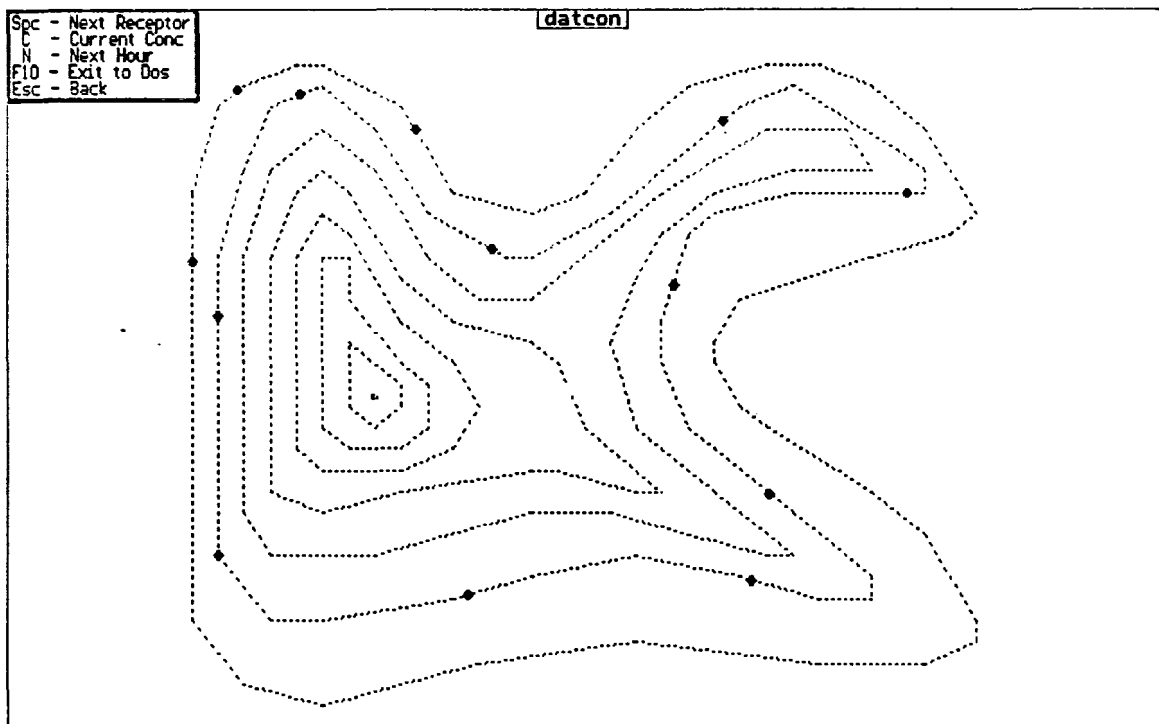


Figure 4-9. Sample screen display from the CHIDIS program, showing user options.

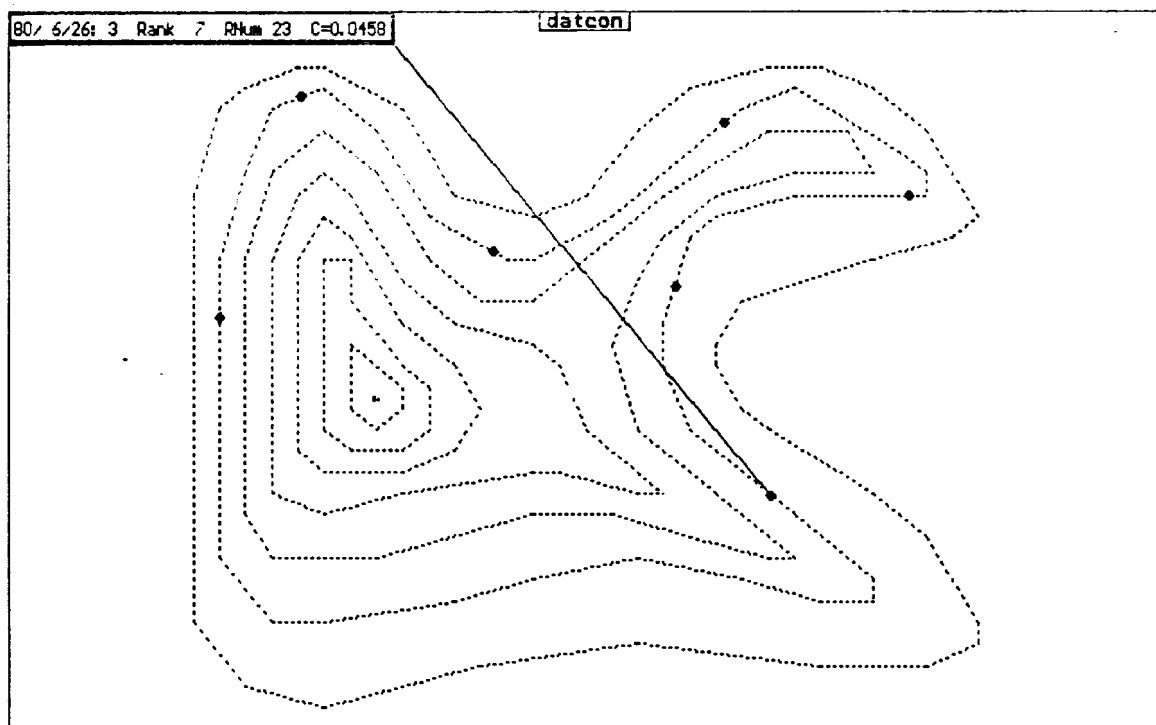


Figure 4-10. Sample screen display from the CHIDIS program, showing receptor locations and the concentration value for the most recently displayed receptor.

4.3.3 CONTOUR

The second concentration display program, CONTOUR, can only be run from the menu driver and is described in greater detail in Section 5.2.8. CONTOUR allows the user to see concentration isopleths drawn on a background of unedited hill contours. The CONTOUR program is based on the NCAR plotting routines (McArthur, 1983) and uses the Barnes (1973) scheme for gridding the data.

SECTION 5

INSTRUCTIONS FOR USING THE MENU DRIVER

5.1 INTRODUCTION

The CTDMPPLUS modeling system involves the use of a number of programs and input files. The required input files are discussed in detail in Section 3. To facilitate use of the model, a menu driver was developed that helps users select programs to be run and options and files to be used. The main components of the menu driver are shown in Table 5-1. The menu system is designed to aid users with short CTDMPPLUS runs of a few hours or days. Although CTDMPPLUS can be run on a mainframe or a PC, the menu system is designed to work on a PC; using the menu system and CTDMPPLUS together requires a PC with 640K bytes of memory. Users must be familiar with the files required by CTDMPPLUS, as well as the fundamentals of model operation, in order to use the menu system. (Reviewing the terrain and meteorological preprocessor manuals and previous sections of this manual will provide this information.) The requirements for the naming and directory location of files used by the menu driver are described in Sections 5.2.1 and 5.2.2.

5.2 USER INSTRUCTIONS

5.2.1 File Naming

A standard method for naming files has been developed for use with the menu driver. File names consist of a descriptive name and a required extension. For example, the "PROFILE" file for use in modeling the CCB dataset would be named "CCB.PFL". The selection of the descriptive term (i.e., CCB) is left to the user, but the file name extensions must be as indicated in Table 5-2 in order to use the menu driver. During the operation of the menu driver, when a user is asked to input a filename, only the descriptive name should be entered as the menu driver will attach the appropriate extension and pathname.

5.2.2 Directory Setup

The menu system is designed to work with a specific directory structure, which the user must create on the hard disk. The files must be named as indicated in section 5.2.1 and in the directories as listed in Figure 5-1. Files not properly named and located in the proper directory will not be available for use with the menu system.

TABLE 5-1. COMPONENTS IN THE CTDMPLUS MENU DRIVER

Main program	Subprograms
Terrain preprocessor	FITCON HCRIT PLOTCON RECGEN
Meteorological preprocessors	METPRO READ62
CTDMPLUS	
Concentration postprocessors	CHIDIS CONTOUR

TABLE 5-2. STANDARD CTDMPPLUS FILE EXTENSIONS

Description	Required Name	Extension
FITCON options file	FOPTIONS	.OPT
Contour master file		.XY
FITCON diagnostic output		.DAG
FITCON plot file		.PLT
FITCON output file		.FO
HCRIT options file	HOPTIONS	.HOP
HCRIT output file		.HCO
HCRIT plot file		.HPT
RECGEN receptor file		.RCT
METPRO OPTIONS file	OPTIONS	.MOP
SURF1 file	SURF1	.SF1
SURF2 file	SURF2	.SF2
RAWIN file	RAWIN	.RAW
METPRO output file	OUTPUT	.MOF
RAWIN options file	OPT62	.R62
TD6201 file	TD6201	.TD
RAWIN diagnostic output	R62OUT	.ROF
CTDM.IN file	CTDM.IN	.CIN
PROFILE file	PROFILE	.PFL
SURFACE file	SURFACE	.SFC
EMISSION file	EMISSION	.EMS
TERRAIN file	TERRAIN	.HCO
RECEPTOR file	RECEPTOR	.RCT
CONC file	CONC	.CON
CTDM.OUT file	CTDM.OUT	.OUT
CHIRET output file	CHIOUT	.CHI
Gridded data file		.GRD

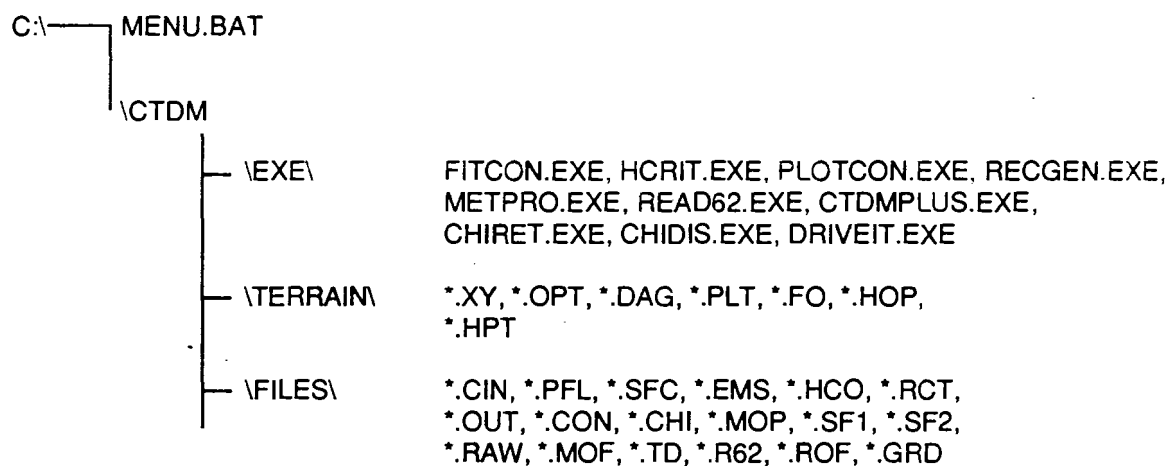


Figure 5-1. Directory setup for menu driver use.

5.2.3 Initiating the Program

The menu driver can be initiated from any directory by typing MENU. This will run the MENU batch file located in the root directory. The batch file changes the current directory to \CTDM\EXE\ and executes the menu driver program, DRIVEIT. The main selection menu shown in Figure 5-2 will then be displayed.

The menu system does not allow for editing files, so all files to be used must be edited and exist in the proper directories as listed in Figure 5-1 prior to initiating the menu system.

Certain special keys are used in the menu system:

- (Esc)** - back up one screen
- (F10)** - end the program and exit to DOS
- (F9)** - execute a particular FORTRAN program
- (F8)** - end selection of files
- (F7)** - overwrite an existing file.

In several instances, the user is given the option to view a particular file. This is done using the DOS command

```
TYPE <filename> | MORE
```

which enables the user to see the file one page at a time. Pressing any key will display the next page, while Ctrl-C will return the user to the menu system. A response of "N" to the view option will also return the user to the menu system.

5.2.4 Terrain Preprocessor Programs

The terrain preprocessor menu is displayed when the user chooses option 1 from the main menu. The user may then choose to execute one of four programs: FITCON, HCRIT, PLOTCON, or RECGEN. Note that FITCON and HCRIT both require an options file. Previous versions ran interactively, but this was not practical for multiple runs with the same hill.

The FITCON program is initiated by selecting option 1 from the terrain preprocessor menu (see Figure 5-3). The user is prompted to choose a contour master file (filename.XY) from a list of available files. The filename of the contour master file is used to determine if a related FITCON options file exists (filename.OPT). If the options file exists, the parameters listed in it are used to initialize the values for the next run, otherwise, default values are used. The options file is displayed as shown in Figure 5-4. The user is then given the opportunity to change any of the parameters in the options file. Validation of each field (e.g., range checking, checking for file existence) occurs when **(Enter)** is pressed and errors are

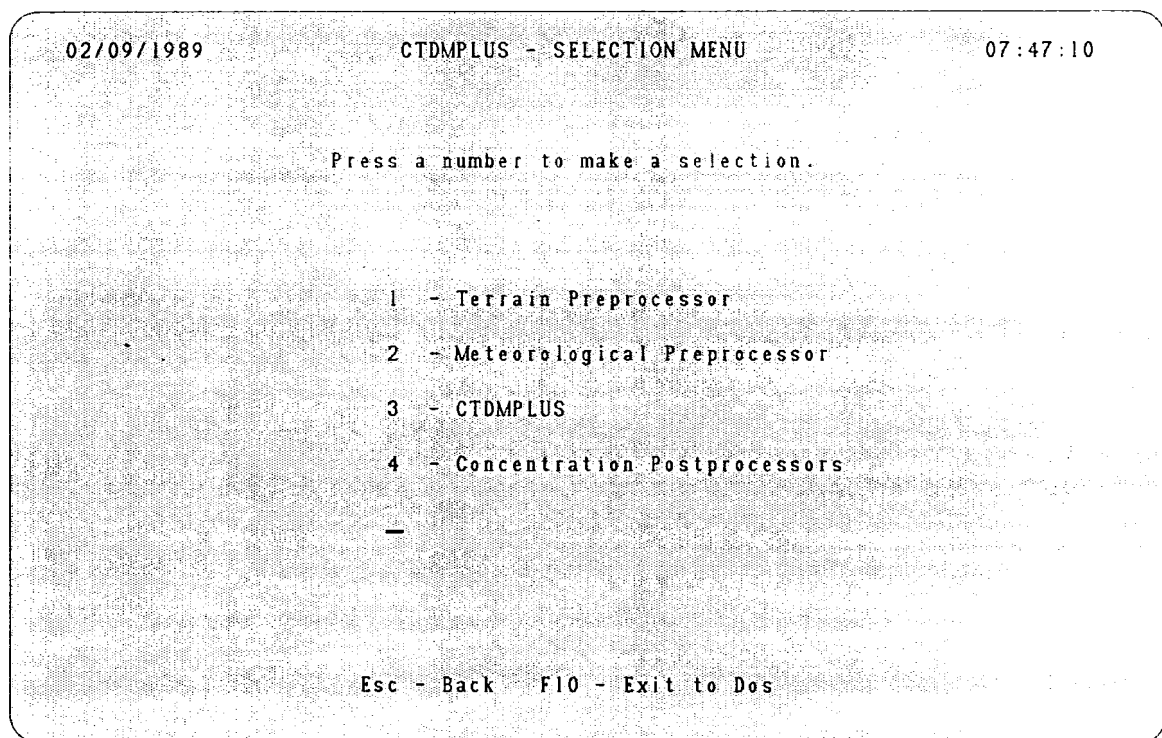


Figure 5-2. Screen display from the menu driver system, showing the main selection menu.

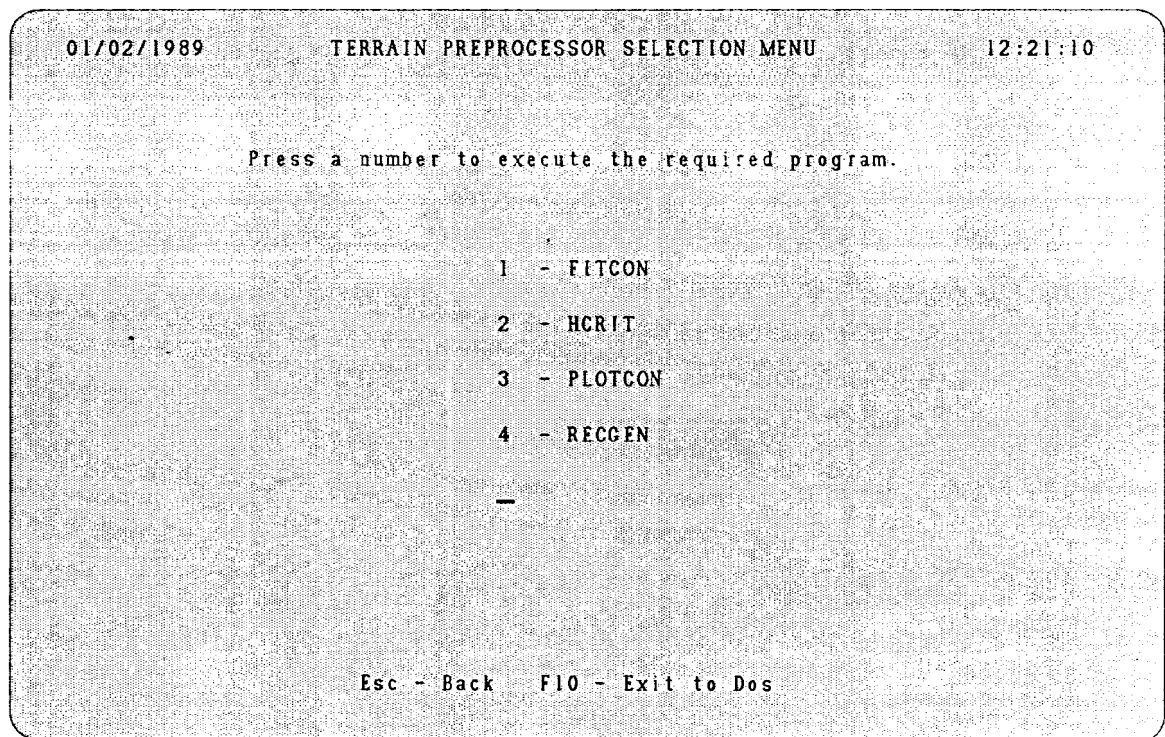


Figure 5-3. Screen display from the menu driver system, showing the terrain preprocessor menu.

01/02/1989	FITCON OPTIONS	12:21:58
------------	----------------	----------

Use the arrow keys to highlight the option to be changed.

CONTOUR MASTER FILE (.XY):	DATCON
DIAG. OUTPUT FILE (.DAG):	tc0
HILL ID NUMBER:	1
HILL NAME:	DATCON
HILL TOP ELEVATION:	80.0000
HILL CENTER X-COORDINATE:	7.0000
HILL CENTER Y-COORDINATE:	14.5000
ANGULAR FILTERING (Y or N):	n
ANGULAR FILTER SIZE (1-22.5):	1.0
CONTOUR SELECTION MODE (1,2, OR 3):	1
LOWER BOUND OF ID NUMBERS (MODE 2 ONLY):	1
UPPER BOUND OF ID NUMBERS (MODE 2 ONLY):	1
CONTOUR ID NUMBER FILE (MODE 3 ONLY):	DATCON
CREATE A PLOT FILE? ? (Y or N):	Y
FITCON PLOT FILE (.PLT):	tc0
FITTED OUTPUT FILE (.FO):	tc0

F9 - Run FITCON	DOWN	UP	Esc - Back	F10 - Exit to Dos
-----------------	------	----	------------	-------------------

Figure 5-4. Sample screen display from the menu driver system, showing the FITCON options screen.

displayed at the bottom of the screen. Pressing the **F9** key causes each field to be validated a final time and FITCON to be run. FITCON cannot be executed while errors exist in the options. After FITCON completes execution, the user is given the option to look at the diagnostic output file (filename.DAG). The fitted ellipses from the FITCON run can be viewed graphically using PLOTCON, or the user may elect to continue on with HCRIT.

The HCRIT program is initiated by selecting option 2 from the terrain preprocessor menu. The user is then prompted to choose a FITCON output file (.FO) from a list of available files. The cursor will initially be on the file that matches the .XY file chosen in the last FITCON run, if one exists. The filename of the .FO file is used to determine if a related HCRIT options file (.HOP) exists. From this point, the sequence of events follows that listed above for FITCON. A sample HCRIT options file is shown in Figure 5-5. After the HCRIT run finishes, the user is prompted to press ENTER to return to the terrain menu. The cut-off contours may be displayed graphically by using PLOTCON. Note that an HCRIT run will create the CTDMPPLUS terrain file (.HCO) for only one hill and the file will be placed in the \CTDM\FILES\ directory. Files must be combined (outside of the menu driver) for CTDMPPLUS runs involving multiple hills.

The PLOTCON program is activated by choosing option 3 from the terrain preprocessor menu. The user is prompted to select a FITCON plot file (.PLT) from a list of available files. The next screen gives the user the option to see edited or unedited contours. After the contours have been displayed, the user has the option of seeing the fitted ellipses (from FITCON) or cut-off hill contours (from HCRIT). After displaying the ellipses, the user is again given the option to see the cut-off contours. For viewing the cut-off contours, the user chooses an HCRIT plot file (.HPT) and the starting elevation for displaying the cut-off contours. After one set of cut-off contours has been displayed, the user may press **Esc** to return to the starting elevation menu, or **Enter** to see the next set of contours.

5.2.5 Receptor Generator

The receptor generator program, RECGEN, is initiated by choosing option 4 of the terrain preprocessor menu. The operation of RECGEN is described in detail in Section 4.1.

5.2.6 Meteorological Preprocessors

The meteorological preprocessor menu, shown in Figure 5-6, is displayed by selecting option 2 from the main menu. The user, at this point, may elect to run METPRO with existing files or create a new "RAWIN" file using the READ62 preprocessor.

01/02/1989	HCRIT OPTIONS	12:22:24														
Use the arrow keys to highlight the option to be changed.																
<table border="0" style="width: 100%;"> <tr> <td style="width: 60%;">FITCON OUTPUT FILE (.FO):</td> <td style="width: 40%; text-align: right;">TC0</td> </tr> <tr> <td>HCRIT OUTPUT FILE (.HCO):</td> <td style="text-align: right;">TC0</td> </tr> <tr> <td>CREATE A PLOT FILE? (Y or N):</td> <td style="text-align: right;">Y</td> </tr> <tr> <td>HCRIT PLOT FILE (.HPT):</td> <td style="text-align: right;">TC0</td> </tr> <tr> <td>SELECTION MODE FOR CRIT. ELEV.:</td> <td style="text-align: right;">1</td> </tr> <tr> <td>NUMBER OF CRIT. ELEV. (MODE 2 ONLY):</td> <td style="text-align: right;">1</td> </tr> <tr> <td>LOWEST CRIT. ELEV. (MODE 2 ONLY):</td> <td style="text-align: right;">0.0000</td> </tr> </table>			FITCON OUTPUT FILE (.FO):	TC0	HCRIT OUTPUT FILE (.HCO):	TC0	CREATE A PLOT FILE? (Y or N):	Y	HCRIT PLOT FILE (.HPT):	TC0	SELECTION MODE FOR CRIT. ELEV.:	1	NUMBER OF CRIT. ELEV. (MODE 2 ONLY):	1	LOWEST CRIT. ELEV. (MODE 2 ONLY):	0.0000
FITCON OUTPUT FILE (.FO):	TC0															
HCRIT OUTPUT FILE (.HCO):	TC0															
CREATE A PLOT FILE? (Y or N):	Y															
HCRIT PLOT FILE (.HPT):	TC0															
SELECTION MODE FOR CRIT. ELEV.:	1															
NUMBER OF CRIT. ELEV. (MODE 2 ONLY):	1															
LOWEST CRIT. ELEV. (MODE 2 ONLY):	0.0000															
F9 - Run HCRIT DOWN UP Esc - Back F10 - Exit to Dos																

Figure 5-5. Sample screen display from the menu driver system, showing the HCRIT options screen.

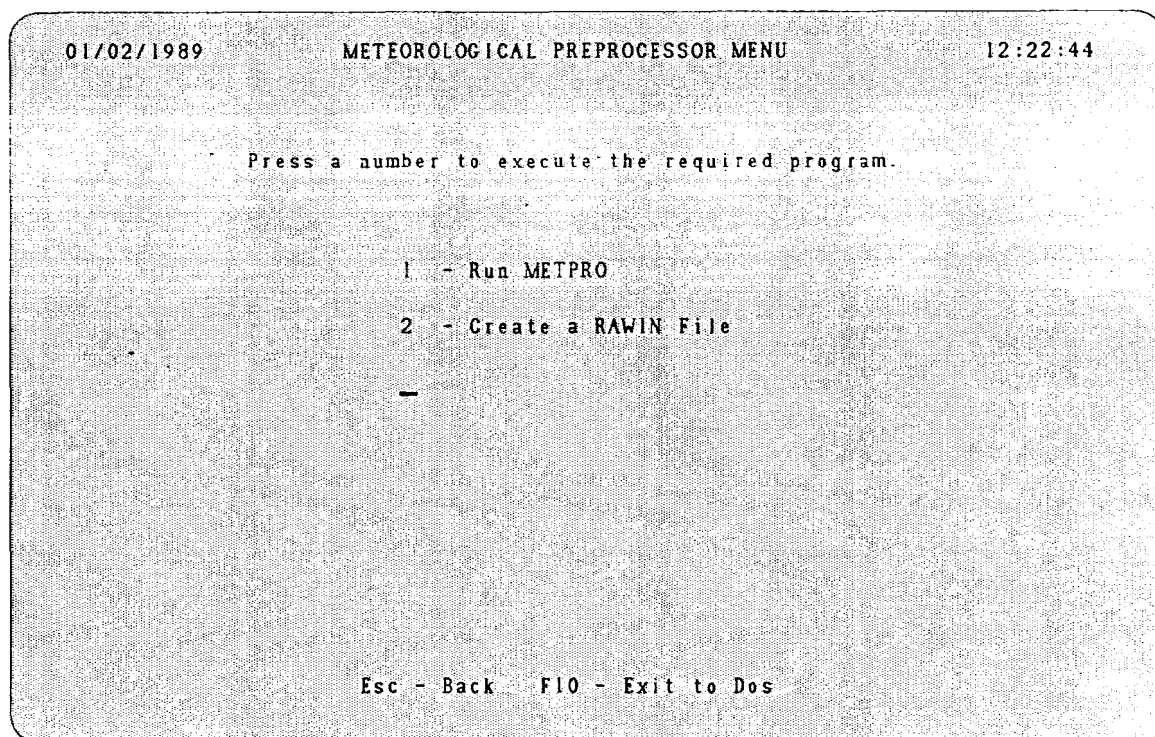


Figure 5-6. Screen display from the menu driver system, showing the meteorological preprocessor menu.

The execution of METPRO is initiated by choosing option 1 from the meteorological preprocessor menu. In running METPRO, the user is first prompted to choose an "OPTIONS" file (.MOP). A sample of the screen display for selecting files is shown in Figure 5-7. The mode switch in the options file is read and selection of files for "PROFILE", "SURF1", "SURF2", and "RAWIN" continues as needed for each mode. After file selection has been completed, the chosen files are displayed for final approval. Files that are not required for a particular mode have an "N/A" displayed in the area for the filename. If a filename needs to be changed, the number corresponding to the file is pressed and the selection menu for that file is displayed. The user may end selection at any time by pressing **(F8)**. The **(F9)** key is pressed to execute METPRO with the listed files. An error message will be displayed if files needed for execution have not been selected. The METPRO program will create a "SURFACE" file with the same filename as the options file and an extension of .SFC, which will be placed in the \CTDM\FILES\ directory. If this file already exists, a warning message will be displayed. The user will have the option of overwriting the existing file or creating a backup copy of the old file (&SF). After execution, the user is given the option to look at the diagnostic output (.MOF) file or to return to the meteorological preprocessor menu.

File selection for the READ62 preprocessor proceeds in similar fashion to that for METPRO. The READ62 program creates the "RAWIN" file (.RAW) needed for METPRO mode 3 and for daytime hours in CTDMPLUS. After execution of the program, the user may look at the diagnostic output file (.R62) or return to the meteorological preprocessor menu.

5.2.7 Running CTDMPLUS

Choosing option 3 from the main menu (Figure 5-2) will start the file selection process for CTDMPLUS. The CTDM.IN file is chosen first and is read to determine which optional files are needed. The user is prompted to select the "PROFILE", "SURFACE", "RECEPTOR", "TERRAIN", and, if necessary, the "EMISSION" and "RAWIN" files. The function keys, **(F8)** and **(F9)**, operate in the same manner as for METPRO. An example of the screen showing the selected files is given in Figure 5-8. The execution of CTDMPLUS will produce two output files, "CONC" and "CTDM.OUT", which are then renamed to filename .CON and filename .OUT, respectively. Upon completion of the run, the user may view the diagnostic output file or return to the main menu.

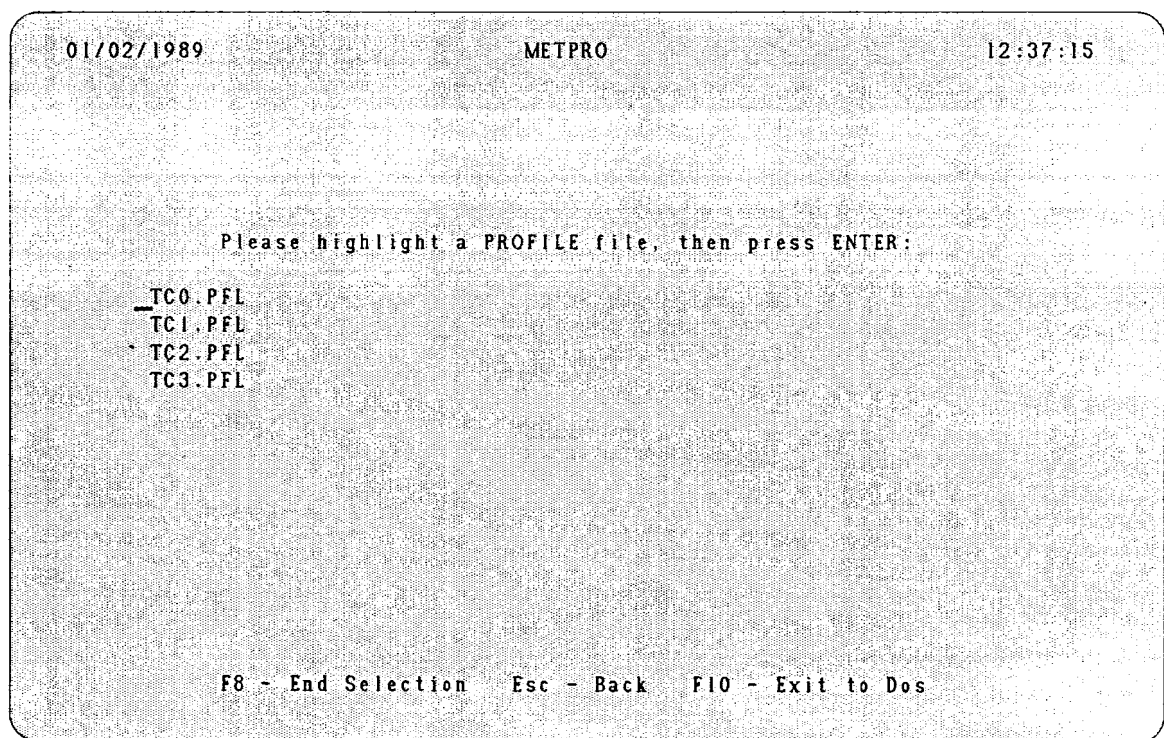


Figure 5-7. Sample screen display from the menu driver system, showing the selection of a file for use with METPRO.

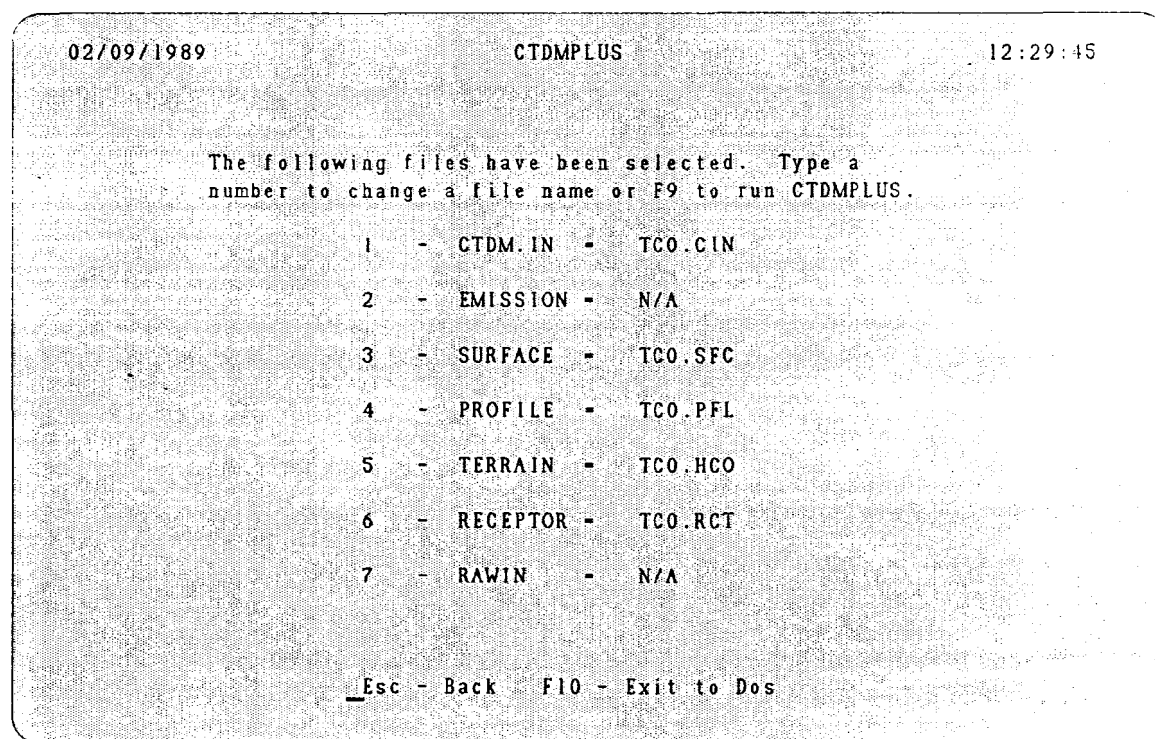


Figure 5-8. Sample screen display from the menu driver system, showing the list of files selected for use with CTDMPPLUS.

5.2.8 Concentration Postprocessors

The concentration postprocessor menu is displayed by selecting option 4 from the main menu (Figure 5-2). The user may elect to run CHIRET, CHIDIS or CONTOUR (see Figure 5-9). CHIRET is a FORTRAN program that reads the concentration and receptor information and creates an output file of sorted concentrations that is used by both CHIDIS and CONTOUR. CHIDIS, a program that displays concentration values at the receptors in decreasing order is described in Section 4.3.1. CONTOUR, which displays concentration isopleths, is described below.

If CHIRET is chosen from the menu, the user is asked to select a concentration file (*.CON) from a list of available files. Next, the corresponding receptor file is chosen. Then, the user must enter the name to be given to the output file (*.CHI). A batch job will be run to execute CHIRET. The execution of CHIRET continues as described in section 4.3.1. After CHIRET has been run, the user is returned to the CONTOUR menu. When the CONTOUR program is selected from the concentration postprocessor menu, the user is given the option to grid the data or run CONTOUR. If the gridding routine is run, the user will be prompted to select a ".CHI" file and provide a name for the output file of gridded data (*.GRD). Upon completion, the gridding routine creates the output file which contains the data in gridded form, ready for contouring.

To display the concentration isopleths, the user must select a ".GRD" file from the list of available files. Next, the user decides whether to display the hill contours in addition to concentration contour. If the hill is to be plotted, the user must select, from a list of available files, the FITCON plot file that contains the hill information. Then, the user is asked to indicate the method for determining the contour interval. The user may choose default values or enter the start, stop, and contour interval values. Finally, the isopleths are displayed, on a background of hill contours if that option was selected. See Figure 5-10 for a sample display. Note that CONTOUR will only provide the user with meaningful results if the receptors are widely scattered over the hill.

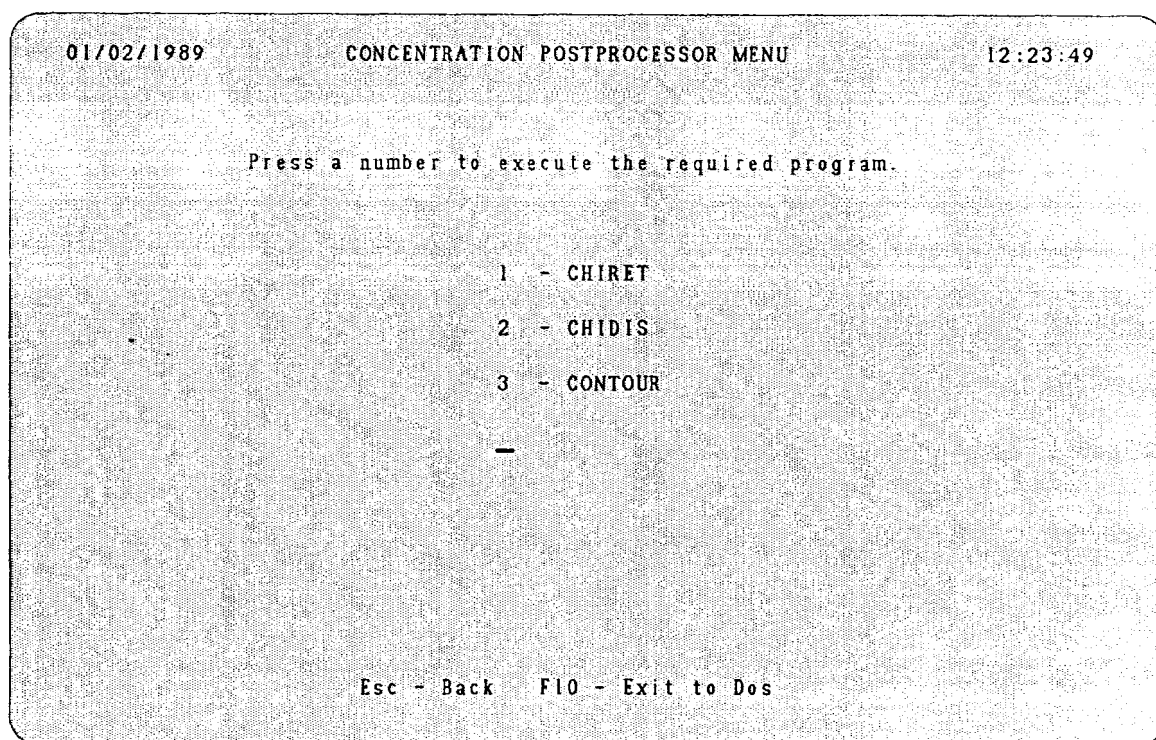


Figure 5-9. Screen display from the menu driver system, showing the concentration postprocessor menu.

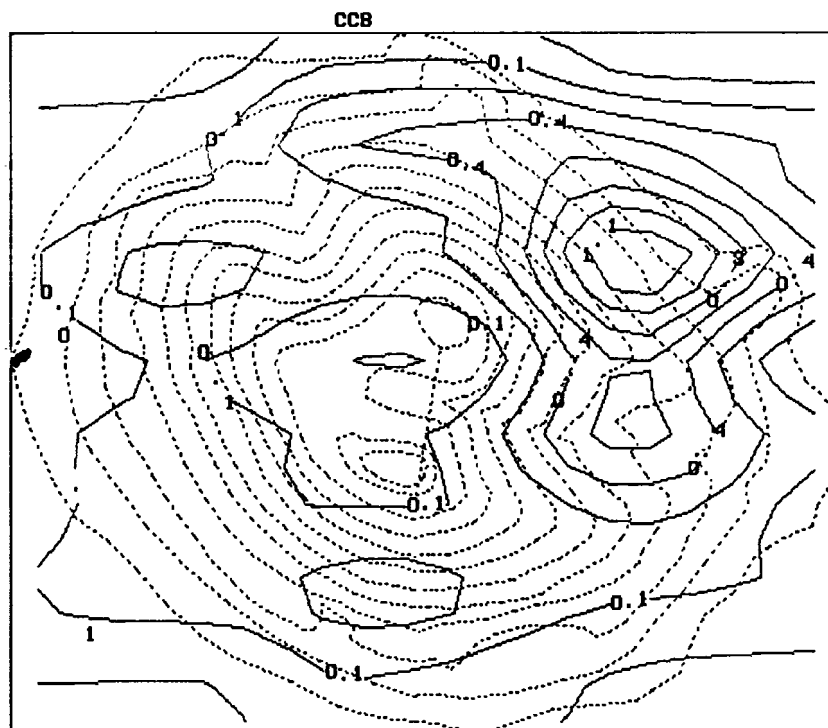


Figure 5-10. Sample screen display from the CONTOUR program, showing the concentration isopleths (solid lines) and hill contours (dashed lines).

REFERENCES

- Agterberg, R., F. T. M. Nieuwstadt, H. van Duuren, A. J. Hasselton, and G. D. Krijt, 1983: Dispersion experiments with sulfur hexafluoride from the 213 m high mast at Cabauw in the Netherlands. Royal Netherlands Meteorological Institute, DeBilt.
- Barad, M. L., Ed., 1958: Project Prairie Grass: a field program in diffusion. Geophysical Research Paper No. 59, Vols. I and II, AFCRF-TR-58-235, Air Force Cambridge Research Center, Bedford, MA.
- Barnes, S.L., 1973: Mesoscale objective map analysis using weighted time series analysis. National Oceanic and Atmospheric Administration Technical Memorandum ERL NSSL-62. National Severe Storms Laboratory, Norman, OK.
- Batchelor, G. K., 1970: *An Introduction to Fluid Dynamics*. Cambridge University Press, London NW1.
- Bjorklund, J. R., and J. F. Bowers, 1982: User's instructions for the SHORTZ and LONGZ computer programs. Vol. I. EPA-903/9-82-004a, U.S. Environmental Protection Agency, Region III, Philadelphia, PA.
- Briggs, G. A., 1973: Diffusion estimation for small emissions. ATDL Contribution File No. 79, Atmospheric Turbulence and Diffusion Laboratory, U.S. Environmental Protection Agency, Research Triangle Park, NC.
- Briggs, G. A., 1975: Plume rise predictions. In *Lectures on Air Pollution and Environmental Impact Analyses*. American Meteorological Society, Boston, MA.
- Briggs, G. A., 1984: Plume rise and buoyancy effects. Chapter 8 in *Atmospheric Science and Power Production*, D. Randerson, Ed. DOE/TIC-27601, U.S. Department of Energy.
- Briggs, G.A., 1985: Analytical parameterization of diffusion: the convective boundary layer. *J. Climate Appl. Meteor.*, **24**, 1167-1186.
- Briggs, G. A., W. L. Eberhard, J. E. Gaynor, W. R. Moninger, and T. Uttal, 1986: Convective diffusion measurements compared with laboratory and numerical experiments. Preprint, Fifth Joint Conference on Applications of Air Pollution Meteorology, American Meteorological Society, Chapel Hill, NC, 340-343.
- Briggs, G. A., and K. R. McDonald, 1978: Prairie Grass revisited: optimum indicators of vertical spread. *Proceedings of the Ninth International Technical Meeting on Air Pollution Modeling and its Applications*, No. 103, NATO, 209-220.
- Brighton, P. W. M., 1978: Strongly stratified flow past three-dimensional obstacles. *Quart. J. Roy. Meteor. Soc.*, **104**, 289-307.
- Burt, E. W., 1977: Valley model user's guide. EPA-450/2-77-018, U.S. Environmental Protection Agency, Office of Air Quality Planning and Standards, Research Triangle Park, NC.

- Businger, J. A., 1973: Chapter 2: Turbulent transfer in the atmospheric surface layer. In *Workshop on Micrometeorology*, D. A. Haugen, Ed. American Meteorological Society, Boston, MA.
- Carson, D. J., 1973: The development of a dry inversion-capped convectively unstable boundary layer. *Quart. J. Roy. Meteor. Soc.*, **99**, 450-467.
- Clark, R. N., D. G. Reid, and A. J. Troup, 1971: The Wangara experiment: boundary layer data. Technical Paper 19, Division of Meteorology and Physics, Commonwealth Scientific and Industrial Research Organization, Australia.
- Crapper, G. D., 1959: A three-dimensional solution for waves in the lee of mountains. *J. Fluid Mech.*, **6**, 51-76.
- Csanady, G. T., 1974: Equilibrium theory of the planetary boundary layer with an inversion lid. *Boundary Layer Meteor.*, **6**, 63-79.
- Drazin, P. G., 1961: On the steady flow of a fluid of variable density past an obstacle. *Tellus*, **13**, 239-251.
- Golder, D., 1972: Relations among stability parameters in the surface layer. *Boundary Layer Meteor.*, **3**, 47-58.
- Guldberg, P. H., J. P. Myers, K. W. Wiltsee, and P. Morgenstern, 1977: Handbook for the single source (CRSTER) model. EPA-450/2-77-013, U.S. Environmental Protection Agency, Office of Research and Development, Research Triangle Park, NC.
- Hanna, S. R., 1983: Lateral turbulence intensity and plume meandering during stable conditions. *J. Climate Appl. Meteor.*, **22**, 1424-1430.
- Hanna, S. R., 1986: Lateral dispersion from tall stacks. *J. Climate Appl. Meteor.*, **25**, 1426-1433.
- Hanna, S. R., and R. J. Paine, 1987: Convective scaling applied to diffusion of buoyant plumes from tall stacks. *Atmos. Environ.*, **21**, 2153-2162.
- Hanna, S. R., J. C. Weil, and R. J. Paine, 1986: Plume model development and evaluation--hybrid approach. EPRI Contract No. RP-1616-27, Electric Power Research Institute, Palo Alto, CA.
- Hovind, E. L., M. W. Edelstein, and V. C. Sutherland, 1979: Workshop on atmospheric dispersion models in complex terrain. EPA-600/9-79-041, U. S. Environmental Protection Agency, Research Triangle Park, NC.
- Hunt, J. C. R., and R. J. Mulherarn, 1973: Turbulent dispersion from sources near two-dimensional obstacles. *J. Fluid Mech.*, **61**, 245-274.
- Hunt, J. C. R., and W. H. Snyder, 1980: Experiments on stably and neutrally stratified flow over a model three-dimensional hill. *J. Fluid Mech.*, **96**, 671-704.
- Johnson, W. B., and E. E. Uthe, 1971: Lidar study of the Keystone stack plume. *Atmos. Environ.*, **5**, 703-724.

- Kaimal, J. C., W. L. Eberhard, W. L. Moninger, J. E. Gaynor, S. W. Troxel, T. Uttal, G. A. Briggs, and G. E. Start, 1986: Project CONDORS: convective diffusion observed by remote sensors. Report No. 7, NOAA/ERL/Boulder Atmospheric Observatory, Boulder, CO.
- Kato, H., and O. M. Phillips, 1969: On the penetration of a turbulent layer into stratified fluid. *J. Fluid Mech.*, **37**, 643-655.
- Lamb, R. G., 1979: The effect of release height on material dispersion in the convective boundary layer. Preprints, Fourth Symposium on Turbulence, Diffusion, and Air Pollution, American Meteorological Society, Reno, NV.
- Lamb, R. G., 1981: Diffusion in the convective boundary layer. In *A Short Course on Atmospheric Turbulence and Air Pollution Modeling*, F. T. M. Nieuwstadt and H. van Dop, Eds. D. Reidel Publishing Company, Boston, MA.
- Li, Z.-K., and G. A. Briggs, 1988: Simple PDF models for convectively driven vertical diffusion. *Atmos. Environ.*, **22**, 54-74.
- Lumley, J. L., and H. A. Panofsky, 1964: *The Structure of Atmospheric Turbulence*. John Wiley and Sons, New York, NY.
- McArthur, G. R., 1983: An introduction to the SCD graphics system. NCAR Technical Note NCAR/TN-161+1A, National Center for Atmospheric Research, Boulder, CO.
- Megarejo, J. W., and J. W. Deardorff, 1974: Stability functions for the boundary-layer resistance laws based upon observed boundary layer heights. *J. Atmos. Sci.*, **31**, 1324-1333.
- Mills, M. T., R. J. Paine, E. M. Insley, and B. A. Egan, 1987: The complex terrain dispersion model (CTDM) terrain preprocessor system--user guide and program descriptions. U.S. Environmental Protection Agency, Atmospheric Sciences Research Laboratory, Research Triangle Park, NC.
- Misra, P. K., 1982: Dispersion of non-buoyant particles inside a convective boundary layer. *Atmos. Environ.*, **16**, 239-243.
- Nieuwstadt, F. T. M., 1981: The steady-state height and resistance laws of the nocturnal boundary layer: theory compared with Cabauw observations. *Boundary Layer Meteor.*, **20**, 3-17.
- Paine, R. J., 1987: User's guide to the CTDM meteorological preprocessor (METPRO) program. U.S. Environmental Protection Agency, Atmospheric Sciences Research Laboratory, Research Triangle Park, NC.
- Paine, R. J., and B. A. Egan, 1987: User's guide to the rough terrain diffusion model (RTDM)--revision 3.20. ERT Document PD-535-585, ERT, Inc., Concord, MA.
- Paine, R. J., D. G. Strimaitis, M. G. Dennis, R. J. Yamartino, M. T. Mills, and E. M. Insley, 1987: User's guide to the complex terrain dispersion model. Vol. 1. EPA-600/8-87-058a, U.S. Environmental Protection Agency, Research Triangle Park, NC.

- Pasquill, F., 1976: Atmospheric dispersion parameters in Gaussian plume modeling. Part II--Possible requirements for change in the Turner workbook values. EPA-600/4-76-030b, U.S. Environmental Protection Agency, Research Triangle Park, NC.
- Perry, S. G., and W. H. Snyder, 1989: Laboratory simulations of daytime mixed layer heights in complex terrain. Accepted for presentation at the Sixth Joint Conference on Applications of Air Pollution Meteorology, American Meteorological Society, Anaheim, CA.
- Riley, J. J., H. T. Liu, and E. W. Geller, 1976: A numerical and experimental study of stably stratified flow around complex terrain. EPA-600/4-76-021, U.S. Environmental Protection Agency, Research Triangle Park, NC.
- Sheppard, P. A., 1956: Airflow over mountains. *Quart. J. Roy. Meteor. Soc.*, **82**, 528-529.
- Smith, R. B., 1980: Linear theory of stratified hydrostatic flow past an isolated mountain. *Tellus*, **32**, 348-364.
- Snyder, W. H., and J. C. R. Hunt, 1984: Turbulent diffusion from a point source in stratified and neutral flows around a three-dimensional hill. Part II--Laboratory measurement of surface concentrations. *Atmos. Environ.*, **18**, 1969-2002.
- Snyder, W. H., R. S. Thompson, and M. S. Shipman, 1986: Streamline trajectories in neutral and stratified flow over a three-dimensional hill. Appendix to *EPA Complex Terrain Model Development: Fifth Milestone Report*. EPA-600/3-85-069, U.S. Environmental Protection Agency, Research Triangle Park, NC.
- Taylor, G. I., 1921: Diffusion by continuous movements. *Proc. London Math. Soc. Ser. 2*, **20**, p. 196.
- Tennekes, H., 1981: Similarity relations scaling laws and spectral dynamics. In *Atmospheric Turbulence and Air Pollution Modeling*, F. T. M. Nieuwstadt and H. van Dop, Eds. D. Reidel Publishing Company, Boston, MA.
- U.S. Environmental Protection Agency, 1986: Guideline on air quality models (revised). EPA-450/2-78-027R, Office of Air Quality Planning and Standards, Research Triangle Park, NC.
- Venkatram, A., 1983: On dispersion in the convective boundary layer. *Atmos. Environ.*, **17**, 529-533.
- Venkatram, A., D. Strimaitis, and D. DiCristofaro, 1984: A semi-empirical model to estimate vertical dispersion of elevated releases in the stable boundary layer. *Atmos. Environ.*, **18**, 923-928.
- Venkatram, A., and R. Vet, 1981: Modeling of dispersion from tall stacks. *Atmos. Environ.*, **15**, 1531-1538.
- Weil, J. C., 1977: Evaluation of the Gaussian plume model at Maryland power plants. Reference No. PPSP-MP-16, Maryland Power Plant Siting Program, Martin Marietta Corporation, Baltimore, MD.
- Weil, J. C., 1979: Assessment of plume rise and dispersion models using lidar data. Reference No. PPSP-MD-24, Maryland Power Plant Siting Program, Martin Marietta Corporation, Baltimore, MD.
- Weil, J. C., and R. P. Brower, 1983: Estimating convective boundary layer parameters for diffusion applications. Martin Marietta Corporation for the Maryland Department of Natural Resources, Baltimore, MD.

- Weil, J. C., and W. F. Furth, 1981: A simplified numerical model of dispersion from elevated sources in the convective boundary layer. Extended abstract, Fifth Symposium on Turbulence, Diffusion, and Air Pollution, American Meteorological Society, Atlanta, GA, 76-77.
- Willis, G. E., and J. W. Deardorff, 1976: A laboratory model of diffusion into a convective planetary boundary layer. *Quart. J. Roy. Meteor. Soc.*, **102**, 427-445.
- Willis, G. E., and J. W. Deardorff, 1978: A laboratory study of dispersion from an elevated source in a convective mixed layer. *Atmos. Environ.*, **12**, 1305-1313.
- Willis, G. E., and J. W. Deardorff, 1981: A laboratory study of dispersion in the middle of the convectively mixed layer. *Atmos. Environ.*, **15**, 109-117.
- Yamartino, R. J., 1984: A comparison of several "single pass" estimators of the standard deviation of wind direction. *J. Clim. Appl. Meteor.*, **23**, 1362-1366.
- Yamartino, R. J., 1987: Appendix A--Exact solutions to the linearized equation for stratified flow over terrain in multidimensional space. In *EPA Complex Terrain Model Development Final Report*. EPA-600/3-88/006, U.S. Environmental Protection Agency, Research Triangle Park, NC.

APPENDIX A

DETAILS OF LIFT AND WRAP ALGORITHMS

A.1 TERRAIN FACTORS T_z and T_y

For axi-symmetric strain, the theory of Hunt and Mulhearn (1973) shows that

$$\sigma^2(t) = \frac{2}{\beta^2(t)} \int_0^t \beta^2(t') K(t') dt' \quad (A-1)$$

where σ denotes either σ_y or σ_z , β is the strain function for the corresponding component, and K is the diffusivity for that component. In the case of σ_z , the strain function β_z for small deflections is approximately

$$\beta_z(t) = e^{-\frac{\partial}{\partial z}(\delta_z(t))} \quad (A-2)$$

where $\delta_z(t)$ is the vertical deflection experienced by a streamline at time t .

The derivation of Equation A-1 depends on a local analysis of the flow field near the centerline of the plume. The strain function is treated as a constant about the centerline, varying only with distance (time) along the flow. In using this result, we assume that the strain function can be assigned a representative value for the layer that contains the bulk of the plume material.

Let $T_h(z_m, t)$, the factor for distortion streamlines in the vertical, be the ratio of the spacing of streamlines in the vertical in the strained flow to that in the incident flow, evaluated at time t along a streamline whose height far from the hill is z_m . The streamline of height z_m is chosen to represent the layer in which the plume resides. Then the distortion factor for the layer at time t is defined as:

$$T_h(z_m, t) = 1 + \frac{\partial}{\partial z} [\delta_z(z, t)]|_{z_m} \quad (A-3)$$

With this mean distortion, the height $\eta(z, t)$ of a streamline above the surface of the hill at time t is approximately

$$\eta(z, t) = z T_h(z_m, t) \quad (\text{A-4})$$

where z is the height of streamline well upwind of the hill. Because of the form of Equation A-4, T_h is equivalent to a "height-correction factor" for a plume.

To evaluate T_z , consider the argument of the exponential function in the vertical distribution factor of Equation 40 (Section 2.5) when the elevation of the receptor above the surface is zero. The primary quantity in this argument is the ratio z_r/σ_{z*} , where σ_{z*} is given in Equation 38 (Section 2.5). The corresponding ratio in the approach of Hunt and Mulhearn is $\eta(z_r, t)/\sigma_z(t)$ where $\eta(z_r, t)$ is given by Equation A-4, and $\sigma_z(t)$ is given by Equation A-1. T_z is evaluated by equating these two quotients.

Using Equations A-2 and A-3, the strain function can be rewritten in terms of T_h as:

$$\beta_z(t) = e^{-(T_h-1)} \quad (\text{A-5})$$

For weak strain, T_h is of the order 1, so that $\beta_z(t) = 1/T_h(z_m, t)$. Adopting the weak-strain form of the product $\beta_z T_h$, the expression for T_z becomes:

$$\frac{1}{T_z^2} = \frac{\int_{t_0}^t 2K_z(t') e^{-2(T_h(z_m, t')-1)} dt'}{\sigma_z^2 - \sigma_{z0}^2} \quad (\text{A-6})$$

Note that the denominator is the difference of the squares of the plume size across the interval $t - t_0$ in the absence of any effects of terrain.

This expression is implemented in CTDMPLUS by breaking the integral in 25 subintervals along the streamline trajectory over the hill. Within each subinterval, the strain function is assumed to be constant, equal to its value at the midpoint of the subinterval. This allows the integral for one of the subintervals to be written as:

$$\int_{t_1}^{t_2} 2K_z(t') \beta_z^2(t') dt' = \beta_z^2(t_m) (\sigma_{za}^2(t_2) - \sigma_{za}^2(t_1)) \quad (\text{A-7})$$

where β_z is obtained from Equation A-5. The altered value of σ_z (σ_{za}) is given by Equation 12 (Section 2.5), except σ_w and T_L have been altered by the changes in the flow over the hill.

The Lagrangian time-scale in the absence of any strain in the flow is given by the relation

$$\frac{1}{T_{Lo}} = \frac{N_o}{\gamma^2} + \frac{\sigma_{wo}}{\Gamma z_s} \quad (A-8)$$

where the subscripts 'o' denote the flat-terrain quantities. The strain in the flow alters the stratification (temperature gradient), the turbulence velocity, and the length scale of the dominant eddies, so that

$$\frac{1}{T_L} = \frac{N_o/\gamma^2}{\sqrt{T_h(z_m, t)}} + \frac{\sigma_{wo}}{\Gamma z_s} \frac{T_{sw}}{T_h(z_m, t)} \quad (A-9)$$

where T_{sw} is the ratio σ_w/σ_{wo} . The value of T_{sw} is estimated from inner-layer theory (Britter et al. 1981) so that $T_{sw} = T_u$, the speedup factor for the flow at time t . This is equivalent to saying that the turbulence intensity (i_z) is not altered by the flow over the hill.

A parallel development factor for T_y leads to a similar result. The distortion factor in the horizontal direction is denoted by $T_t(z_m, t)$ so that

$$\frac{1}{T_y^2} = \frac{\int_{t_o}^t 2K_y(t') e^{-2(T_t(z_m, t')-1)} dt'}{\sigma_y^2 - \sigma_{yo}^2} \quad (A-10)$$

This integral is also broken into subintervals, as in Equation A-7. In this case though, $\sigma_{ya}(t)$ is given by the linear growth form:

$$\sigma_{ya}(t) = T_{sv} \sigma_{vo} t \quad (A-11)$$

because this form holds for distances of travel of nearly 10 km, T_s is set to unity.

A.2 EFFECTIVE RECEPTOR POSITION AND THE DISTORTION FACTORS (LIFT)

The receptor position in Equation 39 (Section 2.5) is denoted as (h_R', y_R') , where the primes indicate that the distance of the receptor from the centerline of the plume has been altered by the presence of the hill. The property of the flow that is conserved as the flow is deformed over the hill is the number of streamlines. Upwind of the hill, streamlines are straight and parallel. Over the hill, the spacing is variable and the streamlines suffer deflections. Because concentrations are computed for a parallel flow in which the influence of terrain is manifest in the H_c -partition of plume material, in the altered rates of diffusion, and in the altered streamline that passes through the receptor, the chief task in computing (h_R', y_R') is in identifying the streamline that passes through the source, and the streamline that passes through the receptor. The position of these two streamlines in the unperturbed flow upwind of the hill defines the effective receptor location relative to the centerline of the plume. These streamlines are obtained from the flow model described in Section A-4.

The design of the flow model is particularly well-suited to obtaining h_R' and y_R' because it is formulated as a "backwards-looking" solution. It is designed to compute the deflection experienced by a streamline that passes through a given point over the hill. If the given point is a receptor, then the model will compute the deflection experienced by the streamline that passes through that receptor. Knowing the actual position of the receptor, the deflections allow h_R' and y_R' to be computed.

The deformation factors T_h and T_l and the speedup factor T_u are also obtained from the model. These are computed along the path of the streamline chosen to be representative of the layer containing the plume material. Far from the hill, this streamline is taken to be half of the way between H_c and the elevation of the center of mass of plume material above H_c .

Because a particular streamline must be followed along the flow (a "forward-looking" process), its position at any time t must be found by an iterative process. Each "guess" at where the streamline may be at time t produces a computed position in the incident flow. New guesses are dependent on the difference between the last computed position, and the position of the targeted streamline.

A.3 INTERNAL MIXING LAYER (LIFT)

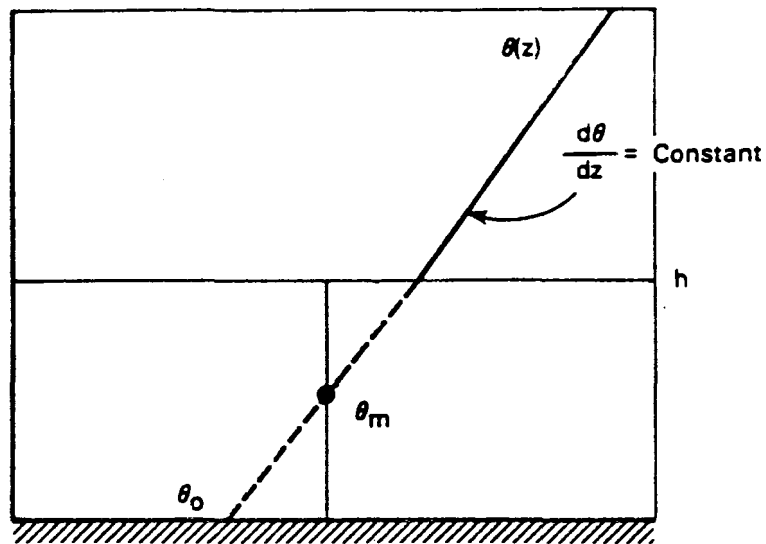
A central assumption involved in the use of the LIFT equations is that the turbulence field is homogeneous. While this assumption is violated in nearly all applications of the Gaussian plume model, there is one situation in modeling the dispersion of plume material over a hill where such a violation is severe.

An elevated plume in a very stably-stratified flow may reside in a region of nearly laminar flow, with very little turbulence. The turbulent boundary layer beneath this region can be very shallow. When H_c is greater than the depth of the turbulent flow, the entire laminar region may flow over terrain, and an internal boundary layer must form at the base of this layer. If this internal boundary layer were ignored, then the diffusivity of plume material would remain virtually zero, and the effect of the terrain would only be seen in the dividing streamline height partition of plume material.

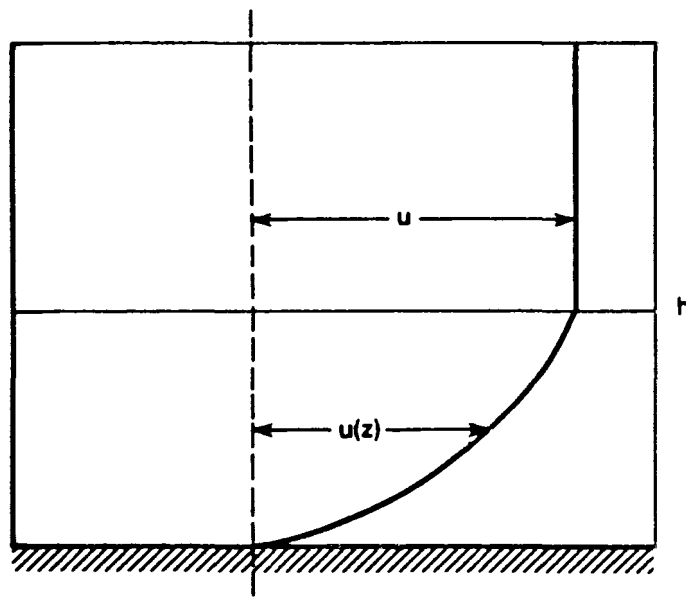
To provide a more realistic treatment of the very stable limit, a simple turbulent surface layer is considered in LIFT. Within this surface layer, the vertical distribution of plume material is uniform, and the concentration is obtained by sampling the vertical distribution in the absence of the surface layer, and taking the average value over the depth of the layer.

The depth of the surface stable layer is estimated by focusing on the initial stages in the development of such a layer, when turbulent mixing is very strong. Assume that the turbulence in the layer produces a layer of constant potential temperature (see Figure A-1). As a result of the rapid mixing in the layer, assume that the buoyancy effects are negligible in the layer, so that the wind speed takes on a logarithmic structure in the vertical. Wind speed is continuous at the top of the layer, but the gradient is not.

Csanady (1974) discusses a theory for estimating the evolution of the depth of such a surface layer. He uses the result of laboratory simulations by Kato and Phillips (1969) in which a layer is thickening into a fluid with constant Brunt-Vaisala frequency N , as a result of a constant stress applied at the bottom of the layer:



Potential Temperature Profile



Wind Speed Profile

Figure A-1. Illustration of the structure assumed for the developing internal mixing layer over the hill above H_c .

$$\frac{1}{u_*} \frac{dh}{dt} = \frac{2.5 u_*^2 \theta_m}{g \Delta \theta h} \quad (\text{A-12})$$

Here, h is the thickness of the layer, u_* is the surface friction velocity, g is the acceleration due to gravity, θ_m is the potential temperature of the mixed layer, and $\Delta \theta$ is the jump in potential temperature at the top of the layer. In essence, the entrainment depends on the turbulence generated at the surface of the layer, and not on any assumptions about shear-generated turbulence at the interface.

The friction velocity in Equation A-12 is given by

$$u_* = \frac{ku}{\ln(h/z_o)} \quad (\text{A-13})$$

where u is the mean wind speed outside of the layer, k is von Karman's constant, and z_o is the roughness length for the surface of the hill. Rewriting Equation A-12, an implicit equation for h :

$$\left(\frac{h}{u/N}\right)^3 \left\{ \left(\ln \frac{h}{z_o}\right)^3 - \left(\ln \frac{h}{z_o}\right)^2 + \frac{2}{3} \left(\ln \frac{h}{z_o}\right) - \frac{2}{9} \left(1 - \left(\frac{z_o}{h}\right)^3\right) \right\} = \frac{x - x_o}{u/N} \quad (\text{A-14})$$

This implicit equation has two undesirable traits. The growth of the mixing layer is extremely rapid for very small time-of-travel (downwind distance) from the point where the flow first encounters the hill above H_c and the estimates of mixing depths "blow up" for weak stratification. The first of these traits is removed by demanding that the rate-of-growth not exceed unity (slope of the interface equates 45°). The second trait is removed by limiting how large u/N can be in equation A-14.

For convenience, u/N is set equal to the minimum of u/N and H_c . This is done because we wish to turn on the mixing layer primarily for those cases in which turbulence at plume height is decoupled from the surface. As H_c becomes less than half the hill height, there is a strong likelihood that the turbulent boundary layer in the approach flow encompasses most of the depth of the flow over the hill. Hence, in using the minimum of u/N and H_c , the stability is artificially increased for H_c less than $H/2$ so that the depth of the mixing layer will decrease. As H_c goes to zero, the mixing layer is completely absent, as desired.

A.4 FLOW MODEL (LIFT)

CTDMPLUS simplifies the treatment of stratified flow over a hill by separating the flow into two regimes: a lower portion, below H_c , which is either blocked (in the case of a long ridge) or flows around the

hill, and an upper portion, above H_c , which has sufficient kinetic energy to flow up and over the hill. This simplification means that for a flow of constant speed, u , which lifts up and over the hill, one always has the property that $(H - H_c)N/u \leq 1$; or equivalently, that the Froude number for this portion of the flow exceeds unity and the flow is not "strongly" stratified. This fact, coupled with the assumption that the hill is not too steep (i.e., less than about 15°) enables one to use the linearized equations of motion for steady-state Boussinesq flow (Smith, 1980):

$$\rho_o u \frac{\partial u'}{\partial x} = - \frac{\partial p'}{\partial x} \quad (\text{A-15a})$$

$$\rho_o u \frac{\partial v'}{\partial x} = - \frac{\partial p'}{\partial y} \quad (\text{A-15b})$$

$$\rho_o u \frac{\partial w'}{\partial x} = - \frac{\partial p'}{\partial z} - \rho' g \quad (\text{A-15c})$$

$$\frac{\partial u'}{\partial x} + \frac{\partial v'}{\partial y} + \frac{\partial w'}{\partial z} = 0 \quad (\text{A-15d})$$

and

$$\rho' = - \left(\frac{\partial p_o}{\partial z} \right) \eta \quad (\text{A-15e})$$

These equations, in which $\partial/\partial x$, $\partial/\partial y$, and $\partial/\partial z$ indicate derivatives with respect to downstream, cross-stream, and vertical coordinates respectively, relate the perturbation velocities u' , v' , and w' to the perturbation density, ρ' , pressure p' , and vertical fluid displacement, $\eta = \eta(x, y, z)$, and to the unperturbed initial velocity u and density ρ_o . Adding the kinematic condition for steady flow in a shear-free approach flow

$$w' = u \frac{\partial \eta}{\partial x} \quad (\text{A-16})$$

Equations (A-15) can be reduced to the single partial differential equation:

$$\frac{\partial^2}{\partial x^2} (\nabla^2 \eta) + n^2 \nabla_H^2 \eta = 0 \quad (\text{A-17a})$$

where

$$n = \frac{N}{u}, \text{ and } N^2 = -\left(\frac{g}{\rho_o}\right) \frac{\partial \rho_o}{\partial z}. \quad (\text{A-17b})$$

Yamartino (1987) discusses exact solutions to Equation (A-17), but steep terrain or strong stratification tend to invalidate these because higher-order terms in Equations A-18 (e.g., quadratic in a perturbations quantity) can be no longer neglected. Thus, the great complexity associated with the exact solution is abandoned in favor of a more easily integrated, approximate solution. The easiest way to reach the approximate solution is to integrate Equation (A-17) twice with respect to x ,

$$\nabla^2 \eta + n^2 \left(\eta + \int_{-\infty}^x \int_{-\infty}^{x'} \frac{\partial^2 \eta}{\partial y^2} dx'' dx' \right) \quad (\text{A-18a})$$

and approximate the troublesome last term as

$$\int_{-\infty}^x \int_{-\infty}^{x'} \frac{\partial^2 \eta}{\partial y^2} dx'' dx' = \eta \cdot \left(\frac{L_x^2}{L_y^2} \right), \quad (\text{A-18b})$$

where L_x , L_y are the length scales of the hill in the along-, cross-wind directions, respectively. This approximation, which proves to be exact for an infinite field of cosine hills, leads to the Helmholtz equation,

$$\nabla^2 \eta + m^2 \eta = 0 \quad (\text{A-19a})$$

where

$$m = n \left(1 + \frac{L_x^2}{L_y^2} \right)^{1/2}. \quad (\text{A-19b})$$

It has the simple particular solution

$$\eta = -\frac{\partial G}{\partial z} \quad (\text{A-20})$$

with $G = \cos(mR)/R$ and $R^2 = x^2 + y^2 + z^2$.

This is the Green's function solution for a delta function hill (i.e., a mathematically narrow but high hill of unit volume). It is extended to a general hill shape $h(x,y)$ via the convolution theorem and the lower boundary condition that the flow at the surface follow the hill shape. Thus, for an arbitrary hill

$$I = \iint dx' dy' h(x-x', y-y') G(x', y', z') \quad (A-21)$$

and

$$\eta = -\frac{\partial I}{\partial z'} \quad (A-22a)$$

where use of the height above terrain z' , instead of absolute z reflects the fact that the lower boundary condition has been linearized.

The other quantities needed for a complete description of the flow are obtained by using Equation A-22a and going back to the basic equations of motion, yielding:

$$\frac{u'}{u} = -\left[\frac{\partial^2}{\partial x'^2}(I) + n^2 I \right] = \frac{\rho'}{\rho_0 u^2} \quad (A-22b)$$

$$\frac{v'}{u} = -\frac{\partial}{\partial x} \frac{\partial}{\partial y}(I) + n^2 \int_{-\infty}^x \frac{\partial I}{\partial y} dx' \quad (A-22c)$$

and

$$\frac{w'}{u} = -\frac{\partial^2 I}{\partial x'^2} \quad (A-22d)$$

It should be noted that lateral perturbation velocity, v' , and the subsequent definition of lateral deflection, δ , as

$$\delta = \int_{-\infty}^x dx' \left(\frac{v'}{u} \right) = -\left[\frac{\partial I}{\partial y} + n^2 \int_{-\infty}^x \int_{-\infty}^{x'} \frac{\partial I}{\partial y} dx'' dx' \right] \quad (A-22e)$$

make the additional assumption that streamline deflections are small enough that integrating along the x -axis at y, z' from $x = -\infty$ to x is equivalent to integrating along the streamline from $x = -\infty$. Equation A-22e also provides another example of how higher-order terms are neglected, as a simple geometrical picture of lateral deflection would indicate that the denominator factor u should actually be the true x -component of velocity, or approximately $u + u'$. Note that the deflections η and δ are those experienced by a streamline that passes through the point (x, y, z') . They tell us where that streamline originates in the incident flow.

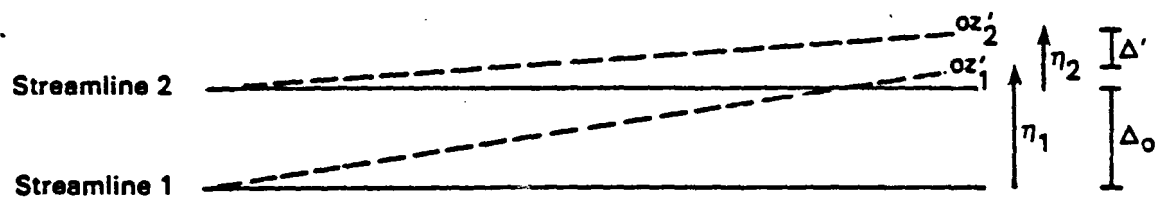
The local strain factors T_l and T_h used in CTDMPLUS can also be related to I through these quantities:

$$T_H = \left(1 - \frac{\partial \eta}{\partial z}\right)^{-1} = \left(1 + \frac{\partial^2 I}{\partial z'^2}\right)^{-1} \quad (\text{A-22f})$$

$$T_l = \left(1 - \frac{\partial \delta}{\partial y}\right)^{-1} = \left(1 + \frac{\partial^2 I}{\partial y'^2} + n^2 \int_{-\infty}^x \int_{-\infty}^{x'} \frac{\partial^2 I}{\partial y'^2} dx'' dx'\right)^{-1} \quad (\text{A-22g})$$

As before, T_h and T_l are factors that relate the spacing between adjacent streamlines in the deformed flow to the spacing in the incident flow. The gradient of the deflection (either $\partial \eta / \partial z$ or $\partial \delta / \partial y$) measures the difference in the deflection experienced by adjacent streamlines and hence, the degree to which the streamlines converge or diverge. In this backward-looking formulation, the deflection is a function of the streamline position (coordinates) after deformation (see Figure A-2), where the vertical position is the height above the surface of the terrain, z' . As detailed in the figure, the finite-difference form of Equation A-22f (and A-22g) is readily obtained from the definitions of streamline positions before and after the deformation. Note that $\partial \eta / \partial z = 1$ is a singular point. This condition would result if streamlines that pass through z_1' and z_2' were to originate at the same height in the incident flow. Also note that Equation A-22f differs from Equation A-3 because the deflection in Equation A-3 is that for a forward-looking formulation.

Before evaluating Equations A-21 and A-22 for a realistic hill shape, it is worthwhile to look back to the solution, $G = \cos(mR)/R$, given by Equation A-21, as properties of the delta function hill solution will show up for finite hills as well. One positive aspect is that as stratification disappears (i.e., N, n, m go to zero) the exact neutral result $G = 1/R$ is recovered. Thus, the approximation expressed by Equation A-18b will not affect neutral flow but only the modifications to the neutral flow solution created by stratification. That these stratification influences might not be too severe can be anticipated by noting that expansion of



$$T_h = \frac{\Delta'}{\Delta_0} = \frac{z'_2 - z'_1}{(z'_2 - \eta_2) - (z'_1 - \eta_1)} = \frac{\Delta z'}{\Delta z' - \Delta \eta} = \frac{1}{1 - \frac{\Delta \eta}{\Delta z'}}$$

Figure A-2. Derivation of the factor T_h in finite-difference form. The dashed lines represent the path of two adjacent streamlines, as they are deflected by the presence of terrain.

the cosine term, as $\cos(mR) \approx 1 - (1/2)m^2 R^2$, indicates that changes to the flow are second-order in m (i.e., m^2) rather than first-order. However, a disturbing aspect of this $\cos(mR)$ dependence is its isotropic nature; that is, z has no special significance in the equation, despite the fact that the density stratification and thus the atmosphere's "springiness" is a z -oriented phenomenon. Exact solutions to Equation A-17 do not display this isotropic behaviour. Thus, one physically significant ramification of approximation (Equation A-18b) becomes apparent. Such isotropic and thus lateral springiness does, however, occur in the aforementioned infinite field of cosine hills problem but steps must be taken to suppress this effect in the single isolated hill problem.

Finally, the connection to the neutral limit solution, $G = 1/R$, suggests a way to inject wind speed shear (with height) back into this shear-free solution. Crapper (1959) points out that the vertical deflection in a neutral, shear-flow is just

$$\eta = \left[\frac{u(0)}{u(z')} \right] \cdot \frac{z'}{R^3} \quad (\text{A-23a})$$

whereas $G = 1/R$ yields

$$\eta = \frac{z'}{R^3} \quad (\text{A-23b})$$

in the shear-free case. Unfortunately, even this simple factor is awkward to superimpose back onto G exactly. The approximation chosen for this model yields a final Green's function of

$$G = \left[\frac{u(0)}{u(z')} \right]^{1/2} \frac{\cos(mR)}{R} \quad (\text{A-24})$$

Any unwanted residual consequences of this approximation are suppressed by enforcing the constraint that $-\partial I / \partial z' = \eta = h(x, y)$ at $z' = 0$.

Referring back to Equation A-22, one notes that all quantities of interest depend on integrals and derivatives of the basic quantity I , given by Equation A-21. Evaluation of I requires a carefully chosen shape of hill. Selection of an appropriate hill shape was governed by

- i) the desire to treat as general a shape and orientation as possible, and

- ii) the necessity for performing the integrations in Equation A-21 analytically.

A Gaussian-shaped hill is used because it contains the overall orientation and scales of the "cut-off" hill, and because it has a tractable mathematical form. The most general Gaussian shape that is considered involves a hill of height h , having elliptical contours with major axis L_a , and a minor axis L_b , oriented at an angle ψ which is counter-clockwise with respect to the flow direction. For a coordinate system with the x-axis aligned with the direction of flow, the hill is prescribed by

$$h(x, y) = h \exp \left\{ - \left[\frac{x^2}{L_x^2} + \frac{y^2}{L_y^2} + 2\gamma xy \right] \right\} \quad (A-25)$$

where

$$\frac{1}{L_x^2} = \left[\frac{\cos^2 \psi}{L_b^2} + \frac{\sin^2 \psi}{L_a^2} \right], \quad \frac{1}{L_y^2} = \left[\frac{\cos^2 \psi}{L_a^2} + \frac{\sin^2 \psi}{L_b^2} \right],$$

and

$$\gamma = \left[\frac{1}{L_b^2} - \frac{1}{L_a^2} \right] \cos \psi \sin \psi.$$

For the symmetric hill with $L_a = L_b = L$, the expression simplifies greatly, as $L_x = L_y = L$ and $\gamma = 0$.

In fact, once the convoluted form of the hill function (i.e. $h(x, y)$ is rewritten as $h(x - x', y - y')$) is substituted into the integral for I , one finds that the exact analytic integration can be accomplished for a receptor position (x, y, z') at the crest (and just off the crest) of such a symmetric Gaussian hill. But this analytic result must be approximated as adequate software does not widely exist for the complex error function portion of this solution. The expression finally used is

$$\begin{aligned} I = & \frac{h(x, y) L_n}{(1 + b_o^2) \left(1 + \frac{z'}{L_n}\right)^2} \cdot \left[\frac{u(0)}{u(z')} \right]^{1/2} \left\{ \left(1 + \frac{z'}{L_n}\right) \cdot \cos(mz') \right. \\ & - \alpha_1 \cdot \frac{\sin(mz')}{m - \alpha_2} \\ & \cdot \left(\frac{x_m}{L_x} \right) \left[m \cdot \cos(mz') + \left(\frac{2}{L_n} + \frac{1}{2} \frac{\alpha}{u(0)} \right) \cdot \sin(mz') \right] \} \quad (A-26) \end{aligned}$$

where

$$b_o = \frac{B_o m L_z}{\sqrt{\pi}} \quad , \quad L_z = R_L \left[\frac{1}{2} \left(\frac{1}{L_x^2} + \frac{1}{L_y^2} \right) \right]^{1/2} \quad ,$$

$$L_n = \frac{1}{2} \sqrt{\pi} L_z \quad ,$$

α is from the shear equation $u(z') = u(0) + \alpha z'$,

$$\alpha_1 = \frac{b_o^2}{L_n} - \frac{1}{2} \frac{\alpha}{u(0)} \quad ,$$

$$\alpha_2 = \frac{2}{\pi^{3/2}} \cdot L_z \cdot \left(1 + \frac{L_x^2}{L_y^2} \right)^{1/2} \quad ,$$

and

$$x_m = x + \gamma L_x^2 y \quad .$$

The two parameters, B_o and R_L , arose because there was a conflict between small and large argument, low-order expansions of the complex error function, and ambiguity in the definition of L_z , respectively. The parameter B_o was set to $(\pi/2)^{1/2}$, the geometric mean of the small and large argument limit values, whereas R_L was tuned to $\ln(2) \approx 0.693$ based on optimization studies using the tow tank data described by Snyder et al. (1986).

The expression for I given above is best described as an admixture of analytic results for the symmetric hill and empirical extensions for the asymmetric hill subject to the constraints that the surface boundary condition be obeyed and that known results be covered for the 2-d ridge limit of $L_y \rightarrow \infty$ and $\psi = 0$. Higher-order terms (e.g., $(\gamma/L_y)^2$ or other such terms arising far from the crest) are neglected. In addition, we took the liberty of switching-off the (x_m/L_x) term upwind of the hill (i.e., $x < 0$), as it seemed to create excessive early streamline rise as the hill was approached and because appropriate damping terms in x_m^2 has already been neglected in the denominator.

Evaluation of the flow variables in Equation A-22 involve straightforward integrations and differentiations of the basic quantity, I , given by Equation A-26. To follow this process most easily and to bridge the gap between mathematical notation (e.g., Equation A-26) and the computer code in SUBROUTINE FLOW, we note that Equation A-26 may be rewritten as

$$I = HHXYM \cdot TZF \cdot \sum_{i=0}^2 T_i \cdot AF_i \quad (A-27)$$

where $HHXYM = h(x, y) L_n / (1 + b_n^2)$ contains the dominant x and y dependences in I , and

$$TZF = \left(1 + \frac{z'}{L_n}\right)^{-2} \cdot \left[\frac{u(0)}{u(z')}\right]^{1/2}$$

contains the overall multiplicative z' dependencies arising from the complex error function approximation and wind speed shear, respectively, and is denoted $TZFAC$ in the code. The sum over terms, $T_i \cdot AF_i$, is organized such that all the trigonometric functions involving the vertical coordinates z' , or the 'angular' variable, mz' , are contained in AF_i , whereas multiplicative constants and remaining coordinate dependences (i.e., x_m/L_x) are absorbed into T_i . Thus, for the quantity I , we have

$$\begin{aligned} T_0 &= 1, \\ T_1 &= -\alpha_1, \text{ and} \\ T_2 &= -\alpha_2 \cdot \left(\frac{x_m}{L_x}\right) \text{ for } x_m \geq 0 \text{ and} \\ &= 0 \text{ for } x_m < 0, \end{aligned}$$

whereas the AF_i quantities, which along with their z' derivatives

$$\begin{aligned} AD_i &= \frac{\partial}{\partial z'}(AF_i) \text{ and} \\ ADD_i &= \frac{\partial^2}{\partial z'^2}(AF_i) \end{aligned}$$

will be used repeatedly in integrated and differentiated forms of I , are presented in Table A-1.

The grouping of terms by variable expressed by Equation A-27 facilitates computation of derivatives by the well-known "chain-rule"

TABLE A-1

 AF_i TERMS AND THEIR DERIVATIVES

$$AF_0 = \left(1 + \frac{z'}{L_n}\right) \cos(mz')$$

$$AD_0 = \frac{\cos(mz')}{L_n} - \left(1 + \frac{z'}{L_n}\right)m \sin(mz')$$

$$ADD_0 = -\frac{2m \sin(mz')}{L_n} - \left(1 + \frac{z'}{L_n}\right)m^2 \cos(mz')$$

$$AF_1 = \frac{\sin(mz')}{m}$$

$$AD_1 = \cos(mz')$$

$$ADD_1 = -m \sin(mz')$$

$$AF_2 = m \cos(mz') + \left(\frac{2}{L_n} + \frac{1}{2} \frac{\alpha}{u(0)}\right) \sin(mz')$$

$$AD_2 = m^2 \sin(mz') + \left(\frac{2}{L_n} + \frac{1}{2} \frac{\alpha}{u(0)}\right)m \cos(mz')$$

$$ADD_2 = -m^2 \cdot AF_2$$

Note: Undesirable streamline deflection behaviour was suppressed by evaluating the sine and cosine terms in AF_0 , AD_0 , and ADD_0 at $z' = 0$.

$$\frac{\partial}{\partial x} A \cdot B \equiv B \cdot \frac{\partial A}{\partial x} + A \cdot \frac{\partial B}{\partial x} .$$

Thus, for example, the quantity $\partial I / \partial z'$, denoted *IDZ* in the code, becomes

$$\frac{\partial I}{\partial z'} = TZFDZ \cdot I + HHXYM \cdot TZF \cdot \sum_{i=0}^2 T_i \cdot AD_i \quad (A-28)$$

where $TZFDZ = (\partial / \partial z' TZF) / TZF$

or

$$TZFDZ = -\frac{2/L_n}{\left(1 + \frac{z'}{L_n}\right)} - \frac{1}{2} \frac{\alpha}{u(z')} .$$

Yet higher derivatives show the economy of the chosen *I* expression compartmentalization and its resistance to the errors that can occur when many, many terms are generated through differation. For example,

$\partial^2 I / \partial z'^2$, denoted *TDZZ* in the code, is simply

$$\begin{aligned} \frac{\partial^2 I}{\partial z'^2} &= TZFDZZ \cdot I + 2 \cdot TZFDZ \frac{\partial I}{\partial z'} \\ &+ HHXYM \cdot TZF \cdot \sum_{i=0}^2 T_i \cdot ADD_i \end{aligned} \quad (A-29)$$

where

$$TZFDZZ = \frac{\left(\frac{\partial^2}{\partial z'^2} TZF\right)}{TZF}$$

or

$$TZFDZZ = (TZFDZ)^2 + \frac{2/L_n^2}{\left(1 + \frac{z'}{L_n}\right)^2} + \frac{1}{2} \frac{\alpha^2}{u^2(z')} .$$

Derivatives of I with respect to x and y are also required, and hence necessitate derivatives of the hill shape function $h(x,y)$ term $HHXYM$. Determining the quantities

$$\begin{aligned}\frac{\partial}{\partial x} (HHXYM) &= -2 \left(\frac{x_m}{L_x} \right) \cdot \frac{HHXYM}{L_x} , \\ \frac{\partial^2}{\partial x^2} (HHXYM) &= -2 \left[1 + 2 \left(\frac{x_m}{L_x} \right)^2 \right] \cdot \frac{HHXYM}{L_x^2} , \\ \frac{\partial}{\partial y} (HHXYM) &= -2 \left(\frac{y_m}{L_y} \right) \cdot \frac{HHXYM}{L_y} , \text{ and} \\ \frac{\partial^2}{\partial y^2} (HHXYM) &= -2 \left[1 + 2 \left(\frac{y_m}{L_y} \right)^2 \right] \cdot \frac{HHXYM}{L_y^2} ,\end{aligned}$$

where $y_m = y + \sqrt{L_x^2} x$, then enables one to rapidly develop the terms:

$$\frac{\partial I}{\partial x} = -2 \left(\frac{x_m}{L_x} \right) \cdot \frac{I}{L_x} + HHXYM \cdot TZF \cdot \sum_{i=0}^2 T_i^* \cdot AF_i \quad (\text{A-30})$$

where now $T_0^* = T_1^* = 0$, because

$T_i^* = \partial T_i / \partial x$ in this case and T_0 and T_1 are independent of x , and $T_2^* = -\alpha_2 / L_x$;

$$\frac{\partial^2 I}{\partial x^2} = -2 \left[1 + 2 \left(\frac{x_m}{L_x} \right)^2 \right] \cdot \frac{I}{L_x^2} - 4 \left(\frac{x_m}{L_x} \right) \frac{\partial I / \partial x}{L_x} \quad (\text{A-31})$$

as all $(\partial^2 T_i / \partial x^2)$ vanish and the extra factor of two (e.i., the 4) arises because

$$\begin{aligned}\frac{\partial^2}{\partial x^2} (AB) &= \frac{\partial}{\partial x} \left[B \cdot \frac{\partial A}{\partial x} + A \cdot \frac{\partial B}{\partial x} \right] = B \cdot \frac{\partial^2 A}{\partial x^2} + 2 \frac{\partial A}{\partial x} \cdot \frac{\partial B}{\partial x} + A \frac{\partial^2 B}{\partial x^2} ; \\ \frac{\partial^2 I}{\partial x \partial z'} &= -2 \left(\frac{x_m}{L_x} \right) \cdot \frac{\partial I / \partial z'}{L_x} + HHXYM \cdot TZFDZ \cdot \sum_{i=0}^2 T_i^* \cdot AF_i \\ &+ HHXYM \cdot TZF \cdot \sum_{i=0}^2 T_i^* \cdot AD_i ;\end{aligned} \quad (\text{A-32})$$

$$\frac{\partial I}{\partial y} = -2 \frac{(y_m/L_y)I}{L_y} + HHXYM \cdot TZF \cdot \sum_{i=0}^2 T_i^* \cdot AF_i \quad (A-33)$$

where T_i^* are redefined now as

$$T_i^* = \frac{\partial T_i}{\partial y} \quad \text{and yield}$$

$$T_0^* = T_1^* = 0$$

$$\text{and } T_2^* = -\frac{\alpha_2}{L_y} ;$$

$$\frac{\partial^2 I}{\partial y^2} = -2 \left[1 + 2 \left(\frac{y_m}{L_y} \right)^2 \right] \frac{I}{L_y^2} - 4 \left(\frac{y_m}{L_y} \right) \frac{\partial I / \partial y}{L_y} ; \quad (A-34)$$

$$\frac{\partial^3}{\partial y^3} = -8 \left(\frac{y_m}{L_y} \right) \frac{I}{L_y^3} - 4 \left(\frac{y_m}{L_y} \right) \frac{\partial^2 I / \partial y^2}{L_y} - 2 \left[3 + 2 \left(\frac{y_m}{L_y} \right)^2 \right] \frac{\partial I / \partial y}{L_y^2} ; \text{ and} \quad (A-35)$$

$$\begin{aligned} \frac{\partial^2 I}{\partial x \partial y} = & -2 \left[\gamma + 2 \frac{x_m y_m}{L_x^2 L_y^2} \right] \cdot I \\ & - 2 \left(\frac{x_m}{L_x} \right) \frac{\partial I / \partial y}{L_x} - 2 \left(\frac{y_m}{L_y} \right) \frac{\partial I / \partial x}{L_y} . \end{aligned} \quad (A-36)$$

The above seven quantities are denoted IDX , $IDXX$, $IDXZ$, IDY , $IDYY$, $ID3Y$, and $IDXY$, respectively, in the computer algorithm FLOW.

Computation of the integrated quantities, defined now symbolically as

$$I^x \equiv \int_{-\infty}^x dx' I(x') \quad \text{and}$$

$$I^{xx} \equiv \int_{-\infty}^x dx' \int_{-\infty}^x dx'' I(x'')$$

and denoted LX and LXX respectively in the code, now requires that several indefinite integrals can be computed. Referring back to Equation A-27 shows that x 's arise in $HHXYM$ due to the Gaussian hill shape function $h(x,y)$, expressed by Equation A-25, as well in the coefficient T_2 . Thus, it is convenient to consider first the integrals

$$g_j^x = \int_{-\infty}^x dx \exp \left[- \left(\frac{x}{L_x} \right)^2 - \left(\frac{y}{L_y} \right)^2 - 2\gamma xy \right] \left(\frac{x_m}{L_x} \right)^j \quad (A-38)$$

for $j = 0, 1$ and where $x_m = x + \gamma L_x^2 y$, as before. Upon completion of the square in the exponential, the results can be found from integral tables to be

$$g_j^x = L_x \exp \left[- \left(\frac{y}{L_y} \right)^2 \gamma_p \right] G_j^x \quad (A-39)$$

where $\gamma_p = 1 - \gamma L_x^2 L_y^2$ and where the G_j^x are presented in Table A-2. Subsequent integration in x to yield g_j^{xx} , defined as

TABLE A-2

DIMENSIONLESS G_j^x AND G_j^{xx} TERMS

$$G_j^x = \int_{-\infty}^{(x_m/L_x)} d\epsilon \exp(-\epsilon^2) \epsilon^j = G_j^x\left(\frac{x_m}{L_x}\right)$$

and

$$G_j^{xx} = \int_{-\infty}^{(x_m/L_x)} d\epsilon G_j^x(\epsilon)$$

definitions yield:

$$G_0^x = \frac{1}{2} \sqrt{\pi} \left[1 + \text{ERF}\left(\frac{x_m}{L_x}\right) \right] ,$$

$$G_1^x = -\frac{1}{2} \exp\left[-\left(\frac{x_m}{L_x}\right)^2\right] ,$$

$$G_0^{xx} = \left(\frac{x_m}{L_x}\right) G_0^x - G_1^x , \text{ and}$$

$$G_1^{xx} = -\frac{1}{2} G_0^x .$$

These are included in flow algorithm as *GOX*, *GLx*, *GOXX*, and *GLXX* , respectively.

Note: Subsequent numerical studies showed that it was preferable to substitute $[1 - |\text{ERF}(x_m/L_x)|]$ for $[1 + \text{ERF}(x_m/L_x)]$. This has the major effect of allowing streamlines to return laterally to their initial upwind positions more rapidly after passing the hill. This adjustment can be rationalized on the basis that Equation A-26 is most valid near the crest of a hill.

$$g_j^{xx} = \int_{-\infty}^x dx' g_j^x \left(\frac{x_m}{L_x} \right)$$

yields formally

$$g_j^{xx} = L_x^2 \exp \left[- \left(\frac{y}{L_y} \right)^2 \gamma_p \right] G_j^{xx} , \quad (\text{A-40})$$

where the G_j^{xx} are also presented in Table A-2. Computation of the G_j^{xx} are made possible by use of the infrequently tabulated inetgral of an error function:

$$\int dx \operatorname{ERF}(x) = x \operatorname{ERF}(x) + \frac{1}{\sqrt{\pi}} \exp(-x^2) .$$

Armed with these quantities, one may express I^x as

$$I^x = \left(\frac{HHLX2E}{L_x} \right) \cdot TZF \cdot \sum_{i=0}^2 T_i^* AF_i \quad (\text{A-41})$$

where

$$HHLX2E = \frac{hL_n L_x^2 \exp \left[- \left(\frac{y}{L_y} \right)^2 \gamma_p \right]}{1 + b_0^2}$$

is the variable name used in the code, and where

$$T_0^* = G_0^x ,$$

$$T_1^* = -\alpha_1 \cdot G_0^x , \text{ and}$$

$$T_2^* = -\alpha_2 \cdot G_1^x .$$

Similarly, the doubly integrated quantity, I^{xx} , is then just

$$I^{xx} = HHLX2E \cdot TZF \cdot \sum_{i=0}^2 T_i^* \cdot AF_i \quad (\text{A-42})$$

where the T_i^* are redefined as

$$\begin{aligned} T_0^* &= G_0^{xx} , \\ T_1^* &= -\alpha_1 \cdot G_0^{xx} , \text{ and} \\ T_2^* &= -\alpha_2 \cdot G_1^{xx} . \end{aligned}$$

Achieving the goal of providing all the quantities specified in Equation A-22 now only demands that a few differentiation operations be performed with respect to y . These are in turn facilitated by the observations that since the G_j^x and G_j^{xx} are only functions of x_m/L_x , but $x_m = \gamma L_x^2 y$ contains y , then the differentiation by y is equivalent to a differentiation by x except that d/dy generates the multiplicative factor γL_x^2 instead of $1/L_x$. Thus we obtain the useful quantities

$$\begin{aligned} H_j &= \frac{\partial}{\partial y} (G_j^x) \\ &= \gamma L_x \cdot \exp\left[-\left(\frac{x_m}{L_x}\right)^2\right] \left(\frac{x_m}{L_x}\right) , \end{aligned} \quad (\text{A-43})$$

referenced as *HHJ* (i.e., *HHO* and *HHI* for $j=0,1$) in the code, and the relations

$$\begin{aligned} \frac{\partial}{\partial y} G_j^{xx} &= \gamma L_x G_j^x , \text{ and} \\ \frac{\partial^2}{\partial y^2} G_j^{xx} &= \gamma L_x \cdot \frac{\partial}{\partial y} G_j^x = \gamma L_x H_j \end{aligned}$$

for use in the differentiation process. Keeping track of the terms generated via the chain rule, one then obtains:

$$\frac{\partial I^{xx}}{\partial y} = -2\left(\frac{y}{L_y^2}\right) \gamma_p I^{xx} + HHLX2E \cdot TZF \cdot \sum_{i=0}^2 T_i^* \cdot AF_i \quad (\text{A-44})$$

where

$$T_0^* = \gamma L_x G_0^x ,$$

$$T_1^* = -\alpha_1 \gamma L_x G_0^x , \text{ and}$$

$$T_2^* = -\alpha_2 \gamma L_x G_1^x ;$$

$$\frac{\partial I^x}{\partial y} = -2 \left(\frac{y}{L_y^2} \right) \gamma_p I^x + \frac{HHLX2E}{L} \cdot TZF \cdot \sum_{i=0}^2 T_i^* \cdot AF_i \quad (A-45)$$

and

$$\begin{aligned} \frac{\partial^2 I^{xx}}{\partial y^2} = & -2 \left(\frac{\gamma_p}{L_y^2} \right) I^{xx} \cdot \left[1 + 2 \left(\frac{y}{L_y} \right)^2 \gamma_p \right] \\ & - 4 \left(\frac{y}{L_y^2} \right) \gamma_p \cdot \frac{\partial I^{xx}}{\partial y} \\ & + HHLX2E \cdot TZF \cdot \gamma L_x \cdot \sum_{i=0}^2 T_i^* \cdot AF_i , \end{aligned} \quad (A-46)$$

where

$$T_0^* = H_0 ,$$

$$T_1^* = -\alpha_1 \cdot H_0 , \text{ and}$$

$$T_2^* = -\alpha_2 \cdot H_1$$

in both Equation A-45 and A-46; and

$$\begin{aligned}
\frac{\partial^3 I^{xx}}{\partial y^3} = & -4 \left(\frac{\gamma_p^2}{L_y^3} \right) \left(\frac{y}{L_y} \right) I^{xx} \cdot \left[3 + 2\gamma_p \left(\frac{y}{L_y} \right)^2 \right] \\
& -6 \left(\frac{\gamma_p}{L_y^2} \right) \frac{\partial I^{xx}}{\partial y} \left[1 + 2\gamma_p \left(\frac{y}{L_y} \right)^2 \right] \\
& -6 \left(\frac{\gamma_p}{L_y^2} \right) \left(\frac{y}{L_y} \right) \cdot \frac{\partial^2 I^{xx}}{\partial y^2} \\
& + HHLX2E \cdot TZF \cdot (\gamma L_x)^2 \cdot \sum_{i=0}^2 T_i^* \cdot AF_i ,
\end{aligned} \tag{A-47}$$

where

$$T_0^* = -2H_1 ,$$

$$T_1^* = +2\alpha_1 \cdot H_1 , \text{ and}$$

$$T_2^* = -\alpha_2 \cdot (H_0 - 2H_2) .$$

The above four quantities in Equations A-44 through A-47 are denoted by *IXXDY*, *IXDY*, *IXXDYY*, and *IXXD3Y*, respectively, in the FLOW algorithm.

One may notice that the quantities $\partial^3/\partial y^3$ in Equation A-35 and $\partial^3 I^{xx}/\partial y^3$ in Equation A-47 have been defined for no apparent purpose. However, they appear when one considers derivatives $\partial\delta/\partial y$ and $\partial^2\delta/\partial y^2$ of δ from Equation A-22e, that are needed for a "fully-implicit" style computation of the lateral deflection. This compensates for the fact that lateral deflections can be quite large and therefore badly violate the "small deflection" assumption invoked for Equation A-22e. The resulting lateral deflections are unfortunately smaller than before the correction, but streamline crossover situations (which create a severe problem for an iterative streamline solver) for large aspect ratio hills are eliminated.

Examples of the flow deformation resulting from the algorithm in CTDMPLUS are shown in Figures A-3 (facing downwind) and A-4 (cross-flow view).

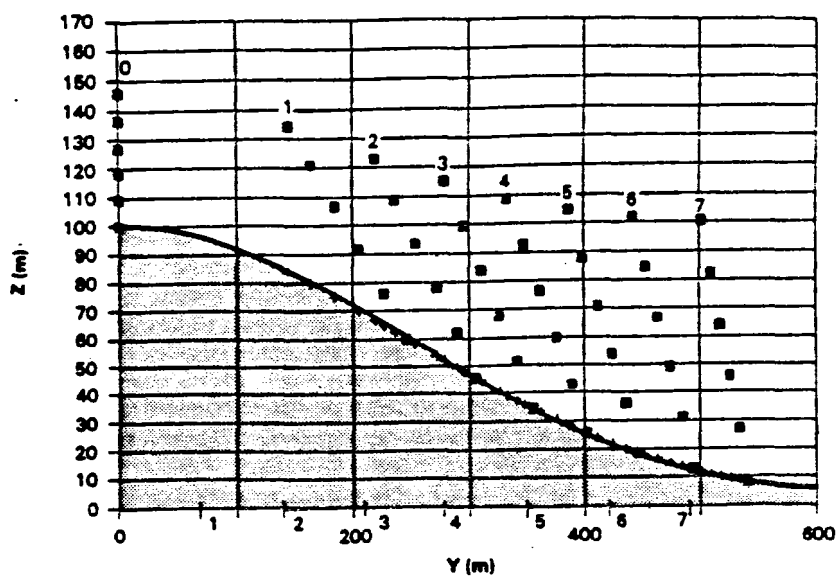


Figure A-3. Behavior of an array of marked streamlines emitted in vertical columns upwind of a Gaussian hill, as seen by an observer looking downwind in stable conditions (Froude # = 1). Initial streamline spacing is 20 m in the vertical (up to 100 m) and 69.3 m in the horizontal upwind of the hill (see streamline column #'s 0-7 at base of diagram and above hill).

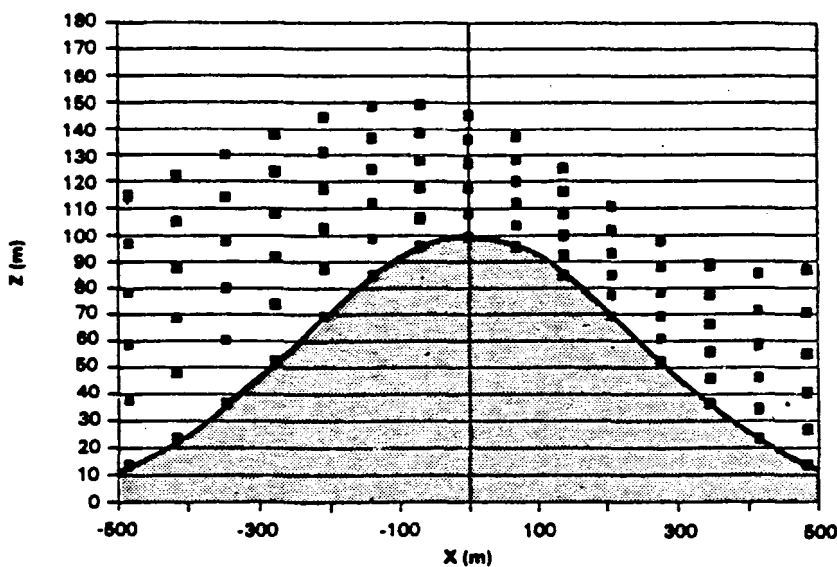


Figure A-4. Pattern of streamlines that pass over the crest of the hill as viewed from the side in stable conditions. Flow is from left to right. Initial streamline spacing is 20 m in the vertical up to 100 m.

A.5 MODEL FOR STREAMLINES (WRAP)

The central features of WRAP are the distance between the streamline that passes through the source and the stagnation streamline, and the relative locations of the source, the receptor, and the point of impingement. These require a flow model to obtain streamlines. Because the flow is two-dimensional in this strongly stratified flow, potential flow solutions are used to obtain the streamlines.

The hill below H_c is represented as a cylinder of elliptical cross-section, set on end. This shape is chosen because it contains the overall scale of the hill, and it is simple enough that streamlin patterns can be expressed analytically. As already stated, the ellipse used for the entire flow below H_c is the result of fitting an ellipse to the height-contour that corresponds to the minimum of H_c and the plume height. The potential flow solution is expressed in elliptical coordinates following the notation of Batchelor (1970).

Let the x-axis be aligned with the major axis of ellipse, let a be the length of the semi-major axis, and b be the length of the semi-minor axis. Then the elliptical coordinates (μ, ν) are related to the cartesian coordinates by the relations

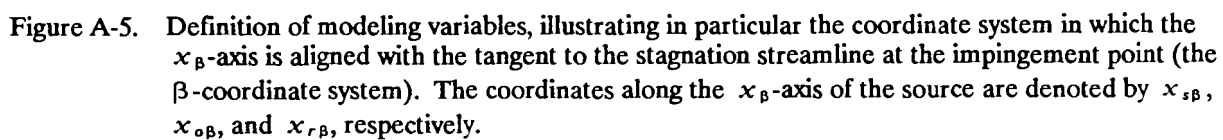
$$\begin{aligned} x^2 &= (a^2 - b^2) \cosh^2(\mu + \mu_0) \cos^2(\nu) \\ y^2 &= (a^2 - b^2) \cosh^2(\mu + \mu_0) \cos^2(\nu) \end{aligned} \quad (A-48)$$

Note that $\mu = \mu' - \mu_0$, where μ_0 is the value of μ' along the boundary of the ellipse (μ is the constant along the ellipses in the family of confocal ellipses of which the boundary of the hill is a member). Using the elliptical coordinates, a streamline in the flow is given by

$$\psi = S_\infty(a + b) \sinh(\mu) \sin(\nu + \alpha_w) \quad (A-49)$$

where S_∞ is the speed of the incident flow, and α_w is its direction. Note that α_w is zero when the flow is directed along the -x direction, and increases in the clockwise direction, as noted in Figure A-5.

The wind speed and direction measured at a tower near a hill may be influenced by the presence of the hill, so that the observed mean speed and direction must be estimated at infinity to determine the incident flow. This is calculated from the theory of two-dimensional potential flow around an ellipse. Let (μ_T, ν_T) be the coordinates of the point at which the speed and direction (S_T, ϕ_T) are measured, where ϕ_T is the direction counter-clockwise from the major axis of the ellipse. Then the wind direction is parallel to the tangent to the streamline defined by $\psi = \psi_T$ at the point (μ_T, ν_T) so that α_w is given by



$$-\tan(\alpha_w) =$$

$$\frac{\left[\frac{\tan(v_T)}{\cosh^2(\mu_T)} + \tan(\phi_T) \tanh(\mu_T) \cos^2(v_T) \right] + r \tan(\phi_T) [\tan^2(v_T) + \tanh^2(\mu_T)]}{(\tan^2(v_T) \tanh^2(\mu_T) + 1) + r \left[\frac{\tanh(\mu_T)}{\cos^2(v_T)} + \tan(\phi_T) \frac{\tan(v_T)}{\cosh^2(\mu_T)} \right]} \quad (A-50)$$

and the speed at infinity (far away from the influence of the hill) is given by

$$S_\infty = \frac{S_T}{r+1} \left(\frac{\frac{(r^2-1)\sin^2(v_T)+1}{\sinh^2 \mu_T} + r^2 + 1 + \frac{2r}{\tanh(\mu_T)}}{1 + \frac{\sin^2(v_T + \alpha_w)}{\sinh^2(\mu_T)}} \right)^{1/2} \quad (A-51)$$

The quantity r is the ratio of the major axis length to the minor axis length, a/b .

Once the incident flow angle relative to the major axis of the ellipse and the speed S_∞ are known, the stream function through the source (ψ_s) can be calculated from

$$\psi_s = -S_\infty(\alpha + b) \sinh(\mu_s) \sin(v_s + \alpha_w) \quad (A-52)$$

The stagnation point can also be calculated. Along the stagnation streamline, $\psi_0 = 0$, so that Equation A-49 becomes

$$0 = -S_\infty(\alpha + b) \sinh(\mu) \sin(v + \alpha_w) \quad (A-53)$$

Because this must be satisfied for all μ , v must be equal to $-\alpha_w$ along the stagnation streamline at the stagnation point. This coordinate system is needed to provide a convenient Cartesian coordinate system that allows the streamline through the source to be a single valued function of x for all α_w . The rotation angle, β , is given by

$$\tan(\beta) = -\frac{a}{b} \tan(\alpha_w) \quad (A-54)$$

The distance between the streamline through the source (ψ_s) and the stagnation streamline ($\psi_0 = 0$) far from the hill is related to the value of ψ_s and the wind speed at infinity, S_∞ . Because the speed of the flow equals the gradient of the stream function far from the hill, we find

$$d = \frac{\psi_s}{S_\infty} \quad . \quad (A-55)$$

However, because σ_v may be measured closer to the hill, the speed at the source is substituted for S_∞ to estimate d near the source.

APPENDIX B

TEST CASE FOR CTDMPPLUS

Input and output files are shown for a test run of CTDMPPLUS. Specific figure references to these files are given below.

<u>File Name</u>	<u>Context</u>	<u>Reference</u>
"CTDM.IN"	Input options; source and receptor information	Figure B-1
"TERRAIN"	Hill Parameterizations	Figure B-2
"RECEPTOR"	Receptor data	Figure B-3
"PROFILE"	Meteorological tower data	Figure B-4
"SURFACE"	Preprocessed meteorological variables	Figure B-5
"RAWIN"	Preprocessed rawinsonde data	Figure B-6
"CONC"	Text file of concentrations	Figure B-7
"CTDM.OUT"	Output listing for this run	Figure B-8

```

CTDMPLUS TEST RUN
3 1 2 1 1 0 1 1 1 1
1.0 0.3048 39.5915 89.4885 6 1
TOWER 0.0 0.0 945.0
STACK-1 0.0 0.0 945.0 189.70 3.36 410.15 25.06 455.05 0
STACK-2 0.0 30.0 940.0 190.00 3.36 420.15 25.06 255.05 0
ENDS
0.76

```

Figure B-1. File "CTDM.IN" used in test run of CTDMPPLUS (see Table 3-3).

1 13	.2240E+04	PIEDMONT HILL				
900.000	.6176E+03-.2092E+04	180.000	3072.000	1294.400		
1000.000	.6176E+03-.2092E+04	180.000	2953.000	1195.700		
1100.000	.6176E+03-.2092E+04	180.000	2834.000	1097.000		
1200.000	.6176E+03-.2092E+04	180.000	2715.000	998.300		
1300.000	.6176E+03-.2092E+04	180.000	2595.000	953.600		
1400.000	.6176E+03-.2092E+04	180.000	2454.000	927.100		
1500.000	.6176E+03-.2092E+04	180.000	2321.000	847.600		
1600.000	.6176E+03-.2092E+04	180.000	2210.000	796.200		
1700.000	.6176E+03-.2092E+04	180.000	2055.000	745.600		
1800.000	.6176E+03-.2092E+04	170.000	1887.000	679.500		
1900.000	.6176E+03-.2092E+04	170.000	1669.000	625.200		
2000.000	.6160E+03-.2095E+04	160.000	1268.000	582.200		
2100.000	.6072E+03-.2110E+04	160.000	1032.000	405.300		
900.000	.6176E+03-.2093E+04	175.111	3.557	3.076	2061.602	764.782
1000.000	.6176E+03-.2093E+04	175.111	3.960	3.437	1930.771	708.782
1100.000	.6175E+03-.2093E+04	174.666	3.949	3.443	1862.632	680.194
1200.000	.6175E+03-.2094E+04	174.128	3.936	3.384	1791.539	654.256
1300.000	.6175E+03-.2094E+04	173.470	3.924	3.311	1716.603	627.123
1400.000	.6175E+03-.2094E+04	172.650	3.898	3.267	1638.731	596.291
1500.000	.6175E+03-.2094E+04	171.589	3.863	3.158	1555.791	566.836
1600.000	.6175E+03-.2095E+04	170.171	3.871	3.019	1461.472	535.555
1700.000	.6175E+03-.2095E+04	168.189	3.924	2.853	1356.096	501.217
1800.000	.6175E+03-.2096E+04	167.729	4.132	2.606	1231.882	465.700
1900.000	.6174E+03-.2097E+04	166.960	4.898	2.303	1078.237	423.987
2000.000	.6181E+03-.2098E+04	170.275	5.122	2.220	966.383	348.302
2100.000	.6290E+03-.2086E+04	180.000	2.000	2.000	1115.968	266.738

Figure B-2. File "TERRAIN" used as input in test run of CTDMPPLUS (see Table 3-5).

MET TOWER	710.	-400.	0.0	1982.	1
FOLLY	550.	-500.	0.0	1850.	1
TREEHOUSE	550.	-700.	0.0	1978.	1
SLIPPERY HILL	490.	-1030.	0.0	2096.	1
RIDGE END	770.	-160.	0.0	1939.	1
OVERLOOK	230.	-980.	0.0	2090.	1
SOUTHSIDE	0.	-1480.	0.0	2110.	1
COW PASTURE	320.	-1480.	0.0	2208.	1

Figure B-3. File "RECEPTOR" used in test run of CTDMPPLUS (see Table 3-6).

80	6	26	1	10.	0	300.	1.2	299.3	5.0	.03	-999.9
80	6	26	1	100.	1	300.	3.9	299.3	5.0	.03	-999.9
80	6	26	10	10.	0	328.	2.2	299.4	-999	.49	-999.9
80	6	26	10	100.	1	328.	2.5	299.4	-999	.49	-999.9

Figure B-4. File "PROFILE" used in test run of CTDMPLUS (see Table 3-7).

80	6	26	178	1	92.	30.	0.057	11.2	0.150E+00
80	6	26	178	10	-999.	1242.	0.293	-7.4	0.150E+00

Figure B-5. File "SURFACE" used in test run of CTDMPLUS (see Table 3-8).

6201	14842	80 626 0	43		12	
990.7/	200./302.5/170/	2	978.0/ 315./300.8/173/	2	950.0/ 573./298.6/179/	2
850.0/1538./290.0/199/	2	839.0/1649./289.4/194/	2	821.0/1834./288.4/187/	1	800.0/2054./289.1/140/
788.0/2183./289.6/ 28/	1	750.0/2604./290.6/ 11/	3	749.0/2615./290.7/ 12/	3	700.0/3187./285.7/ 32/
6201	14842	80 62612	46		11	
991.3/ 200./292.0/ 0/ 0		976.0/ 335./297.1/235/	1	959.0/ 489./297.1/240/	3	950.0/ 572./296.5/249/
900.0/1041./293.1/268/	2	880.0/1236./291.6/266/	2	870.0/1334./293.1/262/	2	850.0/1535./294.2/262/
800.0/2059./294.2/325/	3	750.0/2612./289.8/ 1/	5	700.0/3194./284.9/ 6/	6	

Figure B-6. File "RAWIN" used in test run of CTDMPPLUS (see Table 3-9).

80	6	26	1	1	8	microS/M**3			
0.541E+00	0.592E-03	0.619E-08	0.000E+00	0.214E-02	0.000E+00	0.000E+00	0.000E+00	0.000E+00	
80	6	26	10	6	8	microS/M**3			
0.213E-01	0.152E+00	0.538E+00	0.960E+00	0.188E-05	0.155E+01	0.115E+01	0.991E+00		

Figure B-7. File "CONC", concentration file from the CTDMPLUS test run (see Table 3-11).

CTDMPLUS TEST RUN

INPUT/OUTPUT SWITCHES (1 = USE THIS OPTION, 0 = DO NOT USE OPTION)

ICASE: INCLUDE CASE-STUDY PRINTOUT: 0 = NONE, 1 = STABLE ONLY, 2 = UNSTABLE ONLY 3 = ALL HOURS 3
 ITOPN: CREATE TOP 4 TABLE AT END OF RUN 1
 ICONC: CONCENTRATION OUTPUT: 0 = NONE, 1 = BINARY, 2/3 = TEXT 2

INTERNAL PROGRAM SWITCHES

IMIX: (IF 1, USE ON-SITE MIXING HEIGHT OBSERVATIONS (OFF-SITE IF NOT AVAILABLE); IF 0, VICA VERSA) 1
 IWS1: (IF 1, SET MINIMUM WIND SPEED TO 1.0 M/S) 1
 ISIGV: (HORIZ. TURB. INTENSITY DATA (0=SIGMA-THETA 1=SIGMA-V) 0
 IWD: (IF 1, SCALE WIND DIRECTION WITH HEIGHT) 1
 ICHI: (IF 1, MODEL OUTPUTS CHI/Q; OTHERWISE IT OUTPUTS CHI) 1
 ISOR: (IF 1, MODEL GIVES SOURCE CONTRIBUTION TABLE) 1
 IUNSTA: (IF 0, MODEL WILL NOT READ RAWIN FILE OR CALCULATE UNSTABLE HOURS) 1

FOR HORIZONTAL SCALE, MULTIPLY USER UNITS BY 1.0000 TO GET METERS.
 FOR ELEVATION, MULTIPLY USER UNITS BY 0.3048 TO GET METERS.

SITE LATITUDE (> 0 IF NORTH) = 39.591
 SITE LONGITUDE (> 0 IF WEST) = 89.489
 SITE TIME ZONE (> 0 IF WEST) = 6.
 POLLUTANT # (FOR HOURLY EMISSIONS) = 1

METEOROLOGICAL TOWER COORDINATE INFORMATION:

X-COORD: 0.000 (USER UNITS) * 1.0000 = 0.0 (METERS)
 Y-COORD: 0.000 (USER UNITS) * 1.0000 = 0.0 (METERS)
 ELEVATION: 945.000 (USER UNITS) * 0.3048 = 288.0 (METERS)

Figure B-8. File "CTDM.OUT", output listing from CTDMPLUS test run.

CTDMPLUS TEST RUN

* * * S O U R C E I N F O R M A T I O N * * *

STK #	NAME	EMISSION RATE (G/S)	LOCATION X (M)	Y (M)	STK HT (M)	STK DIA (M)	GAS TEMP (K)	EXIT VEL (M/S)
1	STACK-1	455.05	0.00	0.00	191.2*	3.36	410.1	25.06
2	STACK-2	255.05	0.00	30.00	190.0	3.36	420.1	25.06

COMMON BASE ELEVATION = 286.5 (METERS).
THIS BASE ELEVATION IS USED FOR ALL STACKS IN THIS RUN;
ALL STACK HEIGHTS MARKED WITH * HAVE BEEN ADJUSTED TO
RETAIN THE ACTUAL ELEVATION OF THE TOP OF THE STACKS.

MULTIPLY HORIZONTAL USER UNITS BY: 1.000E+00 TO CONVERT TO METERS
MULTIPLY VERTICAL USER UNITS BY: 3.048E-01 TO CONVERT TO METERS

Figure B-8. (Page 2 of 14).

CTDMPLUS TEST RUN

RECEPTOR INFORMATION						
REC NO.	IDENTIFICATION	EAST COORD (USER UNITS)	NORTH COORD (USER UNITS)	HEIGHT ABOVE LOCAL GRD LVL (USER UNITS)	GRD LVL ELEVATION (USER UNITS)	HILL NUMBER
1	MET TOWER	710.00	-400.00	0.0	1982.0	1
2	FOLLY	550.00	-500.00	0.0	1850.0	1
3	TREEHOUSE	550.00	-700.00	0.0	1978.0	1
4	SLIPPERY HILL	490.00	-1030.00	0.0	2096.0	1
5	RIDGE END	770.00	-160.00	0.0	1939.0	1
6	OVERLOOK	230.00	-980.00	0.0	2090.0	1
7	SOUTHSIDE	0.00	-1480.00	0.0	2110.0	1
8	COW PASTURE	320.00	-1480.00	0.0	2208.0	1

MULTIPLY HORIZONTAL USER UNITS BY: 1.000E+00 TO CONVERT TO METERS						
MULTIPLY VERTICAL USER UNITS BY: 3.048E-01 TO CONVERT TO METERS						

Figure B-8. (Page 3 of 14).

TERRAIN INFORMATION (USER UNITS FOR ALL DATA)

MULTIPLY HORIZONTAL USER UNITS BY: 1.000E+00 TO CONVERT TO METERS
 MULTIPLY VERTICAL USER UNITS BY: 3.048E-01 TO CONVERT TO METERS
 TERRAIN INFORMATION (CONT.)

HILL # 1 PIEDMONT HILL

HILL TOP: 2240.0 (USER UNITS)

BEST FIT ELLIPSE INFORMATION FOR WRAP: PIEDMONT HILL

CONTOUR HEIGHT	X-COORD (HILL CENTER)	Y-COORD	MAJOR AXIS AZIM. FROM N	ELLIPSE AXIS LENGTHS MAJOR	MINOR
900.0	617.600	-2092.000	180.0	3072.000	1294.400
1000.0	617.600	-2092.000	180.0	2953.000	1195.700
1100.0	617.600	-2092.000	180.0	2834.000	1097.000
1200.0	617.600	-2092.000	180.0	2715.000	998.300
1300.0	617.600	-2092.000	180.0	2595.000	953.600
1400.0	617.600	-2092.000	180.0	2454.000	927.100
1500.0	617.600	-2092.000	180.0	2321.000	847.600
1600.0	617.600	-2092.000	180.0	2210.000	796.200
1700.0	617.600	-2092.000	180.0	2055.000	745.600
1800.0	617.600	-2092.000	170.0	1887.000	679.500
1900.0	617.600	-2092.000	170.0	1669.000	625.200
2000.0	616.000	-2095.000	160.0	1268.000	582.200
2100.0	607.200	-2110.000	160.0	1032.000	405.300

MULTIPLY HORIZONTAL USER UNITS BY: 1.000E+00 TO CONVERT TO METERS
 MULTIPLY VERTICAL USER UNITS BY: 3.048E-01 TO CONVERT TO METERS
 TERRAIN INFORMATION (CONT.)

Hc CUT-OFF HILL INFORMATION FOR LIFT: PIEDMONT HILL

CONTOUR HEIGHT	X-COORD (HILL CENTER)	Y-COORD	MAJOR AXIS AZIM. FROM N	<--- INVERSE POLYNOMIAL VARIABLES --->			
				MAJ EXP	MIN EXP	MAJ SCALE	MIN SCALE
900.0	617.600	-2093.000	175.1	3.557	3.076	2061.602	764.782
1000.0	617.600	-2093.000	175.1	3.960	3.437	1930.771	708.782
1100.0	617.500	-2093.000	174.7	3.949	3.443	1862.632	680.194
1200.0	617.500	-2094.000	174.1	3.936	3.384	1791.539	654.256
1300.0	617.500	-2094.000	173.5	3.924	3.311	1716.603	627.123
1400.0	617.500	-2094.000	172.6	3.898	3.267	1638.731	596.291
1500.0	617.500	-2094.000	171.6	3.863	3.158	1555.791	566.836
1600.0	617.500	-2095.000	170.2	3.871	3.019	1461.472	535.555
1700.0	617.500	-2095.000	168.2	3.924	2.853	1356.096	501.217
1800.0	617.500	-2096.000	167.7	4.132	2.606	1231.882	465.700
1900.0	617.400	-2097.000	167.0	4.898	2.303	1078.237	423.987
2000.0	618.100	-2098.000	170.3	5.122	2.220	966.383	348.302
2100.0	629.000	-2086.000	180.0	2.000	2.000	1115.968	266.738

MULTIPLY HORIZONTAL USER UNITS BY: 1.000E+00 TO CONVERT TO METERS
 MULTIPLY VERTICAL USER UNITS BY: 3.048E-01 TO CONVERT TO METERS

SURFACE ROUGHNESS LENGTH OF EACH HILL:

HILL # 1
 ZO (M) 0.760

Figure B-8. (Page 4 of 14).

MAP EDGES: XMIN = -521., XMAX = 1291., YMIN = -1480., YMAX = 30.

* = SOURCE, RECEPTORS SHOWN BY HILL # (0-9,A-Z)

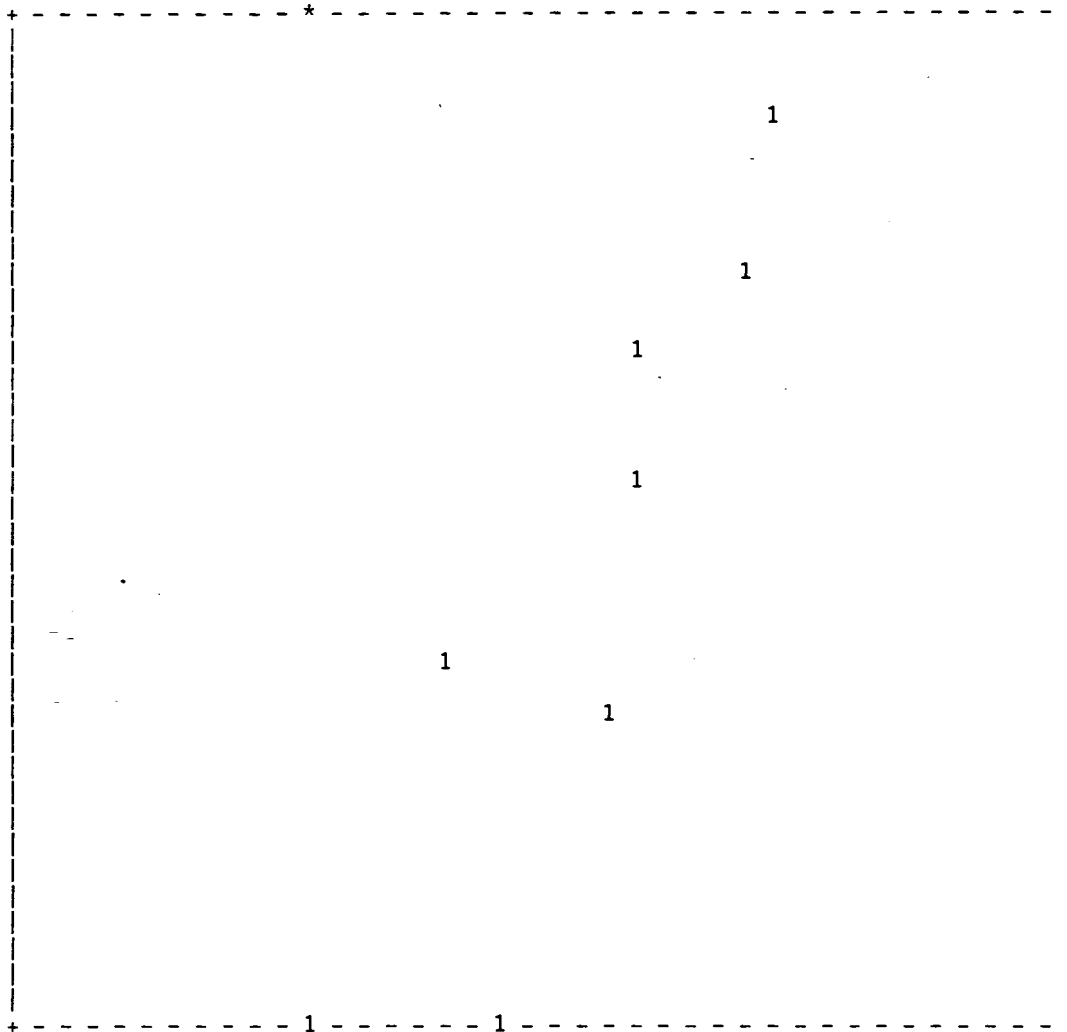


Figure B-8. (Page 5 of 14).

CTDMPLUS TEST RUN

INPUT MET DATA FROM SURFACE AND PROFILE (NOTE: ***** = MISSING DATA):

YR	MO	DA	HR	MIXING HEIGHT (M)	SFC TEMP (K)	SFC U* (M/S)	MONIN- OBUKHOV LENGTH (M)	SFC ROUGH. LENGTH (M)
80	6	26	1	92.0	299.3	0.057	11.2	0.1500

ADJUSTED HEIGHT (M)	WIND DIR. (DEG)	<-WIND SPEED-> SCALAR (M/S)	VECTOR (M/S)	AMB. TEMP (K)	SIGMA- THETA (DEG)	SIGMA-V (M/S)	SIGMA-W (M/S)
11.5	300.0	1.20	1.20	299.30	5.0	0.20	0.03
101.5	300.0	3.90	3.89	299.30	5.0	0.34	0.03

NOTE: SCALAR WIND SPEEDS USED IN CTDM ARE SET TO A MINIMUM OF 1 M/S

NOTE: HEIGHTS ARE REFERENCED TO THE COMMON STACK BASE ELEVATION
THE ADJUSTMENT TO THE INPUT HEIGHT IS 1.5 METERS.

SOURCE #	<----- SOURCE INFORMATION ----->					FINAL PLUME		
	QS (G/S)	TS (K)	VS (M/S)	BUOY FLUX (M4/S3)	MOM FLUX (M4/S2)	RISE (M)		
1	1.0	410.1	25.06	187.5	1293.4	138.05		

VARIABLES AT PLUME HEIGHT:	HEIGHT (M)	WDIR (DEG)	USCAL (M/S)	UVECT (M/S)	SIGV (M/S)	SIGW (M/S)	DTHDZ (DEG/M)
	329.3	300.	3.90	3.89	0.34	0.0390	0.0098

Figure B-8. (Page 6 of 14).

CTDMPLUS TEST RUN

INFORMATION FOR HILL 1: PIEDMONT HILL

HCRIT = 178.5 M; FROUDE # ABOVE HCRIT = 1.00

WRAP INFORMATION:

DISTANCE FROM SOURCE TO HILL CENTER = 2181.3 M; WRAP HT = 178.5 M
 ELLIPSE AXIS LENGTHS: MAJOR = 2159.4 M; MINOR = 834.4 M
 MAJOR AXIS AZIMUTH FROM NORTH = 180.0 DEG
 DISTANCE TO PRIMARY IMPINGEMENT POINT = 287.3 M

LIFT INFORMATION:

DISTANCE FROM SOURCE TO HILL CENTER = 2183.1 M; LIFT MIDPOINT HT = 287.4
 ELLIPSE AXIS LENGTHS: MAJOR = 1528.0 M; MINOR = 554.5 M
 MAJOR AXIS AZIMUTH FROM NORTH = 171.6 DEG
 DISTANCE ALONG FLOW FROM SOURCE TO HILL CENTER = 1581.8 M
 CROSSFLOW DISTANCE FROM SOURCE TO HILL CENTER = 1504.7 M
 DISTANCE TO PRIMARY IMPINGEMENT POINT = 287.1 M

REC #	L / W	SRC-RECP DISTANCE ALONG FLOW (M)	SRC-RECP DISTANCE CROSS FLOW (M)	RECEPTOR HT ABOVE STK BASE (M)	EFF. SRC-RECP HT DIFF (M)	FLAT TERRAIN SIG-Y (M)	FLAT TERRAIN SIG-Z (M)	HILL-INDUCED EFFECTIVE SIG-Y (M)	HILL-INDUCED EFFECTIVE SIG-Z (M)	TOTAL CONC (US/M**3)
1	L	815.	36.6	317.6	150.7	71.3	39.5	57.0	39.5	3.1797E-01
1	W	814.	86.0	317.6	11.7	71.2	39.5	71.2	39.5	0.0000E-01
1	TOTAL									3.1797E-01
2	L	726.	189.0	277.4	150.7	63.9	39.5	51.9	39.5	4.7911E-04
2	W	732.	86.0	277.4	51.9	64.3	39.5	64.3	39.5	0.0000E-01
2	TOTAL									4.7911E-04
3	L	826.	347.5	316.4	150.7	72.3	39.5	57.7	39.5	5.2610E-09
3	W	838.	86.0	316.4	12.9	73.2	39.5	73.2	39.5	0.0000E-01
3	TOTAL									5.2610E-09
4	L	939.	615.0	352.3	150.7	81.7	39.5	64.4	39.5	0.0000E-01
4	W	963.	86.0	352.3	-23.1	83.6	39.5	83.6	39.5	0.0000E-01
4	TOTAL									0.0000E-01
5	L	747.	-203.3	304.5	150.7	65.6	39.5	53.1	39.5	2.4281E-04
5	W	737.	86.0	304.5	24.8	64.7	39.5	64.7	39.5	0.0000E-01
5	TOTAL									2.4281E-04
6	L	689.	679.4	350.5	150.7	60.8	39.5	49.7	39.5	0.0000E-01
6	W	716.	86.0	350.5	-21.2	63.0	39.5	63.0	39.5	0.0000E-01
6	TOTAL									0.0000E-01

Figure B-8. (Page 7 of 14).

CTDMPLUS TEST RUN

REC / #	L / W	SRC-RECP DISTANCE (M)	SRC-RECP DISTANCE (M)	RECEPTOR HT ABOVE STK BASE (M)	EFF. SRC-RECP HT DIFF (M)	FLAT TERRAIN SIG-Y (M)	SIG-Z (M)	HILL-INDUCED EFFECTIVE SIG-Y (M)	SIG-Z (M)	TOTAL CONC (US/M**3)
7 L		740.	1205.0	356.6	150.7	65.0	39.5	52.7	39.5	0.0000E-01
7 W		788.	86.0	356.6	-27.3	69.0	39.5	69.0	39.5	0.0000E-01
7 TOTAL										0.0000E-01
8 L		1017.	1008.5	386.5	150.7	88.2	39.5	69.3	39.6	0.0000E-01
8 W		1059.	86.0	386.5	-57.2	91.6	39.5	91.6	39.5	0.0000E-01
8 TOTAL										0.0000E-01

SOURCE #	<----- SOURCE INFORMATION ----->					FINAL PLUME
	QS (G/S)	TS (K)	VS (M/S)	BUOY FLUX (M4/S3)	MOM FLUX (M4/S2)	RISE (M)
2	1.0	420.1	25.06	199.5	1262.7	140.94

VARIABLES AT PLUME HEIGHT:	HEIGHT (M)	WDIR (DEG)	USCAL (M/S)	UVECT (M/S)	SIGV (M/S)	SIGW (M/S)	DTHDZ (DEG/M)
	330.9	300.	3.90	3.89	0.34	0.0390	0.0098

Figure B-8. (Page 8 of 14).

CTDMPLUS TEST RUN

INFORMATION FOR HILL 1: PIEDMONT HILL

HCRIT = 178.5 M; FROUDE # ABOVE HCRIT = 1.00

WRAP INFORMATION:

DISTANCE FROM SOURCE TO HILL CENTER = 2210.0 M; WRAP HT = 178.5 M

ELLIPSE AXIS LENGTHS: MAJOR = 2187.9 M; MINOR = 834.4 M

MAJOR AXIS AZIMUTH FROM NORTH = 180.0 DEG

DISTANCE TO PRIMARY IMPINGEMENT POINT = 289.3 M

LIFT INFORMATION:

DISTANCE FROM SOURCE TO HILL CENTER = 2211.9 M; LIFT MIDPOINT HT = 287.4

ELLIPSE AXIS LENGTHS: MAJOR = 1528.0 M; MINOR = 554.5 M

MAJOR AXIS AZIMUTH FROM NORTH = 171.6 DEG

DISTANCE ALONG FLOW FROM SOURCE TO HILL CENTER = 1596.8 M

CROSSFLOW DISTANCE FROM SOURCE TO HILL CENTER = 1530.7 M

DISTANCE TO PRIMARY IMPINGEMENT POINT = 289.2 M

REC #	L W	SRC-RECP DISTANCE ALONG FLOW (M)	SRC-RECP DISTANCE CROSS FLOW (M)	RECEPTOR HT ABOVE STK BASE (M)	EFF. SRC-RECP HT DIFF (M)	FLAT TERRAIN SIG-Y SIG-Z (M) (M)	HILL-INDUCED EFFECTIVE SIG-Y SIG-Z (M) (M)	TOTAL CONC (US/M**3)
1	L	830.	62.6	317.6	152.4	72.6 40.3	58.6 40.3	2.2282E-01
1	W	830.	94.1	317.6	13.3	72.6 40.3	72.6 40.3	0.0000E-01
1	TOTAL							2.2282E-01
2	L	741.	215.0	277.4	152.4	65.1 40.3	53.3 40.3	1.1321E-04
2	W	746.	94.1	277.4	53.6	65.6 40.3	65.6 40.3	0.0000E-01
2	TOTAL							1.1321E-04
3	L	841.	373.5	316.4	152.4	73.5 40.3	59.2 40.3	9.2630E-10
3	W	852.	94.1	316.4	14.6	74.4 40.3	74.4 40.3	0.0000E-01
3	TOTAL							9.2630E-10
4	L	954.	641.0	352.3	152.4	83.0 40.3	66.1 40.4	0.0000E-01
4	W	974.	94.1	352.3	-21.4	84.6 40.3	84.6 40.3	0.0000E-01
4	TOTAL							0.0000E-01
5	L	762.	-177.3	304.5	152.4	66.9 40.3	54.5 40.3	1.8925E-03
5	W	755.	94.1	304.5	26.4	66.3 40.3	66.3 40.3	0.0000E-01
5	TOTAL							1.8925E-03
6	L	704.	705.3	350.5	152.4	62.0 40.3	51.1 40.3	0.0000E-01
6	W	727.	94.1	350.5	-19.6	63.9 40.3	63.9 40.3	0.0000E-01
6	TOTAL							0.0000E-01

Figure B-8. (Page 9 of 14).

CTDMPLUS TEST RUN

REC / #	L / W	SRC-RECP DISTANCE ALONG FLOW (M)	SRC-RECP DISTANCE CROSS FLOW (M)	RECEPTOR HT ABOVE STK BASE (M)	EFF. SRC-RECP HT DIFF (M)	FLAT TERRAIN SIG-Y SIG-Z (M) (M)	HILL-INDUCED EFFECTIVE SIG-Y SIG-Z (M) (M)	TOTAL CONC (US/M**3)
7	L	755.	1231.0	356.6	152.4	66.3 40.3	54.1 40.3	0.0000E-01
7	W	794.	94.1	356.6	-25.7	69.5 40.3	69.5 40.3	0.0000E-01
7	TOTAL							0.0000E-01
8	L	1032.	1034.5	386.5	152.4	89.4 40.4	71.1 40.4	0.0000E-01
8	W	1066.	94.1	386.5	-55.5	92.2 40.4	92.2 40.4	0.0000E-01
8	TOTAL							0.0000E-01

MAXIMUM CONCENTRATION FOR THIS HOUR IS 0.54 US/M**3 AT RECEPTOR # 1

SOURCE CONTRIBUTION TABLE

DATE 6/26/80 HOUR 1

REC #	STACK # 1	STACK # 2	TOTAL
1	0.3180E+00	0.2228E+00	0.5408E+00
2	0.4791E-03	0.1132E-03	0.5923E-03
3	0.5261E-08	0.9263E-09	0.6187E-08
4	0.0000E+00	0.0000E+00	0.0000E+00
5	0.2428E-03	0.1893E-02	0.2135E-02
6	0.0000E+00	0.0000E+00	0.0000E+00
7	0.0000E+00	0.0000E+00	0.0000E+00
8	0.0000E+00	0.0000E+00	0.0000E+00

Figure B-8. (Page 10 of 14).

CTDMPLUS TEST RUN

INPUT MET DATA FROM SURFACE AND PROFILE (NOTE: ***** = MISSING DATA):

YR	MO	DA	HR	MIXING HEIGHT (M)	SFC TEMP (K)	SFC U* (M/S)	MONIN- OBUKHOV LENGTH (M)	SFC ROUGH. LENGTH (M)
80	6	26	10	1242.0	299.4	0.293	-7.4	0.1500

ADJUSTED HEIGHT (M)	WIND DIR. (DEG)	<-WIND SPEED-> SCALAR (M/S)	VECTOR (M/S)	AMB. TEMP (K)	SIGMA- THETA (DEG)	SIGMA-V (M/S)	SIGMA-W (M/S)
11.5	328.0	2.20	-999.90	299.40	-999.0	-999.90	0.49
101.5	328.0	2.50	-999.90	299.40	-999.0	-999.90	0.49

NOTE: SCALAR WIND SPEEDS USED IN CTDM ARE SET TO A MINIMUM OF 1 M/S
 NOTE: HEIGHTS ARE REFERENCED TO THE COMMON STACK BASE ELEVATION
 THE ADJUSTMENT TO THE INPUT HEIGHT IS 1.5 METERS.

<----- SOURCE INFORMATION ----->						
SOURCE #	QS (G/S)	TS (K)	VS (M/S)	BUOY FLUX (M**4/S**3)	MOM FLUX (M**4/S**3)	PENETR FACTOR
1	1.0	410.1	25.06	187.3	1293.9	0.0000

SOURCE INFORMATION ADJUSTED FOR PENETRATION:

SOURCE #	QS (G/S)	BUOY FLUX (M**4/S**3)
1	1.0	187.3

PLUME LAYER AVERAGE VARIABLES:

HEIGHT	WD	WS
367.6	330.4	2.53

CONVECTIVE SCALING PARAMETERS:

USTAR	WSTAR	FSTAR
0.2930	2.1935	0.0124

Figure B-8. (Page 11 of 14).

CTDMPLUS TEST RUN

REC #	DWN-WND DIST (M)	CRS-WND DIST (M)	TRANS PL HT (M)	SIGMA Y (M)	HDF (1/M)	CWIC (G/M**3)	CONC (US/M**3)
1	698.5	-419.8	284.3	273.5	1.3593E-05	6.8965E-04	9.3745E-03
2	706.4	-231.3	286.5	275.8	8.3686E-05	8.6034E-04	7.1998E-02
3	880.3	-132.5	331.8	323.9	2.9155E-04	9.1427E-04	2.6656E-01
4	1137.6	82.7	0.0	384.1	6.8837E-04	7.0466E-04	4.8507E-01
5	519.4	-590.5	233.4	218.3	2.6320E-08	1.8547E-05	4.8816E-07
6	965.7	284.0	0.0	346.0	9.4806E-04	8.3413E-04	7.9081E-01
7	1286.9	731.0	0.0	415.3	9.1530E-04	6.3467E-04	5.8091E-01
8	1444.9	452.7	0.0	446.6	8.8439E-04	5.6739E-04	5.0179E-01

<----- SOURCE INFORMATION ----->						
SOURCE #	QS (G/S)	TS (K)	VS (M/S)	BUOY FLUX (M**4/S**3)	MOM FLUX (M**4/S**3)	PENETR FACTOR
2	1.0	420.1	25.06	199.3	1263.1	0.0000

SOURCE INFORMATION ADJUSTED FOR PENETRATION:

SOURCE #	QS (G/S)	BUOY FLUX (M**4/S**3)
2	1.0	199.3

PLUME LAYER AVERAGE VARIABLES:

HEIGHT	WD	WS
373.1	330.5	2.53

CONVECTIVE SCALING PARAMETERS:

USTAR	WSTAR	FSTAR
0.2930	2.1935	0.0132

Figure B-8. (Page 12 of 14).

CTDMPLUS TEST RUN

REC #	DWN-WND DIST (M)	CRS-WND DIST (M)	TRANS PL HT (M)	SIGMA Y (M)	HDF (1/M)	CWIC (G/M**3)	CONC (US/M**3)
1	724.2	-405.6	297.4	281.6	1.7722E-05	6.7111E-04	1.1894E-02
2	732.3	-217.1	299.6	283.9	9.7071E-05	8.2709E-04	8.0287E-02
3	906.3	-118.5	345.4	331.5	3.0598E-04	8.8877E-04	2.7194E-01
4	1163.8	96.5	0.0	391.0	6.8578E-04	6.9192E-04	4.7450E-01
5	545.0	-576.2	246.1	227.1	6.3662E-08	2.1805E-05	1.3882E-06
6	992.1	298.0	0.0	353.4	9.3428E-04	8.1337E-04	7.5992E-01
7	1313.6	744.7	0.0	421.9	9.0485E-04	6.2484E-04	5.6539E-01
8	1471.4	466.3	0.0	452.8	8.7274E-04	5.6083E-04	4.8946E-01

MAXIMUM CONCENTRATION FOR THIS HOUR IS 1.55 US/M**3 AT RECEPTOR # 6

SOURCE CONTRIBUTION TABLE

DATE 6/26/80 HOUR 10

REC #	STACK # 1	STACK # 2	TOTAL
1	0.9374E-02	0.1189E-01	0.2127E-01
2	0.7200E-01	0.8029E-01	0.1523E+00
3	0.2666E+00	0.2719E+00	0.5385E+00
4	0.4851E+00	0.4745E+00	0.9596E+00
5	0.4882E-06	0.1388E-05	0.1876E-05
6	0.7908E+00	0.7599E+00	0.1551E+01
7	0.5809E+00	0.5654E+00	0.1146E+01
8	0.5018E+00	0.4895E+00	0.9913E+00

Figure B-8. (Page 13 of 14).

CTDMPLUS TEST RUN

REC	TOP 4 CONCENTRATIONS [US/M**3] AT EACH RECEPTOR			
#	HIGHEST (JCD,HR)	SECOND (JCD,HR)	THIRD (JCD,HR)	FOURTH (JCD,HR)
1	5.41E-01 (178, 1)	2.13E-02*(178,10)	***** (0, 0)	***** (0, 0)
2	1.52E-01 (178,10)	5.92E-04 (178, 1)	***** (0, 0)	***** (0, 0)
3	5.38E-01 (178,10)	6.19E-09 (178, 1)	***** (0, 0)	***** (0, 0)
4	9.60E-01 (178,10)	0.00E-01 (178, 1)	***** (0, 0)	***** (0, 0)
5	2.14E-03 (178, 1)	1.88E-06 (178,10)	***** (0, 0)	***** (0, 0)
6	1.55E+00*(178,10)	0.00E-01 (178, 1)	***** (0, 0)	***** (0, 0)
7	1.15E+00 (178,10)	0.00E-01 (178, 1)	***** (0, 0)	***** (0, 0)
8	9.91E-01 (178,10)	0.00E-01 (178, 1)	***** (0, 0)	***** (0, 0)

Figure B-8. (Page 14 of 14).

United States
Environmental Protection
Agency

Center for Environmental Research
Information
Cincinnati OH 45268

Official Business
Penalty for Private Use, \$300

Please make all necessary changes on the above label,
detach or copy, and return to the address in the upper
left-hand corner.

If you do not wish to receive these reports CHECK HERE ☐
detach, or copy this cover, and return to the address in the
upper left-hand corner.

EPA/600/8-89/041